

EMISSION OF SHORT-LIVED HALOCARBONS BY
SELECTED TROPICAL MARINE PHYTOPLANKTON

LIM YONG KIAN

INSTITUTE OF GRADUATE STUDIES
UNIVERSITY OF MALAYA
KUALA LUMPUR

2017

**EMISSION OF SHORT-LIVED HALOCARBONS BY
SELECTED TROPICAL MARINE PHYTOPLANKTON**

LIM YONG KIAN

**DISSERTATION SUBMITTED IN FULFILMENT OF
THE REQUIREMENTS FOR THE DEGREE OF MASTER
OF PHILOSOPHY**

**INSTITUTE OF GRADUATE STUDIES
UNIVERSITY OF MALAYA
KUALA LUMPUR**

2017

UNIVERSITY OF MALAYA
ORIGINAL LITERARY WORK DECLARATION

Name of Candidate: Lim Yong Kian

Registration/Matric No: HGT140001

Name of Degree: Master of Philosophy (Ocean & Earth Sciences)

Title of Project Paper/Research Report/Dissertation/Thesis ("this Work"):

Emission of short-lived halocarbons by selected tropical marine phytoplankton

Field of Study:

Earth Science (Biotechnology)

I do solemnly and sincerely declare that:

- (1) I am the sole author/writer of this Work;
- (2) This Work is original;
- (3) Any use of any work in which copyright exists was done by way of fair dealing and for permitted purposes and any excerpt or extract from, or reference to or reproduction of any copyright work has been disclosed expressly and sufficiently and the title of the Work and its authorship have been acknowledged in this Work;
- (4) I do not have any actual knowledge nor do I ought reasonably to know that the making of this work constitutes an infringement of any copyright work;
- (5) I hereby assign all and every rights in the copyright to this Work to the University of Malaya ("UM"), who henceforth shall be owner of the copyright in this Work and that any reproduction or use in any form or by any means whatsoever is prohibited without the written consent of UM having been first had and obtained;
- (6) I am fully aware that if in the course of making this Work I have infringed any copyright whether intentionally or otherwise, I may be subject to legal action or any other action as may be determined by UM.

Candidate's Signature

Date:

Subscribed and solemnly declared before,

Witness's Signature

Date:

Name:

Designation:

ABSTRACT

Biogenic volatile halocarbons contribute free halogen radicals to the troposphere and stratosphere, and may play a role in the catalytic destruction of the ozone layer. The contributions and significant impacts of biogenic halocarbon emissions from the tropics are relatively unknown and are of particular interest due to the prevalence of strong convective forces at the tropics and climate change. Of the marine biogenic sources, the marine microalgae (phytoplankton) inhabiting the oceans that cover 70% of the Earth's surface, make them a significant source of the short-lived halocarbons. A change in the environment may affect the emission of halocarbons. In this study, the effects of life-stage and irradiance were investigated. Using controlled laboratory experiments, three selected tropical marine phytoplankton were investigated for emission of halocarbons. Three phytoplankton species were grown in flask cultures and sampled for halocarbon emissions during different growth stages of the batch cultures. Growth was estimated using chlorophyll-a and cell number. Halocarbons were measured using a two-syringe collection system followed detection using a GC-MS equipped with a purge and trap system. The phytoplankton were found to emit a suite of short-lived halocarbons, namely CHBr_3 , CH_3I , CHCl_3 , CHBr_2Cl and CH_2Br_2 at different growth phases. *Amphora* sp. UMACC 370 was shown to be a stronger halocarbon emitter, especially CH_3I ($10.55 - 64.18 \text{ pmol mg}^{-1} \text{ day}^{-1}$), than the other two taxa, *Synechococcus* sp. UMACC 371 and *Parachlorella* sp. UMACC 245 ($1.04 - 3.86 \text{ pmol mg}^{-1} \text{ day}^{-1}$ and $0 - 2.16 \text{ pmol mg}^{-1} \text{ day}^{-1}$, respectively). CH_3I has significantly ($p < 0.05$) higher emission rate compared to the other detected compounds. Results show that the emissions of detected short-lived halocarbons are species- and growth phase-dependent, highlighting the importance of considering cell physiological conditions when determining gas emission rates. Chlorophyll-a and cell density normalized to emission rate of all five compounds were found to be highly correlated ($p < 0.01$). The cultures were also exposed to a range of

irradiance, 0, 40 and 120 $\mu\text{mol photons m}^{-2} \text{ s}^{-1}$. The photosynthetic performance (F_v/F_m , maximum quantum yield) of the cultures when exposed to the range of irradiance was used as an indicator of algal cell stress from photosynthesis. F_v/F_m was measured using the Water Pulsed Amplitude Modulated Fluorometer (PAM). Exposure to 120 $\mu\text{mol photons m}^{-2} \text{ s}^{-1}$ for 12 hours produced significant ($p < 0.05$) decrease in F_v/F_m and increase in halocarbon emissions, especially the release of CH_3I by *Amphora* sp. UMACC 370. The net changes of F_v/F_m , however, were weakly correlated to the significant ($p < 0.05$) changes in overall emission of the five compounds, suggesting that halocarbon emission triggered from oxidative cell stress at higher irradiance may not be directly linked to photosynthesis but instead to mitochondrion respiration, nutrient limitation or a change in lipid composition within the cell membrane.

ABSTRAK

Halokarbon biogenik meruap menyumbang halogen radikal secara bebas ke troposfera dan stratosfera dan mungkin memainkan peranan dalam pemusnahan lapisan ozon. Sumbangan dan kesan nyata pelepasan halokarbon biogenik dari kawasan tropika masih tidak diketahui dan amat diminati disebabkan kelaziman perolakan yang kuat di kawasan tropika dan perubahan iklim. Satu sumber biogenik marin, fitoplankton yang mendiami lautan meliputi 70% daripada permukaan bumi membuat mereka satu sumber halokarbon hayat-pendek yang penting. Perubahan dalam persekitaran tentu boleh mempengaruhi pelepasan halokarbon. Dalam kajian ini, kesan peringkat pertumbuhan dan sinaran cahaya telah disiasat. Menggunakan eksperimen makmal terkawal, tiga fitoplankton marin tropika yang terpilih telah disiasat untuk mengaji pelepasan halokarbon. Tiga spesies fitoplankton telah ditumbuh dalam kelalang dan disampel untuk pelepasan halokarbon semasa peringkat pertumbuhan yang berbeza. Pertumbuhan dianggar menggunakan klorofil-a dan bilangan sel. Halokarbon diukur menggunakan sistem pengumpulan dua picagari dan diikuti pengesanan halokarbon menggunakan GC-MS dilengkapi dengan sistem pembersihan dan perangkap. Fitoplankton didapati melepaskan satu set halokarbon hayat-pendek, iaitu CHBr_3 , CH_3I , CHCl_3 , CHBr_2Cl dan CH_2Br_2 di fasa pertumbuhan yang berbeza. *Amphora* sp. UMACC 370 telah ditunjukkan sebagai halokarbon pemancar yang lebih kuat, terutamanya CH_3I ($10.55 - 64.18 \text{ pmol mg}^{-1} \text{ day}^{-1}$), berbanding dengan dua taksa yang lain, iaitu *Synechococcus* sp. UMACC 371 dan *Parachlorella* sp. UMACC 245 ($1.04 - 3.86 \text{ pmol mg}^{-1} \text{ day}^{-1}$ and $0 - 2.16 \text{ pmol mg}^{-1} \text{ day}^{-1}$, masing-masing). CH_3I mempunyai signifikan ($p < 0.05$) kadar pelepasan yang lebih tinggi berbanding dengan sebatian dikesan lain. Keputusan menunjukkan bahawa pelepasan halokarbon hayat-pendek yang dikesan adalah spesies- dan pertumbuhan fasa pergantungan, menonjolkan kepentingan untuk mempertimbangkan sel keadaan fisiologi apabila menentukan kadar pelepasan gas. Klorofil-a dan ketumpatan sel

dinormalkan kadar pelepasan kesemua lima kompaun telah didapati berkait-rapat ($p < 0.01$). Fitoplankton juga didedahkan dengan pelbagai sinaran, 0, 40 dan 120 $\mu\text{mol foton m}^{-2} \text{ s}^{-1}$. Prestasi fotosintesis (F_v/F_m , hasil kuantum maksimum) daripada tumbuhan yang terdedah kepada julat sinaran digunakan sebagai penunjuk tekanan sel-sel. Pulsed Amplitude Modulated Fluorometer (PAM) digunakan untuk mengukur F_v/F_m . Pendedahan pada 120 $\mu\text{mol foton m}^{-2} \text{ s}^{-1}$ selama 12 jam menghasilkan penurunan F_v/F_m . Pendedahan 120 $\mu\text{mol foton m}^{-2} \text{ s}^{-1}$ selama 12 jam menghasilkan penurunan F_v/F_m dan peningkatan pelepasan halokarbon yang signifikan ($p < 0.05$), terutamanya pembebasan CH_3I oleh *Amphora* sp. UMACC 370. Walaubagaimanapun, perubahan F_v/F_m lemah dikait-rapat dengan perubahan signifikan ($p < 0.05$) pelepasan lima sebatian, menunjukkan bahawa pelepasan halokarbon dicetuskan daripada tekanan oksidatif sel daripada sinaran yang lebih tinggi tidak semestinya diakibatkan fotosintesis tetapi berkemungkinan lebih berkait-rapat dengan pernafasan mitokondrion, had nutrien dan perubahan komposisi lipid dalam membran sel.

ACKNOWLEDGEMENTS

First and foremost, I would like to express my deepest gratitude to my research supervisor, Prof. Dr. Phang Siew Moi, for giving me the opportunity from the very beginning to work on this Master project and later spending her valuable time to supervise, guide and nurture me to ensure my achievements. Her immeasurable advice, thoughts and care as well as unswerving determination has truly been my motivation to not only successfully complete my research but to a better person in life and in work. I would also like to express my sincere and profound gratitude to my co-supervisor, Prof. Dr. William Sturges for always been so immensely supportive and unselfishly approachable whenever I needed advice from his area of expertise. He is also one of the most affable professors I have ever met in my life. Not to forget, thank you Dr. Gill Malin for all the professional guidance in scientific writing and research work. I have learned so much from you.

Throughout my daily research work, I have been blessed to be surrounded by a group of cheerful and optimistic colleagues. They are; Lee Kok Keong, Dr. Ng Fong Lee (Victoria), Ou Mei Cing, Tan Cheng Yau, Dr. Poong Sze Wan, Tan Pui Ling, Fiona Keng Seh Lin, Dr. Ng Poh Kheng, Nurain Mustaza, Bahram Barati, Muhammad Mussoddiq bin Jaafar, Dr. Emienour Muzalina Mustafa, Vejeysri Vello and Dr. Mahmoud Danaee. Thank you for always been there for me. You have supported and encouraged me towards making University of Malaya, both a centre of excellence and a surrogate home to me.

I would also like to use this opportunity to say a million thanks to my friends outside my research work. They are my panacea to stress. They teach me the importance to harmoniously balance between life and work. To mention a notable few: Matthew Giebel, Maurice Jan, Dave Kerschgens, Jaclyn Lee, Gan Boon Phin, Edwin Scott, Derek Baran, my unforgettable alma mater friends from University of Pittsburgh, and countless more. Thank you for all the social, spiritual and emotional support, and making life purposeful all this while.

Thank you all the wonderful and friendly staff from the Institute of Ocean and Earth Sciences (IOES) and Institute of Graduate Studies (IPS), University of Malaya for always been helpful and resourceful at your very best. You all really are a bunch of genuinely nice people. Not to forget, I thank the Ministry of Education Malaysia for providing MyMaster scholarship and Higher Institute of Centre of Excellence Grant (HICOE-2014F) for the financial support, allowing my research studies here possible.

Last but not least, I thank my eternally loving parents, my beautiful sister and supportive relatives, especially my older cousin, Chee Hock Ming, who has never gave up his belief in me and is continuously motivating me.

Thank you all from my heart.

TABLE OF CONTENTS

Abstract	iii
Abstrak	v
Acknowledgements	vii
Table of Contents	viii
List of Figures	xii
List of Tables	xvi
List of Symbols and Abbreviations	xviii
List of Appendices	xxi
CHAPTER 1: INTRODUCTION	22
1.1 Background	22
1.2 Problem statement	23
1.3 Research questions	23
1.4 Objectives	23
1.5 Thesis outline	24
CHAPTER 2: LITERATURE REVIEW	25
2.1 Halocarbons	25
2.1.1 Halocarbon chemistry	25
2.1.2 Long-lived halocarbons	25
2.1.3 Short-lived halocarbons	26
2.1.4 Environmental role of halocarbons	27
2.2 Climate change	29
2.2.1 Causes and effects of modern climate change	29
2.2.2 Ozone	31
2.2.2.1 Importance of ozone	31

2.2.2.2	Ozone production	31
2.2.3	Effect of halocarbons on atmospheric chemistry	32
2.3	Introduction to marine microalgae.....	34
2.3.1	What are microalgae?	34
2.3.2	Distribution and abundance of microalgae.....	35
2.4	Marine biogenic sources of halocarbons	37
2.4.1	Halocarbon emission by marine microalgae	37
2.4.2	Mechanisms behind the halocarbon emissions	46
2.4.3	Significance of tropical emission of biogenic halocarbons	48
2.4.4	Factors affecting halocarbon emissions by microalgae.....	51
2.4.4.1	Varying environmental conditions	51
2.4.4.2	Halocarbon emissions and photosynthesis	55
CHAPTER 3: METHODOLOGY		57
3.1	Microalgal cultures	57
3.2	Experiment 1: Optimization of selected parameters for studies	62
3.2.1	Selection of suitable growth media	62
3.2.2	Profiling algal growth.....	62
3.2.3	Determination of incubation time.....	63
3.3	Experiment 2: Determining suitable cell density for halocarbon studies	63
3.4	Experiment 3: Effects of algal growth cycle on halocarbon emission	64
3.4.1	Experimental design	64
3.4.2	Analysis for halocarbons	66
3.4.3	Calibration of halocarbon standards	68
3.4.4	Detection limit and precision of the system	68
3.4.5	Cell biomass determination	69
3.5	Experiment 4: Effects of varying irradiances on halocarbon emission	70

3.5.1	Experimental set-up.....	70
3.5.2	Analysis and calibration of halocarbons	71
3.5.3	Cell biomass determination	71
3.5.4	Determination of photosynthetic parameter, F_v/F_m	71
3.6	Statistical Analysis.....	72
CHAPTER 4: RESULTS.....		73
4.1	Experiment 1: Optimization for halocarbon studies.....	73
4.1.1	Growth curves of microalgae in different culture media.....	73
4.1.2	Basic growth profile of the selected microalgae	75
4.1.3	Selection of suitable air-tight incubation hours.....	78
4.2	Experiment 2: Emission of halocarbons at different cell densities.....	79
4.3	Experiment 3: Halocarbon emission at different life-cycle stage.....	82
4.3.1	Growth curves of microalgae	82
4.3.2	Photosynthetic performance as an indication of cells' health state.....	85
4.3.3	Emission of halocarbons	87
4.3.4	Emission rates of halocarbons	91
4.3.4.1	Normalization to chlorophyll-a	91
4.3.4.2	Normalization to cell density	93
4.3.5	Comparison of emission rates of halocarbons by growth phases.....	95
4.3.6	Emission rate as a whole in percentage	98
4.3.7	Correlation of detected halocarbons	99
4.3.8	Axenicity of cultures	100
4.4	Experiment 4: Effects of different irradiances on halocarbon emission.....	100
4.4.1	Growth response and pH changes	100
4.4.2	Changes of F_v/F_m as algal cell stress indicator	104
4.4.3	Comparison of halocarbon emissions amongst microalgae	106

4.4.3.1	Normalization to chlorophyll-a	106
4.4.3.2	Normalization to cell density	108
4.4.4	Comparison between irradiance and F_v/F_m amongst microalgae	110
4.4.5	Correlation of halocarbon emission rates	112
4.4.6	Pairwise comparisons between halocarbon emission rates and irradiances amongst microalgae	113
4.4.6.1	Normalization to chlorophyll-a	113
4.4.6.2	Normalization to cell density	120
4.4.7	Correlation between F_v/F_m and halocarbon emission rates at different irradiances amongst microalgae	126
CHAPTER 5: DISCUSSION		128
5.1	Emission rates amongst the three tropical microalgae	128
5.1.1	Effect of different growth phases	128
5.2	Comparison of emission rates	131
5.2.1	Tropical marine phytoplankton and seaweeds	131
5.2.2	Previous related-studies from polar and temperate regions	132
5.3	Emission rates amongst the five detected compounds	134
5.4	Effect of irradiance and photosynthetic performance on halocarbon emission by selected microalgae	135
5.5	Proposed areas for future research	142
CHAPTER 6: CONCLUSIONS.....		144
References		147
List of Publications and Papers Presented		159
Appendix		160

LIST OF FIGURES

Figure 3.1: <i>Parachlorella</i> sp. UMACC 245 under (a) FESEM using High vacuum mode (60 000x magnification) and (b) light microscope.....	58
Figure 3.2: <i>Synechococcus</i> sp. UMACC 371 under (a) FESEM using High vacuum mode (30 000x magnification) and (b) light microscope.....	59
Figure 3.3: <i>Amphora</i> sp. UMACC 370 under (a) FESEM using High vacuum mode (23 000x to 100 000x magnification) and (b) light microscope.....	60
Figure 3.4: Flow chart of research work	61
Figure 3.5: Two-syringe collection system.....	66
Figure 3.6: Gas-Chromatography Mass-Spectrometry (left) and Purge-&-Trap System (right).....	67
Figure 4.1: Growth curves based on Optical Density (OD _{620nm}) of three tropical marine microalgae, (a) <i>Parachlorella</i> sp. UMACC 245, (b) <i>Synechococcus</i> sp. UMACC 371 and (c) <i>Amphora</i> sp. UMACC 370 under different growth media over a period of 12 days. n = 3	74
Figure 4.2: Growth curves of three tropical marine microalgae over a growth period of 14 days determined by chlorophyll-a. n = 3.....	75
Figure 4.3: Growth curves of three tropical marine microalgae over a growth period of 14 days determined by cell density. n = 3	76
Figure 4.4: Growth curve of three tropical marine microalgae over a growth period of 14 days determined by Optical Density (OD _{620nm}). n = 3	76
Figure 4.5: Carotenoids of three tropical microalgae over a growth period of 14 days ..	77
Figure 4.6: Maximum quantum yield, F_v/F_m of three tropical marine microalgae over a growth period of 14 days. n = 3	77
Figure 4.7: pH of three tropical marine microalgae over a growth period of 14 days. n = 3.....	78
Figure 4.8: Growth curves based on chlorophyll-a. Cell growth phases of three tropical marine microalgae, (a) <i>Synechococcus</i> sp. UMACC 371; (b) <i>Parachlorella</i> sp. UMACC 245; (c) <i>Amphora</i> sp. UMACC 370 based on real-time biomass, chlorophyll-a (mg L ⁻¹) over 12 days of culture period. n = 3	83

Figure 4.9 (a-c): Growth curves based on cell density. Cell growth phases of three tropical marine microalgae, (a) <i>Synechococcus</i> sp. UMACC 371; (b) <i>Parachlorella</i> sp. UMACC 245; (c) <i>Amphora</i> sp. UMACC 370 based on real-time biomass, cell number (cell mL ⁻¹) over 12 days of culture period. n = 3.	84
Figure 4.10: Maximal quantum efficiency, F_v/F_m . The mean of F_v/F_m for (a) <i>Synechococcus</i> sp. UMACC 371; (b) <i>Parachlorella</i> sp. UMACC 245; (c) <i>Amphora</i> sp. UMACC 370 before and after incubation over 12-day culture period. n = 3	86
Figure 4.11: Changes of concentration of halocarbons detected from the three microalgae and Prov50 medium (controls) over a growth period of 12 days for compound (a) CHBr ₃ , (b) CH ₃ I, (c) CHCl ₃ , (d) CHBr ₂ Cl, and (e) CH ₂ Br ₂ . n = 3	87
Figure 4.12: Emission of short-lived halocarbons. Concentration of halocarbon emitted by the three tropical marine microalgae across 12 experimental days for compound (a) CHBr ₃ , (b) CH ₃ I, (c) CHCl ₃ , (d) CHBr ₂ Cl and (e) CH ₂ Br ₂ . Bar charts which contain different alphabets denote significant difference at ($p < 0.05$). n = 3	89
Figure 4.13: Emission rate normalized to chlorophyll-a. Concentration of compound (a) CHBr ₃ , (b) CH ₃ I, (c) CHCl ₃ , (d) CHBr ₂ Cl and (e) CH ₂ Br ₂ normalized to real-time chlorophyll-a for the three tropical microalgae across 12 experimental days. Bar charts which contain different alphabets denote significant difference at ($p < 0.05$). n = 3	91
Figure 4.14: Emission rate normalized to cell density. Concentration of compound (a) CHBr ₃ , (b) CH ₃ I, (c) CHCl ₃ , (d) CHBr ₂ Cl and (e) CH ₂ Br ₂ normalized to cell number for the three tropical microalgae across 12 experimental days. Bar charts which contain different alphabets denote significant difference at ($p < 0.05$). n = 3	93
Figure 4.15: Total emission rate in percentage. Total rate of emission (%) of every five halocarbons in comparison amongst the three tropical marine microalgae based on (a) cell number and (b) chlorophyll-a.....	98
Figure 4.16: Changes (%) in chlorophyll-a before and after 12-hour of light-exposure of the three microalgae under three different irradiance levels.....	101
Figure 4.17: Changes (%) in cell density before and after 12-hour light-exposure of the three microalgae under three different irradiance levels.....	101
Figure 4.18: Changes (%) in dry weight before and after 12-hour light-exposure of the three microalgae under three different irradiance levels.....	102
Figure 4.19: Changes (%) in OD _{620nm} before and after 12-hour light-exposure of the three microalgae under different irradiance levels.....	102
Figure 4.20: Changes (%) in carotenoids before and after 12-hour light-exposure of the three microalgae under different irradiance levels.....	103

Figure 4.21: Changes of pH before (dashed lines) and after (solid lines) 12-hour light-exposure of the three microalgae under three different irradiance levels. n = 3	104
Figure 4.22: Changes of maximum quantum yield, F_v/F_m , before (dashed lines) and after (solid lines) 12-hour light-exposure under three different irradiance levels for the three microalgae. n = 3	105
Figure 4.23: Percent changes of the five halocarbon emission rates normalized to chlorophyll-a by <i>Synechococcus</i> sp. UMACC 371 under three different irradiances levels, 0, 40, 120 $\mu\text{mol photons m}^{-2} \text{s}^{-1}$	107
Figure 4.24: Percent changes of the five halocarbon emission rates normalized to chlorophyll-a by <i>Parachlorella</i> sp. UMACC 245 under three different irradiance levels, 0, 40, 120 $\mu\text{mol photons m}^{-2} \text{s}^{-1}$	107
Figure 4.25: Percent changes of the five halocarbon emission rates normalized to chlorophyll-a by <i>Amphora</i> sp. UMACC 370 under three different irradiance levels, 0, 40, 120 $\mu\text{mol photons m}^{-2} \text{s}^{-1}$	108
Figure 4.26: Percent changes of the five halocarbon emission rates normalized to cell density by <i>Synechococcus</i> sp. UMACC 371 under three different irradiance levels, 0, 40, 120 $\mu\text{mol photons m}^{-2} \text{s}^{-1}$	109
Figure 4.27: Percent changes of the five halocarbon emission rates normalized to cell density by <i>Parachlorella</i> sp. UMACC 245 under three different irradiance levels, 0, 40, 120 $\mu\text{mol photons m}^{-2} \text{s}^{-1}$	109
Figure 4.28: Percent changes of the five halocarbon emission rates normalized to cell density by <i>Amphora</i> sp. UMACC 370 under three different irradiance levels, 0, 40, 120 $\mu\text{mol photons m}^{-2} \text{s}^{-1}$	110
Figure 4.29: Changes of maximum quantum yield, F_v/F_m , across three different irradiance levels (0, 40, 120 $\mu\text{mol photons m}^{-2} \text{s}^{-1}$) by the three microalgae. n =9.....	111
Figure 4.30: Changes of CHBr_3 emission rates normalized to chlorophyll-a from the microalgae under three irradiance levels (0, 40, 120 $\mu\text{mol photons m}^{-2} \text{s}^{-1}$). n= 27	115
Figure 4.31: Changes of CH_3I emission rates normalized to chlorophyll-a from microalgae under three irradiance levels (0, 40, 120 $\mu\text{mol photons m}^{-2} \text{s}^{-1}$). n= 27	116
Figure 4.32: Changes of CHCl_3 emission rates normalized to chlorophyll-a from microalgae under three irradiance levels (0, 40, 120 $\mu\text{mol photons m}^{-2} \text{s}^{-1}$). n= 27	117
Figure 4.33: Changes of CH_2Br_2 emission rates normalized to chlorophyll-a from microalgae under three irradiance levels (0, 40, 120 $\mu\text{mol photons m}^{-2} \text{s}^{-1}$). n= 27	118

Figure 4.34: Changes of CHBr_2Cl emission rates normalized to chlorophyll-a from microalgae under three irradiance levels (0, 40, 120 $\mu\text{mol photons m}^{-2} \text{s}^{-1}$). n= 27 119

Figure 4.35: Changes of CHBr_3 emission rates normalized to cell density from microalgae under three irradiance levels (0, 40, 120 $\mu\text{mol photons m}^{-2} \text{s}^{-1}$). n= 27 121

Figure 4.36: Changes of CH_3I emission rates normalized to cell density from microalgae under three irradiance levels (0, 40, 120 $\mu\text{mol photons m}^{-2} \text{s}^{-1}$). n= 27 122

Figure 4.37: Changes of CHCl_3 emission rates normalized to cell density from microalgae under three irradiance levels (0, 40, 120 $\mu\text{mol photons m}^{-2} \text{s}^{-1}$). n= 27 123

Figure 4.38: Changes of CH_2Br_2 emission rates normalized to cell density from microalgae under three irradiance levels (0, 40, 120 $\mu\text{mol photons m}^{-2} \text{s}^{-1}$). n= 27 124

Figure 4.39: Changes of CHBr_2Cl emission rates normalized to cell density from microalgae under three irradiance levels (0, 40, 120 $\mu\text{mol photons m}^{-2} \text{s}^{-1}$). n= 27 125

Figure 5.1: Dry weight (DW) of three tropical microalgae over a growth period of 12 days 132

LIST OF TABLES

Table 2.1: Types of halocarbon emitted by cultures of marine phytoplankton isolated from different climatic zones	38
Table 3.1: Summary of halocarbons extracted by purge-and-trap and analyzed using GC-MSD and associated quantifying ion, retention time, detection limit and precision	69
Table 4.1: Specific growth rate, μ (day^{-1}) of three tropical marine microalgae based on exponential phase under different growth media. $n = 3$	75
Table 4.2: Comparison of F_v/F_m across 8 hours of air-tight incubation for <i>Parachlorella</i> sp. UMACC 245, <i>Synechococcus</i> sp. UMACC 371 and <i>Amphora</i> sp. UMACC 370	79
Table 4.3: Emission of five halocarbons emitted by cultures of different $\text{OD}_{620\text{nm}}$. Concentration (pmol L^{-1}) of halocarbons emitted by three microalgae of different cell densities ($\text{OD}_{620\text{nm}}$)*. a) <i>Synechococcus</i> UMACC 371; b) <i>Amphora</i> UMACC 370; c) <i>Parachlorella</i> UMACC 245. $n = 3$. Different letters denote standard deviation (SD) homogenous group ($p < 0.05$) according to post-hoc Tukey's test.....	81
Table 4.4: Algal growth stages determined by chlorophyll-a and cell density. Selected range and representative points of exponential and stationary phases for the three tropical marine microalgae are shown.....	85
Table 4.5: Specific growth rate. The mean of specific growth rate (μ) of the three tropical marine microalgae based on their exponential growth phase of chlorophyll-a and cell number. $n = 3$	85
Table 4.6: Emission rate at different growth phases. Concentrations of five halocarbons normalized to chlorophyll-a ($\text{pmol mg chl-a}^{-1} \text{ day}^{-1}$) and cell number ($\text{pmol } (10^9 \text{ cell})^{-1} \text{ day}^{-1}$) at exponential and stationary phase for (a) <i>Synechococcus</i> sp. UMACC 371, (b) <i>Parachlorella</i> sp. UMACC 245 and (c) <i>Amphora</i> sp. UMACC 370.....	95
Table 4.7: Correlation of the halocarbons. Pearson Product-Moment correlation coefficient (r) of the emission rate from the five detected compounds in term of (a) chlorophyll-a, (b) cell number, (c) chlorophyll-a and cell number.....	99
Table 4.8: Mean $F_v/F_m \pm \text{S.D.}$ values of the microalgae measured under different irradiance levels. Data was statistically analyzed using Factorial ANOVA Data presented are mean values of F_v/F_m from a total of 36 replicates ($n = 36$). Different letters denote standard deviation (S.D.) homogenous group ($p < 0.01$) according to post hoc Tukey's test.....	105
Table 4.9: Pairwise comparisons of the F_v/F_m at different irradiance levels (0, 40, 120 $\mu\text{mol photons m}^{-2} \text{ s}^{-1}$) amongst the three microalgae. $n = 27$	111
Table 4.10: Correlation of the halocarbons. Pearson Product-Moment correlation coefficient (r) of the emission rate from the five detected compounds in term of (a) chlorophyll-a, (b) cell density, (c) chlorophyll-a and cell number produced by the three microalgae with irradiance.....	112

Table 4.11: Pairwise comparisons of CHBr ₃ normalized to chlorophyll-a at different irradiances (0, 40, 120 $\mu\text{mol photons m}^{-2} \text{s}^{-1}$) amongst the three microalgae. n = 27 ...	115
Table 4.12: Pairwise comparisons of CH ₃ I normalized to chlorophyll-a at different irradiances (0, 40, 120 $\mu\text{mol photons m}^{-2} \text{s}^{-1}$) amongst the three microalgae. n = 27 ...	116
Table 4.13: Pairwise comparisons of CHCl ₃ normalized to chlorophyll-a at different irradiances (0, 40, 120 $\mu\text{mol photons m}^{-2} \text{s}^{-1}$) amongst the three microalgae. n = 27 ..	117
Table 4.14: Pairwise comparisons of CH ₂ Br ₂ normalized to chlorophyll-a at different irradiances (0, 40, 120 $\mu\text{mol photons m}^{-2} \text{s}^{-1}$) amongst the three microalgae. n = 27 ...	118
Table 4.15: Pairwise comparisons of CHBr ₂ Cl normalized to chlorophyll-a at different irradiances (0, 40, 120 $\mu\text{mol photons m}^{-2} \text{s}^{-1}$) amongst the three microalgae. n = 27 ...	119
Table 4.16: Pairwise comparisons of CHBr ₃ normalized to cell density at different irradiances (0, 40, 120 $\mu\text{mol photons m}^{-2} \text{s}^{-1}$) amongst the three microalgae. n = 27 ...	122
Table 4.17: Pairwise comparisons of CH ₃ I normalized to cell density at different irradiance (0, 40, 120 $\mu\text{mol photons m}^{-2} \text{s}^{-1}$) amongst the three microalgae. n = 27.....	123
Table 4.18: Pairwise comparisons of CHCl ₃ normalized to cell density at different irradiances (0, 40, 120 $\mu\text{mol photons m}^{-2} \text{s}^{-1}$) amongst the three microalgae. n = 27 ...	124
Table 4.19: Pairwise comparisons of CH ₂ Br ₂ normalized to cell density at different irradiances (0, 40, 120 $\mu\text{mol photons m}^{-2} \text{s}^{-1}$) amongst the three microalgae. n = 27 ...	125
Table 4.20: Pairwise comparisons of CHBr ₂ Cl normalized to cell density at different irradiances (0, 40, 120 $\mu\text{mol photons m}^{-2} \text{s}^{-1}$) amongst the three microalgae. n = 27 ...	126
Table 4.21: Pearson correlation coefficient (<i>r</i>) between net changes of maximum quantum yields (F_v/F_m) of the microalgae and their halocarbon emission rates normalized to chlorophyll-a	127
Table 4.22: Pearson correlation coefficient (<i>r</i>) between net changes of maximum quantum yields (F_v/F_m) of the microalgae and their halocarbon emission rates normalized to cell density.	127
Table 5.1: Comparison of emission rate between tropical macroalgae and marine microalgae for CHBr ₃ , CH ₃ I, CH ₂ Br ₂ and CHBr ₂ Cl under dry-weight normalization.	131
Table 5.2: Total mass of emitted halides. Total halogen mass emitted as halocarbons and percentage contribution to the total from bromine, chlorine and iodine. Taxa are arranged in decreasing total mass halogens emitted order	134
Table 5.3: Total mass of emitted halides. Total halogen mass emitted as halocarbons and percentage contribution to the total from bromine, chlorine and iodine. Taxa are arranged in decreasing total mass halogens emitted order	141

LIST OF SYMBOLS AND ABBREVIATIONS

%	: Percentage
<	: Less than
>	: More than
°C	: Degree Celcius
ANOVA	: Analysis of Variance
C _a	: Chlorophyll-a
CAROL	: Algal Collection at The University of North Carolina at Chapel Hill
CCMP	: Culture Collection Marine Phytoplankton
CH ₃ *	: Radical methane ion
CFC	: Chlorofluorocarbon
Chl-a	: Chlorophyll-a
ClONO ₂	: Chlorine Nitrate
cell mL ⁻¹	: cell per millimeter
DW	: Dry Weight
ENSO	: El Nino-Southern Oscillation
ETR _{max}	: Maximum Electron Transport Rate
F ₀	: Minimum fluorescence
F _m	: Maximum fluorescence
F _v /F _m	: Maximum Quantum Yield
FESEM	: Field Emission Scanning Microscope
GC	: Gas Chromatography
GCMS	: Gas Chromatography-Mass Spectrometer
GHG	: Greenhouse Gas

Gg Br yr ⁻¹	: Gigagram Bromine per year
Gg I yr ⁻¹	: Gigagram Iodine per year
g L ⁻¹	: gram per Litre
H ₂ O ₂	: Hydrogen Peroxide
HCl	: Hydrochloric Acid
I*	: Radical iodine
IO	: Iodine Oxide
μ	: Micro
μg Chl-a ⁻¹ h ⁻¹	: Microgram per Chlorophyll a per hour
μmol photon m ⁻² s ⁻¹	: Micromole photon per square metre per second
mmol Br y ⁻¹	: millimole Bromine per year
Mmol yr ⁻¹	: Megamole per year
mg m ⁻³	: milligram per volume
<i>m/z</i>	: Quantifying Ion
MSD	: Mass Spectrometry Detector
ng min ⁻¹ m ⁻²	: nanogram per minute per square metre
nm	: nanometre
NO _x	: Nitrogen Oxide
NPQ	: Non-Photochemical Quenching
NS	: Non-Significant
O ₂	: Oxygen molecule
O ₃	: Ozone molecule
OBIS	: Ocean Biogeographic Information System
OFN	: Oxygen Free Nitrogen
<i>p</i>	: Pearson Correlation Coefficient
PAM	: Pulse Amplitude Modulation

pM	: picoMolar
pmol g DW ⁻¹ h ⁻¹	: picomole gram per Dry Weight per hour
pmol L ⁻¹	: picomole per Litre
pmol mol ⁻¹	: picomole per mole
pptv	: part per trillion volume
PSC	: Polar Stratospheric Cloud
PSII	: Photosystem II
Prov50	: Provasali 50 culture medium
<i>r</i>	: Regression
<i>r</i> ²	: Coefficient of Detemination
rpm	: round per minute
SAM	: S- adenosyl-L-methionine
S.D.	: Standard Deviation
Sig.	: Significance
sp.	: species
SPSS	: Statistical Package for the Social Sciences
Std.	: Standard
UMACC	: University of Malaya Algae Culture Collection
UTEX	: The Culture Collection of Algae at The University of Texas at Austin
<i>uv</i>	: Ultraviolet Radiation
V _a	: Volume of acetone
V _c	: Volume of culture
VOC	: Volatile Organic Compound
X ⁻	: Halide

LIST OF APPENDICES

Appendix A: Phylogenetic tree of <i>Amphora</i> sp. UMACC 370.....	160
Appendix B: Calibration curves of the five compounds.....	161
Appendix C: Composition of three growth media	165
Appendix D: Chromatogram sample generated from the Gas Chromatography - Mass Spectrometry (GCMS) equipped with Purge-and-Trap system.....	167

University of Malaya

CHAPTER 1: INTRODUCTION

1.1 Background

The group of halogenated compounds known as halocarbons, have received less attention for their contributions to climate change than other greenhouse gases such as carbon dioxide, methane and nitrous oxide. Once in the atmosphere, halocarbons give rise to bromine, chlorine and iodine radicals that can cause the catalytic destruction of ozone, resulting in increased penetration of harmful UV radiation to the Earth's surface (Frederick, 2015). Most of the long-lived halogenated compounds are derived from man-made (anthropogenic) chemicals and are notoriously responsible for the drastic loss of stratospheric ozone. Apart from the contribution of anthropogenic activities, scientists are looking further into natural activities that might result in the release of volatile organic compounds, in order to minimize the uncertainties in the estimation of global halocarbon budget. Marine biogenic sources such as phytoplankton (microalgae) are one of the top contributors of the shorter-lived compounds to the atmosphere as they are widely distributed throughout the euphotic zone of all of the Earth's aquatic environments (Moore, 2003). Recent successes in using algae as feedstocks for biofuel, industrial biomaterials and biopharmaceuticals that have initiated large-scale mass cultivation of the phytoplankton may enhance the release of halocarbons quantitatively. A number of short-lived halocarbon compounds released from oceanic sources such as from the marine phytoplankton of polar and temperate regions as well as seaweeds (macroalgae) had been reported following the discovery of increased levels of iodomethane, CH_3I over kelp beds (Keng *et al.*, 2013). Recent studies suggested the possibility of these biogenic short-lived halocarbons contributing and adding to the stratospheric halogen load.

Though literature on halocarbon emissions by the polar and temperate phytoplankton is available, reports from the tropics are relatively unknown. The transport of short-lived halocarbons to the tropical tropopause is very rapid. This fast ascent of the halocarbons

is linked to the occurrence of deep convection that is prevalent in the tropics due to a combination of high insolation and high humidity. This in turn may be modulated by the incidence of El Niño-Southern Oscillation (ENSO) events such as through effects on monsoon dynamics. (Bergman *et al.*, 2012; Navarro *et al.*, 2015; Hossaini *et al.*, 2015). In their analysis of global warming trends, Mora *et al.* (2013) reported that in the next 10 years, and before big temperature, ice-melting shifts are seen in the Arctic, the tropics will suffer “unprecedented” climate change effects.

1.2 Problem Statement

The negative effects of climate change events such as global warming affect the emission (rate) of volatile organohalogen (halocarbons) by marine microalgae. The halocarbons, in turn, can increase the earth’s temperature through depletion of the ozone. Hence, it is crucial that some work in the tropical region be done to better understand the local atmospheric chemistry and its contribution to the global scenario.

1.3 Research Questions

- (i) What are the main halogenated compounds emitted by tropical marine microalgae?
- (ii) How do different physiological growth phases of the tropical marine microalgae affect the emission of halocarbons?
- (iii) How does irradiance affect the emission of halocarbons?

1.4 Objectives

The overall objective of this research project is to investigate and understand short-lived halocarbon emission by tropical marine microalgae. The sub-objectives undertaking this research are:

- (1) To identify the main halocarbons emitted by tropical marine microalgae

- (2) To profile the halocarbons during the growth cycle of selected microalgal cultures
- (3) To study the effect of irradiance and photosynthetic performance on halocarbon emission by selected tropical marine microalgae in the laboratory

1.5 Thesis outline

This thesis is divided into six chapters described briefly as follows:

- (i) Chapter 1 introduces the background of this study and addresses the associated problems and research questions with appropriate objectives.
- (ii) Chapter 2 defines relevant terms, describe research scopes and previous works by referring to the literature.
- (iii) Chapter 3 provides the experimental design and methodology from the beginning of microalgal culturing to finding out the emission of halocarbons.
- (iv) Chapter 4 presents the experimental results in proper format and validates the model of study.
- (v) Chapter 5 discusses the results in comparison with relevant literature accordingly.
- (vi) Chapter 6 gives an overview of the research presented and concludes the findings and their contribution.

CHAPTER 2: LITERATURE REVIEW

2.1 Halocarbons

2.1.1 Halocarbon chemistry

Halocarbons, also commonly known as halogenated compounds or organohalogens, are molecules that comprise of carbon atoms covalently bonded to one or more halogens such as chlorine (Cl), bromine (Br), iodine (I) and Fluorine (F) in the presence or absence of hydrogen (McMurray, 2008). Halocarbons can be toxic and volatile, and are generally unreactive (Sneader, 2005). Bromo- and iodo-carbons are considered more reactive than chlorocarbons and even more so than fluorocarbons, due to the higher stability of the corresponding halide anions and the stronger single-bonded strength of the latter (McMurray, 2008). Halocarbons can be classified into long-lived and short-lived.

2.1.2 Long-lived halocarbons

Long-lived halocarbons are halogenated compounds with atmospheric lifetimes longer than six months (WMO, 2014). They contribute to the halogen load in the inner atmosphere layer, the stratosphere. This has to do on the account of the fact that long-lived halocarbons are not significantly degraded in the troposphere during their transport to the stratosphere since they exist longer than the time needed to move to the stratosphere (WMO, 2014).

Long-lived anthropogenic halocarbons are involved in affecting the atmospheric chemistry. They include, but not limited to, the chlorofluorocarbons (CFCs), hydrochlorofluorocarbons (HCFCs), chloromethane (CH_3Cl), tetrachloromethane (CCl_4) and many other halons (WMO, 2014). Some CFCs compounds such as CFC-11, CFC-12 and CFC-113 have very long lifetimes ranging from 45 years to 100 years (WMO, 2014). Long-lived anthropogenic compounds are predominantly made up of chlorine atoms and they were found to be responsible for the major stratospheric ozone loss (UNEP, 2010).

Volcanic eruptions also release some of the long-lived halocarbons like CCl_4 and CH_3Cl , but the contribution to the halogen loads, overall, is negligible since the chlorines are easily dissolved in water and washed out of the atmosphere in rain (Jordan, 2003).

2.1.3 Short-lived halocarbons

Short-lived halocarbons, also commonly referred as trace gases, are halogenated compounds with atmospheric lifetimes of six months or less (Laube *et al.*, 2008). These trace gases can also be classified into very short-lived halocarbons, depending on their specific range of atmospheric lifetimes. They play a part in contributing and adding free halogen radicals to the troposphere and stratosphere, even though long-lived halocarbons are more notoriously known as the main long-term culprit of halogen radical contributors (Laube, 2008).

Examples of chlorinated short-lived compounds include trichloromethane (CHCl_3), dichloromethane (CH_2Cl_2), tetrachloroethylene (C_2Cl_4) and many more. All chlorinated compounds can be either from anthropogenic or natural sources. For instance, CHCl_3 can be produced naturally by seaweeds as well as marine microalgae (Colomb *et al.*, 2008; Nightingale *et al.*, 1995). C_2Cl_4 , an excellent solvent widely used as spot remover and for dry cleaning, are synthetically produced (WMO, 2014).

Brominated short-lived halocarbons include tribromomethane (CHBr_3), dibromomethane (CH_2Br_2) and bromomethane (CH_3Br). Most of the anthropogenic sources of CH_3Br are from the agricultural use during soil fumigation. The remaining anthropogenic sources are from biomass burning, leaded petroleum, industry and structural fumigation (WMO, 2011). The biological production of CH_3Br by marine phytoplankton (microalgae) was reported (Sæmundsdottir & Matrai, 1998). Terrestrial vegetation, seaweeds and marine microalgae were found to be some of the natural sources of CHBr_3 and CH_2Br_2 (Moore *et al.*, 1996; Carpenter *et al.*, 2000). The oceanic emission

of CHBr_3 had been estimated to be 430-1400 Gg Br yr^{-1} , and CH_2Br_2 57-280 Gg Br yr^{-1} (WMO, 2014).

Short-lived organoiodines such as iodomethane (CH_3I), diiodomethane (CH_2I_2), chloriodomethane (CH_2ClI), bromiodomethane (CHBr_2I) and iodoethane ($\text{C}_2\text{H}_5\text{I}$) were some of the widely studied marine-produced volatile iodinated organohalogens. These compounds have received attention in connection to the chemistry of iodine in the atmosphere (Moore, 2003). About 214 Gg I yr^{-1} of iodocarbons were produced by microbial activity in rice paddies and by the burning of biological materials (Bell & Hsu, 2002). These volatile iodomethanes are broken up in the atmosphere as part of the global iodine cycle (Bell & Hsu, 2002).

CH_3I is thought to be the most abundant and has been of particular interest by which iodine plays a role in new particle formation in the atmosphere (Carpenter *et al.*, 2000; Manley & Dastoor, 1987). Most of the iodinated short-lived compounds are released through natural processes, especially from the ocean (WMO, 2014). Macroalgae and microalgae are some of the natural sources that contribute to iodine load in the atmosphere. Anthropogenic sources of iodinated compounds such as CH_3I may also be found from the production of biomass burning and fumigation (UNEP, 2010; Mead *et al.*, 2008)

2.1.4 Environmental role of halocarbons

Synthesized halocarbons have been emitted in robust quantities into the environment for the past few decades while halocarbons from the natural sources in the ecosystems have long been emitted for millions of years, contributing to the halogen fluxes in the atmosphere (Gribble, 1998). C_2Cl_4 , one of the chlorocarbons, was amongst the first synthesized halogenated compounds discovered by Michael Faraday in the early nineteenth century (Faraday, 1821; Clowes, 2014). It was not until the early twentieth

century where many halogenated compounds were created and used for industrial purposes. Ever since the first synthesis of fluorocarbon in the laboratory by Frederic Swarts and later on improved synthesis process of the fluorocarbon by Thomas Midgely, CFCs were broadly used for air-conditioning gases, as aerosol propellants and many more (Sneader, 2005; Thompson, 1932; Swarts, 1908).

Halocarbons, especially the brominated and chlorinated, are known to cause ozone layer depletion. (Forster & Joshi, 2005). A single chlorine atom in the stratosphere can destroy many ozone molecules through a catalytic cycle when ultraviolet radiation is present. Bromine can efficiently destroy up to 40-100 times in destroying ozone molecules than chlorine in the stratosphere (Penkett *et al.*, 1995). In the stratosphere, the halogen radicals produced from halogenated source gases react with ozone molecules in the presence of ultraviolet radiation, ultimately resulting in the loss of ozone layer. These halocarbons may be produced by both natural and anthropogenic processes, such as biogenic pathways at the land and ocean surface of the Earth and industrial releases, respectively (WMO, 2014). The halocarbon released are transported to the stratosphere through vertical transport, e.g. deep convective forces (Aschmann *et al.*, 2009).

Halocarbons are also known to involve in the absorption of infrared radiation from the Earth's surface (WMO, 2014). Halocarbon such as CFCs can exert up to 6000 times of Global Warming Potential (GWP) than other greenhouse gases like carbon dioxide (CO₂), making it much more efficient in absorbing the radiation, and also emit the radiation back to the Earth's surface, resulting higher global temperature on Earth's surface and lower part of the atmosphere (IPCC, 2007).

Iodinated compounds, on the other hand, are not directly involved in the depletion of stratospheric ozone. The number of iodine atoms that reach the stratosphere is greatly reduced due to rapid tropospheric loss (WMO, 2014). However, the release of iodine,

mainly through photolysis in the atmosphere, may be involved in the cyclic catalytic destruction of ozone. These iodine form iodine oxides (IO/OIO) rapidly with ozone, influencing the tropospheric oxidizing capacity (McFiggans *et al.*, 2000) and greenhouse gas processing. This, in turn, would affect the halo-chemistry composition in the stratosphere and create unseen reactions that may enhance the depletion of ozone layer.

2.2 Climate change

2.2.1 Causes and effects of modern climate change

Global warming, refers to the rise in average temperatures of the Earth's surface that is primarily due to the anthropogenic use of fossil fuels, resulting in climate change (Day *et al.*, 2011). Global warming will not only result in higher temperature but also accelerated sea-level rise, changes in rainfall and even in the frequency and intensity of tropical storms (Day *et al.*, 2011). Since the beginning of pre-industrial era, human influences have been the dominant detectable influence on climate change (Houghton *et al.*, 2001). Climate change will interact with other human impacts to produce environmental effects greater than with climate change alone and ultimately leave unwanted impacts on the ecosystem (Day *et al.*, 2011). In other words, living organisms on land and in oceans will inevitably be adversely affected by the climate change impacts. Reasonable assumptions have also been made to suggest that climate change will affect the distribution and deposition of the ozone concentration in the atmospheric boundary layer (Kinney, 2008; Jacob & Winner, 2009; Watson *et al.*, 2016).

Anthropogenic halocarbons such as CFCs are not only notorious for its ability to destroy the stratospheric ozone, but also well-known for its contribution to global warming as the dominating and effective greenhouse gases (GHGs) (Mactavish & Buckle, 2013; Ramanathan & Feng, 2009). GHGs are atmospheric gases that have the ability to absorb and emit radiation within the thermal infrared range on Earth, causing

what is known as the “greenhouse effect”. Some of the major GHGs include anthropogenic carbon dioxide (CO₂), methane and CFCs from human activities, and water vapors from the nature (Kiehl & Trenberth, 1997). Therefore, these anthropogenic halocarbons contribute more to temperature rise on Earth than the CO₂ (Velders *et al.*, 2007).

The sun radiates a net of 240 Watts/m² of energy in the form of ultraviolet (UV) (Scheff & Frierson, 2014), visible and near Infrared Range (IR) to the surface of the Earth after passing through the atmosphere and about half of the solar radiation is absorbed by the Earth’s surface, warming up the Earth. Some of the solar radiation is reflected back to the atmosphere at 103 Watts/m² (Godish *et al.*, 2015). Some of the infrared radiation would pass through the atmosphere and then out into space at 240 Watt/m² while the rest of the IR is converted into heat energy and is absorbed and re-emitted back onto the Earth by GHGs (Godish *et al.*, 2015). Therefore, when there is an accumulation of GHGs molecules in the atmosphere, more heat will be trapped and thus warming up the Earth. In other words, the accumulating abundance of long-lived anthropogenic halocarbon like CFCs in the atmosphere does contribute to the global warming.

The emission of anthropogenic long-lived halocarbons is rampant. Measures and precautions were taken by many international communities to reduce the adverse effects of ozone depletion and global warming contributed by associated halocarbons. The progress to ozone recovery is slowly gaining its momentum towards achieving optimal balance of atmospheric chemistry on Earth because the issues of halocarbon emission by anthropogenic sources were addressed and tackled.

Nonetheless, the sources from natural environments, which have been significantly contributing and adding to the existing halogen load in the stratospheric atmosphere, also play a big role in depleting the ozone layer. Because natural sources of halocarbon emitted

from biomass burning and volcanic activities were insignificant and discounted (Deshler *et al.*, 1996; WMO, 2014), scientists had switched their attention to other main halocarbon contributors, such as seaweeds and marine phytoplankton.

2.2.2 Ozone

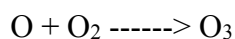
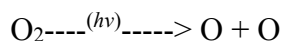
2.2.2.1 Importance of ozone

The ozone layer is the earth's primary shield against the harmful ultraviolet radiation (UNEP, 2010). The ozone layer protects all life on Earth by absorbing 97% to 99% of the solar ultraviolet radiation ($h\nu$), which, if not would undoubtedly damage exposed life forms on Earth's surface. This essentially leads to undesirable conditions such as skin cancer and weakened immune systems; disrupts marine food web; and reduces crop yield (Nash & Newman, 2011).

2.2.2.2 Ozone production

The earth's atmosphere is categorized into several layers. The lowest level layer, the troposphere, extends from the Earth's surface up to about ten kilometers in altitude. The following layer, the stratosphere, continues upwards from ten kilometers to about fifty kilometers connecting to the mesosphere (Fahey & Hegglin, 2011). The ozone layer, discovered in 1913 by a French physicists Charles Fabry and Henri Buisson (Sivasakthivel *et al.*, 2011), is made of up to 90% ozone molecules (O_3) concentrating in the stratosphere (UNEP, 2010).

Stratospheric ozone is formed naturally by chemical reactions involving oxygen molecules (O_2) and sunlight. Solar ultraviolet radiation breaks apart one O_2 to produce two oxygen atoms ($2 O$). Each of these highly reactive atoms combines with an O_2 to produce tri-oxygen molecule (O_3), that is, the ozone (Fahey & Hegglin, 2011).



2.2.3 Effects of halocarbons on atmospheric chemistry

Stratospheric ozone depletion was raised in 1971 for the first time, with the concern that supersonic transport aircraft emission of nitrous oxide and water vapor would adversely affect the ozone levels (Poppoff *et al.*, 1978). Later in 1974, Mario Molina, along with his professor, F. Sherwood Rowland, developed the CFCs ozone depletion theory and discovered that the chlorine atoms, produced by the decomposition of CFCs, can catalytically destroy ozone (Molina & Rowland, 1974). It was concluded that CFCs would not break down on Earth's surface or in the troposphere. Instead, CFCs would rise into the stratosphere and remain for several years. From there, intense *uv* radiation would break their bonds, releasing highly reactive chlorine atoms that quickly and repeatedly react with ozone (UNEP, 2010).



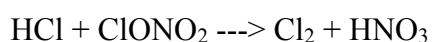
The net reaction, $\text{O} + \text{O}_3 \rightarrow \text{O}_2 + \text{O}_2$

Each chlorine can destroy as many as up to 100,000 molecules before it become inactivated and returned to the troposphere in the form of HCl (Moore & Stanitski, 2014).

In the late 1980s, a massive “hole” in the ozone over Antarctic was discovered. Satellite data showed that the hole, in terms of percentage of O_3 depletion, had been deepening and enlarging every year since 1977 (Hill, 2010). There has been an extreme depletion since 1987 where the area of the hole has widened to the point where it is larger

than the Antarctic continent. The hole tended to worsen progressively in terms of how long it lasts to the Antarctic spring (Sparling, 2001).

The culprit of such ozone hole over the Antarctic lies in the conditions of Antarctic winter and spring that are conducive to O₃ destruction. During winter, the Antarctic stratosphere is denitrified (Toon & Turco, 1991); essentially NO_x compounds and water vapors present in the dry air are frozen due to the extreme cold and isolation created from polar vortex, forming what is referred as the “polar stratospheric clouds (PSC) (Chipperfield, 2015). The frozen compounds, which are not present in gaseous form, are therefore not available to react with and tie up chlorine. On top of that, reactions that free Cl from relatively stable reservoirs (HCl or ClONO₂) take place faster on surfaces, as provided by PSC’s, than they do in gaseous environment (Chipperfield, 2015).



When Spring starts to kick in with the first return of direct sunlight, the freed form of Cl, as well as the Cl₂, are photolyzed and photo-associated into atomic Cl, giving them the freedom to react rapidly and repeatedly with O₃. The NO_x compounds still remain frozen that hence cannot act to form reservoirs such as ClONO₂ thanks to the extreme cold temperature in the early of Spring due to the vortex (NASA, 2009).

Other organohalogens like Bromine (Br), also take part in similar reactions like the chlorine. In fact, bromine atoms, even at lower concentrations, are 50 times more efficient than Cl at attacking O₃ in the chlorine-rich stratosphere (Berg *et al.*, 1983; Penkitt *et al.*, 1995). Br may be responsible for the 20% Antarctic ozone depletion, with 5-10% of the total depletion due to this particular halocarbon, bromomethane (CH₃Br), alone.

The Arctic also experiences ozone depletions, but not as much as those over the Antarctic; losses of ozone over the Arctic has been around 5-10% range while with 50-66% range over Antarctic (Solomon, 1999). This is mainly due to the fact that: 1) the polar vortex over the Arctic during winter is not as intense as that over the Antarctic, 2) there is a shorter time for the critical overlap between cold and first direct sunlight as the Arctic stratosphere warms faster in Spring than that over the Antarctic, and 3) the Arctic doesn't denitrify as completely as the Antarctic stratosphere does (Mohanakuma, 2008; NOAA, 2010).

The issue of O₃ destruction from natural resources like volcanic eruption was raised back in the 1950s, but enough evidence showed that the losses of O₃ and volcanic activities are not correlated (Deshler *et al.*, 1996). Much of the HCl produced by the volcanoes does not make it to the stratosphere and is quickly washed out through the major Cl removal mechanism from the stratosphere (Deshler, 1996). In fact, there was a significant loss of O₃ back in the 1980s but there was no major volcanic activities (WMO, 2007).

Destruction of ozone in the stratosphere also happens via the cyclic chemical reaction (WMO, 2014). The cyclic chemical reaction involves natural occurring species like halogen radicals, nitrogen oxide radicals and hydrogen radicals. Small changes in radical concentrations will cause serious implications on the O₃ as they get regenerated through the ozone-destructing catalytic cycles (Fahey & Hegglin, 2011).

2.3 Introduction to marine microalgae

2.3.1 What are microalgae?

Phytoplankton comprise the microalgae are microscopic plant-like unicellular organisms capable of efficient photosynthesis and biomass production (Tebbani *et al.*, 2014). They comprise a diverse group of prokaryotic and eukaryotic photosynthetic

microorganisms that grow in both freshwater and marine habitats as well as on soil or as epiphytes. (Li *et al.*, 2008). In a balanced ecosystem, microalgae, serving as the primary producers, play an essential role in marine food chains. They serve as food for a wide range of marine species (Helbling & Villafane, 2001).

2.3.2 Distribution and abundance of microalgae

It has been estimated that about 200,000 to 800,000 of microalgae exist; 5000 out of all these are known species of marine microalgae (Hallegraeff, 2003). The distribution and abundance of microalgae species are controlled by abiotic as well as biotic factors in both space and time. Changes in the microbial community can often be difficult to quantify against a background of high temporal and spatial variability. Nonetheless, evidence indicates that increased precipitation and glacial melt from warmer surface ocean temperatures due to global warming reportedly favors dominance of cryptophytes over diatoms in Antarctic coastal waters (Moline & Prézelin 1996; Moline *et al.*, 2004).

Three most important classes of microalgae in terms of abundance include green algae (Chlorophyceae), the diatoms (Bacillariophyceae) and the golden algae (Chrysophyceae) (Carlsson *et al.*, 2007). Cyanophyceae, a special class of microalgae, which is often called blue-green algae, or Cyanobacteria, a phylum of bacteria capable of obtaining energy from sunlight. The blue-green algae are often referred to as Cyanobacteria because they have cell structure and composition similar to those of prokaryotic cells in that they lack cell nucleus and distinctive organelles of eukaryotes, and their structure and chemical composition of the cell wall are the same as those of gram-negative bacteria (Pisciotta *et al.*, 2010). On the other hand, they also possess pigments like of those in eukaryotic algae to carry out photosynthesis (Pisciotta *et al.*, 2010).

Microalgae are widely populated in many different aquatic environments, from freshwater to brackish and marine waters. (Arrigo *et al.*, 2012; Fisherman *et al.*, 2010; Boonyapiwat, 1997).

The north–south trend of decreased calcification of *Emiliana huxleyi* in the Southern Ocean over the past two decades since 1983/1984 indicates that *Emiliana huxleyi* populations are migrating polewards (Cubillos *et al.*, 2007) while the red tide dinoflagellate, *Noctiluca scintillans* are migrating southwards towards the Southern Ocean from Tasmania brought on by a warm-core eddy circulation (McLeod *et al.*, 2012). Species composition and abundance in Albatross Bay, Gulf of Carpentaria, northern Australia examined from 1986-1992 reflects a stable tropical microalgae community in waters without pulses of physical and chemical disturbances (Burford *et al.*, 1995) as there was no distinct species succession of diatoms. The diatoms were the dominating species at the inshore sites. The proportion of green flagellates increased at the offshore sites and the cyanobacterium genus *Trichodesmium* and the diatom genera *Chaetoceros*, *Rhizosolenia*, *Bacteriastrum* and *Thalassionema* dominated the phytoplankton (Burford *et al.*, 1995). Diatoms contribute around 20% of global primary productivity (Malviya *et al.*, 2016) and are predominantly distributed on the Northern Hemisphere (Hasle & Syvertsen, 1996; OBIS, 2015). However, Malviya *et al.* (2016) has shown that most diatom genera were seen in all oceanic provinces although their ribotype abundance patterns based on a molecular rarefaction analysis were highly variable. *Chaetoceros* (both subgenera), *Corethron* and *Fragilariopsis* were highly abundant in the Southern Ocean. *Attheya*, *Planktoniella*, and *Haslea* were seen primarily in the South Pacific Ocean and *Leptocylindrus* was found to be highly abundant in the Mediterranean Sea (Malviya *et al.*, 2016). Based on a significant positive relationship of chlorophyll-a and fucoxanthin pigments, diatoms are found more dominant in terms of numerical abundance than prymnesiophytes in the central eastern Arabian Sea (Roy, 2010). Strzepek & Harrison

(2004) suggested that diatoms, and most probably other eukaryotic algal taxa, might have adapted the ability to survive in different underwater light climate between oceanic and coastal waters, enabling them to decrease their iron requirements without compromising photosynthetic capacity. This facilitates the colonization of the open oceans by diatoms.

2.4 Marine biogenic sources of halocarbons

2.4.1 Halocarbon emissions by marine microalgae

The oceans have been recorded to be the main contributor of volatile organohalogens to the atmosphere, but the sources of organohalogens had been unknown except for macrophytic algae (seaweeds), which primarily are confined to the coastal zone (Moore, 2003).

Krysell (1991) reported that pelagic marine algae are a source of bromoform in the surface waters of the Arctic Ocean. Sturges *et al.* (1993) reported that Arctic ice microalgae emit significant quantities of bromoform that may be converted photochemically into active bromine forms. The active form of bromines, in return, is thought to be one of the main causes of the destruction of surface ozone in the Arctic environment during the spring. The estimates of the total annual bromoform release revealed that polar ice algae might actually contribute globally significant amount of organic bromine compounds, comparable with anthropogenic and macrophyte sources (Sturges *et al.*, 1993). This study was followed by investigations of halocarbon emissions by microalgae originating from different climatic zones from the poles to the tropics. A summary of all the studies on halocarbon emissions by marine microalgae isolated from polar, temperate and tropical zones is reported in Table 2.1 below.

Table 2.1: Types of halocarbon emitted by cultures of marine phytoplankton isolated from different climatic zones.

Taxa	Climate zones (incubation temperature)	Type of halocarbons emitted																Reference
		CH ₃ I	CHCl ₃	CHBr ₃	CHBr ₂ Cl	CH ₂ Br ₂	CH ₂ ClI	CH ₂ I ₂	C ₃ H ₄ Br ₂	CH ₃ Br	CH ₃ Cl	CH ₂ Cl ₂	C ₂ H ₃ Cl	C ₂ HCl ₃	C ₂ Cl ₄	C ₂ H ₂ Cl ₂	C ₂ H ₄ Cl ₂	
<i>Synechococcus</i> sp. UMACC 371	Tropical (25°C)																	Lim <i>et al.</i> (unpublished)
<i>Chlorella</i> sp. UMACC 245	Tropical (25°C)																	Lim <i>et al.</i> (unpublished)
<i>Amphora</i> sp. UMACC 370	Tropical (25°C)																	Lim <i>et al.</i> (unpublished)
<i>Mediopyxis helyxis</i>	Polar/ Temperate																	Thorenz <i>et al.</i> (2014)
<i>Porosira glacialis</i>	Polar/ Temperate																	Thorenz <i>et al.</i> (2014)
<i>Thalassiosira</i> sp.	Polar (2- 4 °C)																	Hughes <i>et al.</i> (2013)
<i>Prochlorococcus marinus</i> CCMP 2389	Temperate (22 °C)																	Hughes <i>et al.</i> (2011)
<i>Synechococcus</i> sp. CCMP 2370	Temperate (22 °C)																	Hughes <i>et al.</i> (2011)
<i>Prochlorococcus marinus</i> CCMP 1986	Temperate (20-21°C)																	Brownell <i>et al.</i> (2010)
<i>Synechococcus</i> sp. CCMP 2370	Temperate (20-21°C)																	Brownell <i>et al.</i> (2010)
<i>Calcidiscus leptoporus</i> AC365	Sub-tropical (20- 25 °C)																	Colomb <i>et al.</i> (2008)
<i>Emiliana huxleyi</i> CCMP 371	Sub-tropical (20- 25 °C)																	Colomb <i>et al.</i> (2008)
<i>Phaeodactylum tricornutum</i>	Sub-tropical (20- 25 °C)																	Colomb <i>et al.</i> (2008)
<i>Chaetoceros neogracilis</i> CCMP 1318	Sub-tropical (20- 25 °C)																	Colomb <i>et al.</i> (2008)
<i>Dunaliella tertiolecta</i>	Sub-tropical (20- 25 °C)																	Colomb <i>et al.</i> (2008)
<i>Emiliana huxleyi</i> CCMP 379	Temperate (15 °C)																	Hughes <i>et al.</i> (2006)

All studies on halocarbon emission are associated only with the marine microalgae. This is largely due to the presence of dissolved halogens in the ocean seawater or synthesized marine mediums such as the F/2 (Guillard & Ryther, 1962) and Prov 50 (CCMP 1996) that makes it possible for the microalgae to methylate and produce halocarbons. *Porosira glacialis*, a diatom, was reported to emit 1000 pmol L⁻¹, 1.0 nmol L⁻¹ and 2250 pM (equivalent to 2250 pmol L⁻¹) of CHBr₃ (Tokarczyk & Moore, 1994; Moore *et al.*, 1995; Moore *et al.*, 1996). Furthermore, there was evidence of CH₃I production by *Emiliana huxleyi*, a Chrysophyte, which was reported to emit CH₃I at 0.35 pmol L⁻¹ (Hughes *et al.*, 2006) and 1.8 pptv (Colomb *et al.*, 2008) contrary to Manley & de la Cuesta (1997), who did not observe CH₃I emission by *E. huxleyi*. Scarratt & Moore (1999) reported a 40 times faster CH₃I production by the red microalga *Porphyridium purpureum* than that found by Manley & de la Cuesta (1997) for *Porosira glacialis*. Colomb *et al.* (2008) reported that microalgae also emitted anthropogenic chlorinated organic compounds, namely chloroform (CH₃Cl), dichloromethane (CH₂Cl₂), trichloroethylene (C₂HCl₃), tetrachloroethylene (C₂Cl₄), chlorobenzene (C₆H₅Cl) and dichlorobenzene (C₆H₄Cl₂). *Phaeodactylum tricornutum*, a diatom was reported to emit 1750 pptv and 900 pM of CH₃Cl, by Colomb *et al.* (2008) and Tait & Moore (1995) respectively.

In the early studies of halocarbon emission directly from open-surface waters, there were difficulties in confirming if the elevated levels of bromoform and dibromomethane in Arctic ice cores from Resolute Bay, were contributed by organisms other than the phytoplankton, namely the zooplankton and bacteria (Moore & Tokarczyk, 1993), . This is also a concern in laboratory studies when non-axenic microalgal cultures were used. Manley & de la Cuesta (1997) reported that the associated bacteria in phytoplankton cultures (*Nitzschia* sp., *Navicula* sp., *P. glacialis* and *Phaeocytosis* sp.) did not contribute to the emission of methyl iodide. If the bacteria were the only or main producers of CH₃I,

there would be a continued increase in the amount of CH₃I during stationary phase of algal growth where only bacterial numbers continued to increase. In addition, if CH₃I was, in fact, produced by the bacteria, the rate of CH₃I production normalized to bacterial cells should have remained constant, and not dropped dramatically. This was confirmed by Tokarczyk & Moore (1994) and Moore *et al.* (1995).

Despite the report of weak CH₃I production by undefined microbial populations obtained from decaying kelp tissue (Manley & Dastoor, 1987), and marine bacteria are capable of producing CH₃I in the ocean (Amachi *et al.*, 2001), there has not been any direct evidence showing that marine bacteria are involved in other halocarbon production in either the ocean seawater or the laboratory.

Granfors *et al.* (2013) investigating the role of young Arctic sea ice in halocarbon cycling, reported that halocarbon levels were increased by microorganisms inhabiting the ice. Heterotrophic bacteria were evenly distributed in the ice and was probably more responsible for contributing the halocarbon than the microalgae that were found in the lower layers of the ice. CH₃I production by bacterial aggregates (Asare *et al.*, 2012) and production of CHBr₃, CH₃I, CH₂Br₂ and CHBr₂Cl by cyanobacteria (Karlsson *et al.*, 2008) had been previously reported. In the latter study, the halocarbons were measured during a cyanobacteria bloom in summer in the Baltic sea; with production rates up to 0.3 pmol [μg chl a]⁻¹ h⁻¹ at midday. Hughes *et al.* (2013) investigated the role of a diatom *Thalassiosira* isolated from the coastal waters of the western Antarctic Peninsula in CHBr₃ and CH₂Br₂ production. Production of CHBr₃ was observed to be linked with a primary metabolic process, while bacteria contributed to inhibition of the compound.

Abrahamsson *et al.* (2004) monitored halocarbon levels in 24 hr stations in the Atlantic part of the Southern Ocean and reported that bromochloromethane, tribromomethane, trichloroethene and diiodomethane were dominant. In an attempt to correlate the

compounds with pigments, their results showed that the haptophytes were identified to be linked to the iodinated compounds. Halocarbon levels were also found to peak twice in the diurnal cycle; once at midday when photosynthesis was most active and in the evening. This had been reported by Ekdahl *et al.* (1998) to be related to respiration in the dark period. The Arabian Sea is a very productive area in the Indian Ocean and a study on the halocarbon production by the marine microalgae showed that halocarbon production was strongly correlated to pigment (Roy, 2010). CHCl_3 , CH_2Br_2 , CHBr_3 and CCl_4 were the most abundant with CHCl_3 significantly correlated with fucoxanthin suggesting the importance of diatoms and prymnesiophytes in the Arabian Sea. Seasonality in halocarbon production was observed with higher production during the summer monsoon induced upwelling that resulted in higher microalgal productivity.

Smythe-Wright *et al.* (2006) reported that high CH_3I concentrations of up to 45 pmol L^{-1} near lower latitude (20°N to 60°N) of Atlantic and Indian oceans correlates well with the abundance of dominating species, *Prochlorococcus* sp.. Solely from this marine source, approximately 5.3×10^{11} g I yr^{-1} of global ocean flux of iodine was reported to contribute to the marine boundary layer, putting up a large fraction of the previously estimated total global flux of iodine (10^{11} - 10^{12} g I yr^{-1}) (O'Dowd *et al.*, 2002). Nonetheless, a laboratory-based study led by Brownell *et al.* (2010), through extrapolating the production of CH_3I by similar species, *Prochlorococcus Marinus* to a global scale, reported an average global production rate of CH_3I ; 0.6 Mmol yr^{-1} . This production rate that accounted for 0.03% of the global marine production, on the contrary, suggests that *Prochlorococcus* sp. is not a significant marine source of contributing CH_3I to the atmosphere.

A seasonal study of tropospheric volatile organic compounds (VOC) at the South Pole and selected Antarctic sites, revealed that while the longer lived species of anthropogenic origins (eg. alkyl nitrate) were more abundant in late winter, the compounds of oceanic origin like the bromoform and methyl iodide, were observed in early winter, after the summer peak in biological activity but before oceanic productivity decreased during winter months (Bayersdorf *et al.*, 2010). Bromoform levels correlated with alkyl nitrate, and may be influenced by similar factors linked to seasonality of marine emissions, sea ice extent; atmospheric removal via OH oxidation; and seasonal differences in transport efficiency of marine air masses.

2.4.2 Mechanisms behind the halocarbon emissions

Two pathways, in terms of monohalomethanes and polyhalomethanes, are involved in the production of halocarbons by phytoplankton.

(i) Monohalocamethane

Monohalogenated compounds are produced by a process of methylation of its corresponding halide ion (Manley, 2002). The direct way of forming monohalomethanes is through the transfer of a methyl group to a halide catalyzed by an enzyme. This mechanism requires a methyl donor, for instance, S-adenosyl-L-methionine (SAM) and a halide ion methyl transferase to transfer the methyl group over to the halide ion. Different types of methyl transferase show different kinetics and substrate specificities (Harper, 2000). Some enzymes are capable of catalyzing several halocarbons simultaneously (Itoh *et al.*, 1997). In general, in decreasing order of reactivity are iodide, bromide and chloride, consistent with their decreasing nucleophilicity (Wuosmaa & Hager, 1990).

Several studies of halomethane production from the methyl-transferase system were reported (Wuosmaa & Hager, 1990; Saini *et al.*, 1995; Hughes *et al.*, 2011). Hughes *et al.*, (2011) proposed that the production of methyl iodide (CH_3I) by *Prochlorococcus marinus* (CCMP 2389) could also be due to the iodination of inorganic iodine species, such as atomic iodine (I^*) and the breakdown of higher molecular weight organic iodine (Fenical, 1982) and by radicals (CH_3^*) or methyl group arising from photochemical reactions (Moore & Zafiriou, 1994). Hughes *et al.* (2011) found connections between the CH_3I production rate with cell stress, increased cell membrane permeability and cell lysis. It was suggested that the cells' response to limiting conditions enhanced the production of CH_3I or that the loss of membrane integrity increased the release of CH_3I precursors to the medium.

(ii) Polyhalomethanes

The formation of polygenated compounds involves enzymatic halogenation via haloperoxidase (Theiler *et al.*, 1978). The enzymatic biohalogenation process involved two steps. Firstly, the haloperoxidase enzyme catalyzes the oxygen-based oxidant co-substrate to react with X^- ($\text{X} = \text{Cl}, \text{Br}$ or I) to produce electrophilic halogen species like XO^- or R_2NX . Subsequently, the electrophilic halogen species attacks a carbonyl activated methyl group and substitute a hydrogen atom. The next H-atom substitution then leads to the formation of di- or trihalogenated methanes, and so on (Theiler, 1978; Kline *et al.*, 2000).

Haloperoxidase are characterized by their ability to oxidize halogen anions. For instance, chloroperoxidases can use chloride, bromide and iodide; bromoperoxidases can use bromide and iodide whilst iodoperoxidases can only use iodide (Moore *et al.*, 1996; Urhahn & Ballschmiter, 1998).

A study from Moore *et al.* (1996) reported the presence of bromoperoxidase in *Nitzschia* sp. (CCMP 580), with the ability to produce brominated compounds; CHBr_3 , CH_2Br_2 and iodinated compounds; CH_2I_2 and CH_2ClI . On the other hand, the presence of iodoperoxidase was reported, revealing the production of only the iodinated compounds.

Marine algae are a rich source of volatile halogenated metabolites, especially halomethanes that make algae contribute substantially to the global budget of such molecules. Nonetheless, it is often very challenging to address the physiological and ecological interactions for such metabolites that are ubiquitous in algae and their environment. This is especially true for marine phytoplankton where their overall concentrations in the water column might be relevant, and locally elevated amount of metabolites in the immediate vicinity of the producing cells (Paul & Pohnert, 2011). However, studies have indicated that the release of volatile halocarbons by marine phytoplankton has more to do with defence mechanism from herbivory predators (Bravo-Linares & Mudge, 2009; Paul & Pohnert, 2011). Due to the presence of halogen, the halogenated metabolites often have exceptionally high biological activities, not only can aid in chemical defense but also can act as antifouling agents for the producing algal cells (Pau & Pohnert, 2011).

2.4.3 Significance of tropical emission of biogenic halocarbons

The intense tropical convection in the tropics, especially that over the oceans, have been suggested as being responsible for the rapid transport of compounds into the stratosphere (Schauffer *et al.*, 1999; Levine *et al.*, 2007; Laube *et al.*, 2008; Fueglistaler *et al.*, 2009; Brinckmann *et al.*, 2012; Hossaini *et al.*, 2015). The recent years have seen a growing interest in the monitoring of atmospheric compounds, including the short-lived halocarbons in the western Pacific/Southeast Asian region, characterized by high primary productivity (Sherman & Hempel, 2009). The convection is strongest here especially

during the Northern Hemisphere winter, and can lift the surface oceanic emissions to the tropical tropopause layer which refers to the transition layer between the troposphere and stratosphere (Fueglistaler *et al.*, 2009; Robinson *et al.*, 2014). Measurements have been taken via whole-air sampling, short-term deployment of gas chromatograph devices and on-board measurements during research cruises. Robinson *et al.* (2014) was the first to report continuous measurement from instruments based in Sabah, Borneo.

The contribution of the coastal primary producers, the macroalgae or seaweeds, to the CHBr_3 and CH_2Br_2 emissions in the Southeast Asian region, was estimated by Leedham *et al.* (2013) to a range of 6-224 mmol Br yr^{-1} that was lower than that (180-350 mmol Br yr^{-1}) reported by Pyle *et al.* (2011a), although the definition of SEA was not similar. In extrapolating further to the global scenario, where tropical oceans are estimated to contribute 75% of global halocarbon budget, the very low values from Leedham *et al.* (2013) suggest that emissions from the open oceans (phytoplankton) may be more important than the coastal emissions. Mohd Nadzir *et al.* (2014) using data collected during a research cruise over the Straits of Malacca, the South China Sea and the Sulu-Sulawesi Sea in 2009, estimated a regional emission of 63 Gg yr^{-1} CHBr_3 for the Southeast Asian region. CHBr_3 was the most abundant bromocarbon, ranging from 5.2 pmol mol^{-1} in the Straits of Malacca to 0.94 pmol mol^{-1} over the open ocean. Robinson *et al.* (2014) reported the biogenic short-lived CHBr_3 , CH_2Br_2 and CHI_3 , from a 15-month survey from the rainforest (Danum) and coastal (Kunak) sites first reported by Pyle *et al.* (2011b). CHBr_3 and CH_2Br_2 concentrations did not show seasonal variations, but short-term variations were evident in the coastal site related to the marine sources including coastal seaweed and both coastal and oceanic phytoplankton. They also concluded that the Southeast Asian region may not be as strong a contributor of brominated short-lived halocarbons as previously reported.

Manley *et al.* (1992) made a comparison on the production rates of bromoform per unit per biomass of microalgae and macroalgae. They concluded that even though the phytoplankton releases were 10-100 times lower, these unicellular organisms had the potential to be a vital source of volatile halocarbons because they occupy an ocean area of about 200 times larger than that occupied by the macroalgae. Of the halocarbons identified from the algae, chloroethane (C_2H_5Cl), trichloroethane ($C_2H_3Cl_3$), dichloroethane ($C_2H_4Cl_2$) and tetrachloroethane (C_2Cl_4) normally associated with anthropogenic origins, have been reported for five cosmopolitan marine phytoplankton, *Calcidiscus leptoporus*, *Emiliana huxleyi*, *Phaeodactylum tricornutum*, *Chaetoceros neogracilis* and *Dunaliella tertiolecta* (Colomb *et al.*, 2008) but not in seaweeds. The two diatoms *P. tricornutum* and *Ch. neogracilis* were the strongest emitters of methyl bromide. The latter three species are mass cultivated for aquaculture feed and as a feedstock for biofuel production. Two diatoms, *Mediopyxis heylisia* and *Porosira glacialis* also released dibromopropane ($C_3H_6Br_2$) which has not been detected in seaweeds (Thorenz *et al.*, 2014). Although there has been more research conducted on the halocarbon emissions by seaweeds than phytoplankton, current available literature allows a preliminary estimation of type and range of halocarbons identified. In general, 39 compounds (10 iodinated, 7 brominated, 13 chlorinated and 9 mixed halocarbons) have been reported as being emitted by the clonal-cultured phytoplankton (18) and field-collected seaweeds (34), with 13 compounds in common; giving a Sørensen's Coefficient of Similarity of 0.50, suggesting that 50% of the detected halocarbon species present in seaweeds are also present in phytoplankton. As 0.5 in similarity also indicates 0.5 in dissimilarity, this suggests a potential emission of previously detected compounds by seaweeds to be seen in phytoplankton, and vice versa.

2.4.4 Factors affecting halocarbon emissions by microalgae

2.4.4.1 Varying environmental conditions

Studies reported on the production of halocarbons by microalgae by manipulating the environmental conditions in the laboratory. The parameters put to test include different light stress/ irradiance (Moore *et al.*, 1996; Scarratt & Moore, 1999; Hughes *et al.*, 2006), photosynthesis activity (Hughes *et al.*, 2006) and elevated ozone levels (Thorenz *et al.*, 2014). Most of the studies on halocarbon emission by phytoplankton are mainly associated with the factor of different growth stages (Moore *et al.*, 1994; Tokarczyk & Moore, 1994; Tait & Moore, 1995; Manley & de la Cuesta, 1997; Sæmundsdottir & Matrai, 1998; Scarratt & Moore, 1999).

(i) Growth phase

The amount of halocarbons emitted are largely measured in terms of which growth phase/stage the microalgae are in. The four growth stages in relation to halocarbon emission can be divided into lag phase, acceleration phase, stationary phase and death phase.

Tokarczyk & Moore (1994) reported a suit of halocarbons, namely CHBr_3 , CHBr_2Cl , CH_2Br_2 emitted at different amounts by *Porosira glacialis* and *Nitzschia sp.* (CCMP 580) at different growth phases under continuous cool white light with $12 \mu\text{mol m}^{-2} \text{s}^{-1}$ photosynthetic active radiation at 6°C . The purge and trap system and gas chromatography equipped with electron capture detector were used to analyze and detect the amount of halocarbon emitted. A maximum of 2260 pmol L^{-1} of CHBr_3 emitted by *Nitzschia sp.* (CCMP 580) was reported during its stationary phase (Day 17) at a cell density of $6 \times 10^5 \text{ cell mL}^{-1}$ while 990 pmol L^{-1} of CHBr_3 emitted by *Porosira glacialis* was reported at a cell density of about $100 \times 10^3 \text{ cell mL}^{-1}$ on the same day in stationary phase. An increase in emission rate of CHBr_3 in exponential growth phase from both

Nitzschia sp. (about 250- 2250 pmol L⁻¹) and *Porosira* culture (100- 800 pmol L⁻¹) was reported. The emission of CH₂Br₂ was also reported, reaching as high as 200 and 350 pmol L⁻¹ in *Nitzschia* sp. and *Porosira* cultures, respectively. Lower concentration of CH₂ClI, about 16 pmol L⁻¹, emitted by *Nitzschia* sp. at a cell density of 600 x10³ cell mL⁻¹ was also reported.

Sæmundsdottir and Matrai (1998) reported a high emission rate of methyl bromide (CH₃Br), 30.1 pg CH₃Br µg⁻¹ Chl-a day⁻¹ by *Phaeocystis* sp. (CCMP 628) starting in late exponential or stationary phase, when cultured under 63 µEinstein s⁻¹ m⁻², 12:12 h light: dark cycle at 22°C. Other species such as *Amphidium carterae*, *Chaetoceros diversum*, *Hemiselmis rufescens*, *Pycnococcus provasolii*, *Pavloca* sp., *Prorocentrum micans* and *Chaetoceros atlanticus* produced 1.7- 9.3 pg CH₃Br µg⁻¹ Chl-a day⁻¹.

Scarratt and Moore (1999) reported the emission of CHCl₃ and CH₃I by the red microalga, *Porphyridium purpureum*. Of all the chlorinated hydrocarbon compounds, including C₂HCl₃, C₂Cl₄, CH₂Cl₂ and CHCl₃, over 4 to 10 days culture, only CHCl₃ was detected, with an emission rate range from 3.9 to 7.8 x10⁻⁷ mol g Chl-a⁻¹ day⁻¹. CH₃I was emitted by the same species and detected with an emission rate ranging from 4.8 x10⁻⁷ to 1.2 x10⁻⁶ mol g Chl a⁻¹ day⁻¹.

A study by Hughes *et al.* (2011) reported that the changes in the emitted CH₃I concentrations are closely followed by increase in cell density in *Prochlorococcus marinus* (CCMP 2389). The amount of CH₃I emitted during the logarithmic phase (Day 1-5) is less than 100pmol L⁻¹. A maximum concentration of 690.5 pmol L⁻¹ of CH₃I was reached during mid- growth phase (Day 14). Manley & de la Cuesta (1997) reported a decrease in CH₃I production by *Nitzschia punctata* in the exponential phase where the number of cells in the culture peaked whilst an increase in the CH₃I (1.4 pmol of CH₃I) production occurred in the lag phase, but decreased to 8 pmol L⁻¹, after 16 days of growth.

In 2008, Colomb *et al.* screened several volatile organic compounds (VOCs) including CHCl_3 , CH_3Cl , CH_3Br and CHBr_3 , in *Emiliania huxleyi*, *Calcidiscus leptoporus*, *Phaeodactylum tricornutum*, *Chaetoceros neogracilis* and *Dunaliella tertiolecta* cultured under constant irradiance of $250 \mu\text{Einstein s}^{-1} \text{m}^{-2}$, temperatures from 20 to 25°C adapting to a 12:12 h light:dark cycle. The sampling of the VOCs emissions were done in the middle of the light cycle during 4 days for *Chaetoceros neogracilis* and *Emiliania huxleyi* and 3 days for the rest of the taxa. *Chaetoceros neogracilis* and *Phaeodactylum tricornutum* were reported to emit CH_3Br the most, with 0.007 and $0.002 \text{ pmol L}^{-1} / \text{Chl-a}$ of CHBr_3 . *Calcidiscus leptoporus* was reported to emit $0.0038 \text{ pmol L}^{-1} / \text{Chl-a}$ of CHBr_3 . *Emiliania huxleyi* and *Chaetoceros neogracilis* emitted $0.002 \text{ pmol L}^{-1} / \text{Chl-a}$ of CHBr_3 whereas *Dunaliella tertiolecta* and *Phaeodactylum tricornutum* emitted $0.0001 \text{ pmol L}^{-1} / \text{Chl-a}$ of CHBr_3 . *Calcidiscus leptoporus* was reported to emit approximately 1100 pptv of CHCl_3 while the rest reported to emit lower than 200 pptv. Colomb *et al.* (2008) also reported *Calcidiscus leptoporus* and *Chaetoceros neogracilis* to emit more than 2000 pptv of CH_3Cl , while *Phaeodactylum tricornutum* and *Dunaliella tertiolecta* reported to emit about 1750 pptv whereas *Emiliania huxleyi* was reported to emit about 500 pptv of CH_3Cl .

Study has shown that the rate of CH_3I production in a monospecific *Synechococcus* culture can vary by at least an order of magnitude depending on physiological state (Hughes *et al.*, 2011). One main factor that affects the emissions in different growth phases is the inoculation level. Morris *et al.* (2008) found that a high inoculation level ($>3.5 \times 10^5 \text{ cell mL}^{-1}$) allows consistent growth in an axenic *P. marinus* culture and below this cells fail to grow well. Failure to grow well leads to cell stress and this negatively affects the cell growth in different growth phases and the emission rate of halocarbons, specifically CH_3I , into the surrounding medium (Morris *et al.*, 2008). The emission of

other halogenated compounds such as brominated and chlorinated compounds, however, may not necessarily be dependent on the cell growth.

(ii) Irradiance

The Sun has the ability to emit as high as approximately $2000 \mu\text{mol m}^{-2} \text{s}^{-1}$ light radiating intensity to the Earth (Tibbitts, 1994). Nonetheless, the irradiance levels are subjected to fluctuation due to the constant changes in the weather. A few studies had put this factor to test to see if the changes of light intensity would influence the emission of halocarbons by the microalgae.

In 1996, Moore *et al.* reported a trend of higher concentrations of CH_2Br_2 and CHBr_2Cl produced in *Nitzschia* sp. (CCMP 580) and *Porosira glacialis* cultures with a higher level of illumination. In $40 \mu\text{mol quanta m}^{-2} \text{s}^{-1}$ as low light, CH_2Br_2 emitted by *Nitzschia* sp. ranged from 0- 200 picoMolar (pM) while in higher light, the range of CH_3Br_3 emitted increased from 0 to 1300 pM over a period of 30 days. Nevertheless, this tendency was contrary to what was found by Hughes *et al.* (2006) and Scarratt & Moore (1996; 1999). Hughes *et al.* 2006 reported $2.5\text{-}2.8 \text{ pmol L}^{-1}$ of CH_3I emission over a period of 25 hours in both low light ($47 \mu\text{mol m}^{-2} \text{s}^{-1}$) and high light ($250 \mu\text{mol m}^{-2} \text{s}^{-1}$) for *Tetraselmis* sp. The same can be seen for *Emiliania huxleyi* and *Thalassiosira pseudonana*, with CH_3I emission ranging $0.2\text{-}0.38 \text{ pmol L}^{-1}$ and $0.2\text{-}0.3 \text{ pmol L}^{-1}$, respectively. Methyl halide production by three phytoplankton species (*Phaeodactylum tricornutum*, *Phaeocystis* sp., *Thalassiosira weissflogii*) was found to be not directly dependent on photosynthesis, but was closely related to biomass (Scarrat & Moore, 1996). *Phaeocystis* had the highest methyl halide production rate, while total CH_3Cl and CH_3Br increased higher during stationary phase of growth. Carbon limitation on the medium increased the production of halocarbons more than nitrogen limitation. Scarratt & Moore (1999) revealed that exposing the cultures of *Porphyridium purpureum* to high light intensity ($800 \mu\text{mol}$

quanta $\text{m}^{-2} \text{s}^{-1}$) in excess of the acclimated irradiance level ($20 \mu\text{mol quanta m}^{-2} \text{s}^{-1}$) did not stimulate the production of the measured halocarbon compounds (CH_2Cl_2 , C_2HCl_3 , C_2Cl_4). In fact, the production of CH_3I dropped when exposed to high irradiance over a period of 24 hours. Scarratt & Moore's findings were supported by the work of Hughes *et al.* (2006) in a sense that light-induced stress does not induce the release of iodocarbon in any of the cultures examined.

(iii) Elevated ozone level

Thorenz *et al.* (2014) reported the only study of the influence of different elevated ozone level on the production of halocarbons by microalgae. To resemble the natural condition of the stratosphere, a glass chamber tube was continuously channelled with synthetic air flow at 3.4 L min^{-1} over stirred algae suspension with ozone (100 ppb) and without ozone, each done separately. It was found that the release of several tested halocarbons, CHBr_3 , CH_3I , CH_2ClI and CH_2I_2 , was not dependent on the high or low ozone level. This conclusion was made based on its insignificant differences in halocarbon emission rates, ranging $0.030\text{-}0.098 \text{ ng min}^{-1} \text{ m}^{-2}$ for CH_3I , $0.003\text{-}0.039 \text{ ng min}^{-1} \text{ m}^{-2}$ for CH_2ClI , $0.073\text{-}0.117 \text{ ng min}^{-1} \text{ m}^{-2}$ for CH_2I_2 and $0.503\text{-}0.549 \text{ ng min}^{-1} \text{ m}^{-2}$ for CHBr_3 for *Porosira glacialis*. *Mediopyxis helysia* emitted a range of $9.90\text{-}21.94 \text{ nmol L}^{-1}$ of iodide and $397\text{-}499 \text{ nmol L}^{-1}$ of iodate, while *P. glacialis* emitted a range of $7.32\text{-}19.71 \text{ ng min}^{-1} \text{ m}^{-2}$ of iodide and $408\text{-}478 \text{ ng min}^{-1} \text{ m}^{-2}$ of iodate.

2.4.4.2 Halocarbon emissions and photosynthesis

The photosynthetic performance based on fluorometry was used by Hughes *et al.* (2006) to measure the maximum quantum yield (F_v/F_m), which is an indicator of algal cell stress and the cell viability of the microalgae. Hughes *et al.* 2006 reported that under 14:10 h light:dark cycle at 15°C , there were no changes in the concentrations of CH_3I and CH_2ClI relative to the control in any of the *Emiliana huxleyi*, *Tetraselmis* sp. and

Thalassiosira pseudonana cultures, although the F_v/F_m in both control (low light at $47 \mu\text{mol photons m}^{-2} \text{ s}^{-1}$) and high light ($250 \mu\text{mol photons m}^{-2} \text{ s}^{-1}$) treatments changed. In both the high and low light conditions, *Emiliania huxleyi* was reported to emit a range of 0.25 to 0.35 pmol L^{-1} of CH_3I and approximately 2.5 to 4.5 pmol L^{-1} of CH_2ClI ; *Tetraselmis* sp. was reported to emit about 2.5 to 2.8 pmol L^{-1} of CH_3I and a range of 0.5 to 0.8 pmol L^{-1} of CH_2ClI ; *Thalassiosira pseudonana* was reported to emit a range of 0.2 to 0.3 pmol L^{-1} of CH_3I while no emission of CH_2ClI was detected in both light conditions. The finding of a decrease in the fluorescence-based F_v/F_m for PSII (Photosystem II) due to high light stress revealed the oxidative damage to the photosynthetic apparatus in the cells. They concluded that iodocarbon release is not associated with light stress and is not likely to be in any connection with the protection against oxidative damage in the microalgae studied.

In another by Hughes *et al.* (2011), it was found that despite the decrease in F_v/F_m over a period of 22 days (from early exponential phase onwards), an increase in CH_3I concentration was observed throughout the 22 days experiment under an irradiance of $40 \mu\text{Einstein m}^{-2} \text{ s}^{-1}$ with 14:10 h light:dark cycle at 22°C . During the increase of cell densities in exponential phase (from $4.0 \times 10^7 \text{ cells mL}^{-1}$ (Day 2) to $8.0 \times 10^7 \text{ cells mL}^{-1}$ (Day 7), *Prochlorococcus marinus* (CCMP 2389) showed a decrease in F_v/F_m of about 0.67 (Day 2) to 0.50 (Day 7) while an increase in CH_3I emission of approximately 20 pmol L^{-1} to 100 pmol L^{-1} in Day 2 and 7 respectively was reported. A decrease in F_v/F_m (0.5 to 0.3) on Day 7 (cell density at $8 \times 10^7 \text{ cell mL}^{-1}$) to 16 (cell density of about $0.5 \times 10^7 \text{ cell mL}^{-1}$) cultures showed an increase in the emission of CH_3I , from about 100 pmol L^{-1} to 450 pmol L^{-1} . *Synechococcus* sp. (CCMP 2370) was reported to emit about 2.0 to 4.0 pmol L^{-1} of CH_3I , which was close to the amount of CH_3I detected in the medium-only control.

CHAPTER 3: METHODOLOGY

3.1 Microalgal cultures

Three common tropical marine algal strains from the University of Malaya Algae Culture Collection (UMACC) were used for all experiments; the cyanophyte *Synechococcus* sp. UMACC 370 and the bacillariophyte *Amphora* sp. UMACC 370 were isolated from shrimp ponds connected to the Straits of Malacca in Kuala Selangor, Malaysia; while the chlorophyte *Parachlorella* sp. UMACC 245 was isolated from the east-coast waters facing the South China Sea in Terengganu, Malaysia. The strains represent three different classes of microalgae that are abundant in the local regions. Stock cultures were grown in Provasoli Medium (Prov50) (CCMP, 1996) under a 12h light:12h dark cycle and at a temperature of 25 ± 1 °C in an incubator shaker set at 100 rpm (PROTECH, model GC-1050). Silicate ($\text{Na}_2\text{SiO}_3 \cdot 9\text{H}_2\text{O}$) was supplemented at 0.01g dm^{-3} to the culture medium for *Amphora* sp. UMACC 370. The cultures were kept and maintained under axenic conditions using standard aseptic techniques; glassware and growth media were sterilized by autoclaving (15 min at 121°C) before use.

The isolated microalgae, *parachlorella* sp. UMACC 245, *synechococcus* sp. UMACC 371 and *amphora* sp. UMACC 370 as shown in respective Figures 3.1, 3.2 and 3.3 were imaged under Field Emission Scanning Microscope (FESEM) and light microscope for taxonomic identification. *Parachlorella* sp. UMACC 245 is unicellular, non-motile, coccoid, and has a size of about $3.5 - 4.0 \mu\text{m}$ in diameter. *Synechococcus* sp. UMACC 371 is unicellular, coccoid, non-motile and has a size of approximately $1.0 - 2.5 \mu\text{m}$ in diameter. *Amphora* sp. UMACC 370 is unicellular, non-flagellates and has a diameter size of about $10 - 11 \mu\text{m}$. Based on the morphology and phylogenetic tree (Appendix A), the isolated *Amphora* sp. UMACC 370 appears to be most closely related to *Amphora Subtropica*, given 100% bootstrap support based on rcbL gene. However, the differences in nucleotide composition between the two sequences of *Amphora* and that the sequence

of *Amphora* sp. UMACC 370's actual identity may not be deposited in Genbank indicates that the isolated *Amphora* sp. UMACC 370 may be a new species.

A flow chart of research work is provided as shown in Figure 3.4.

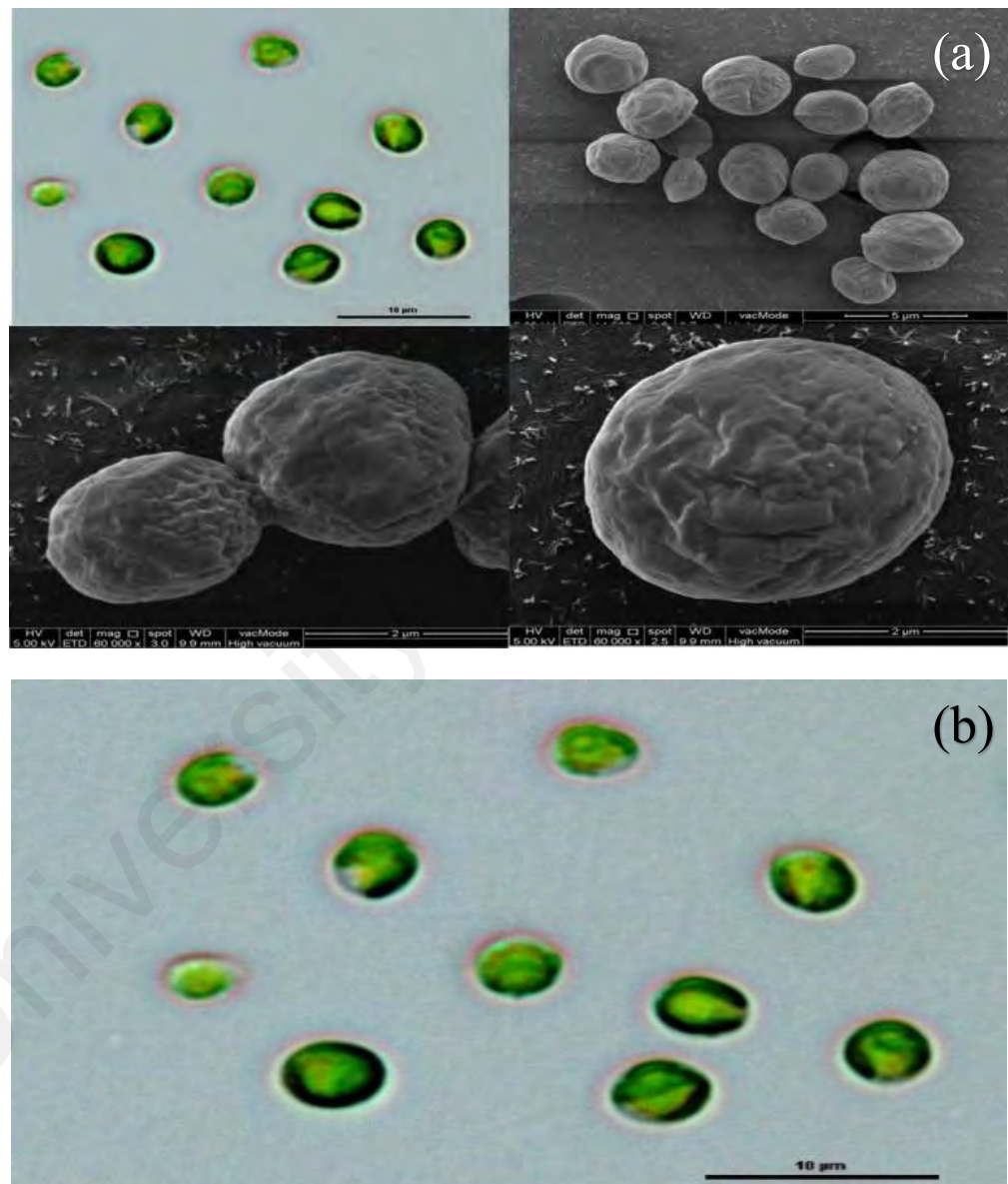


Figure 3.1: *Parachlorella* sp. UMACC 245 under (a) FESEM using High vacuum mode (60 000x magnification) and (b) light microscope.

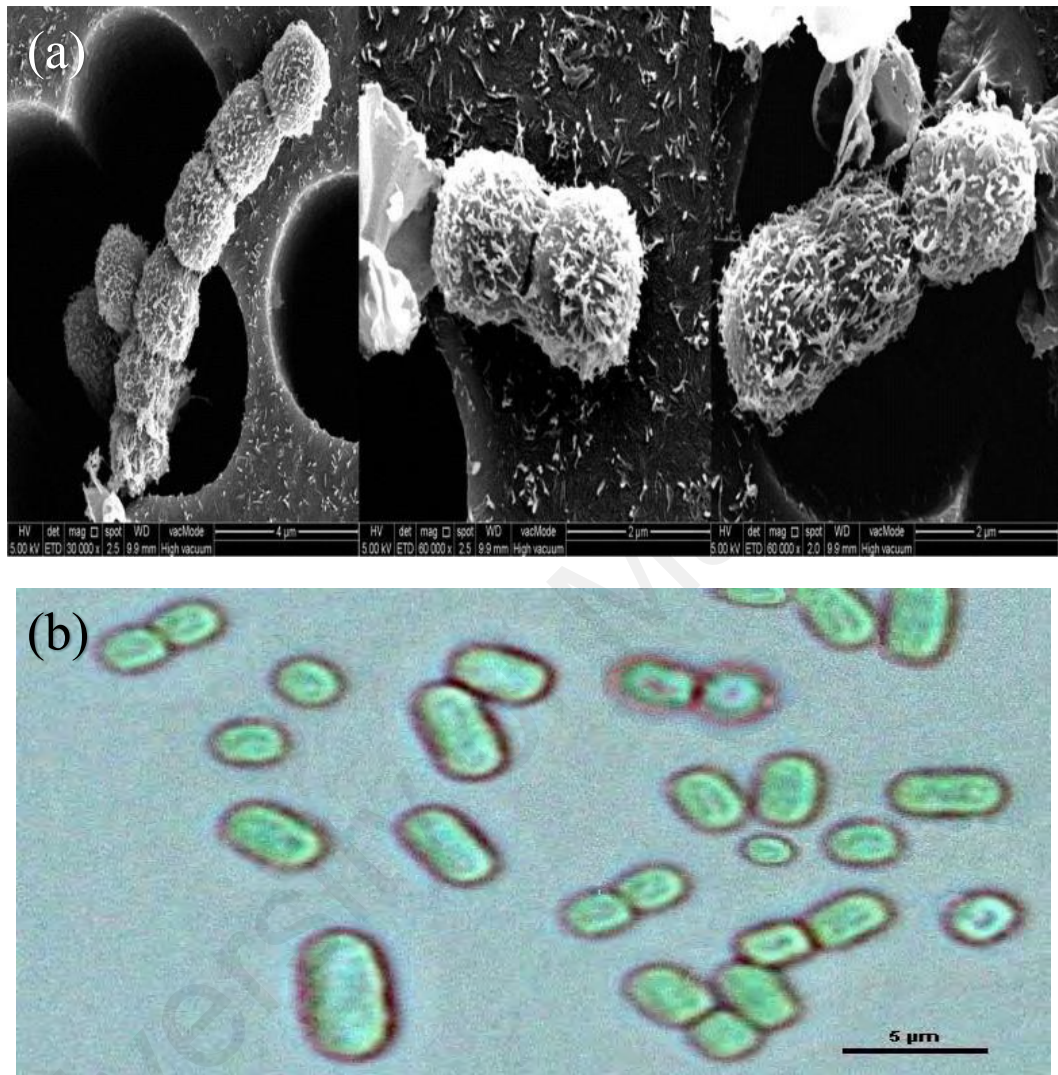


Figure 3.2: *Synechococcus* sp. UMACC 371 under (a) FESEM using High vacuum mode (30 000x magnification) and (b) light microscope.

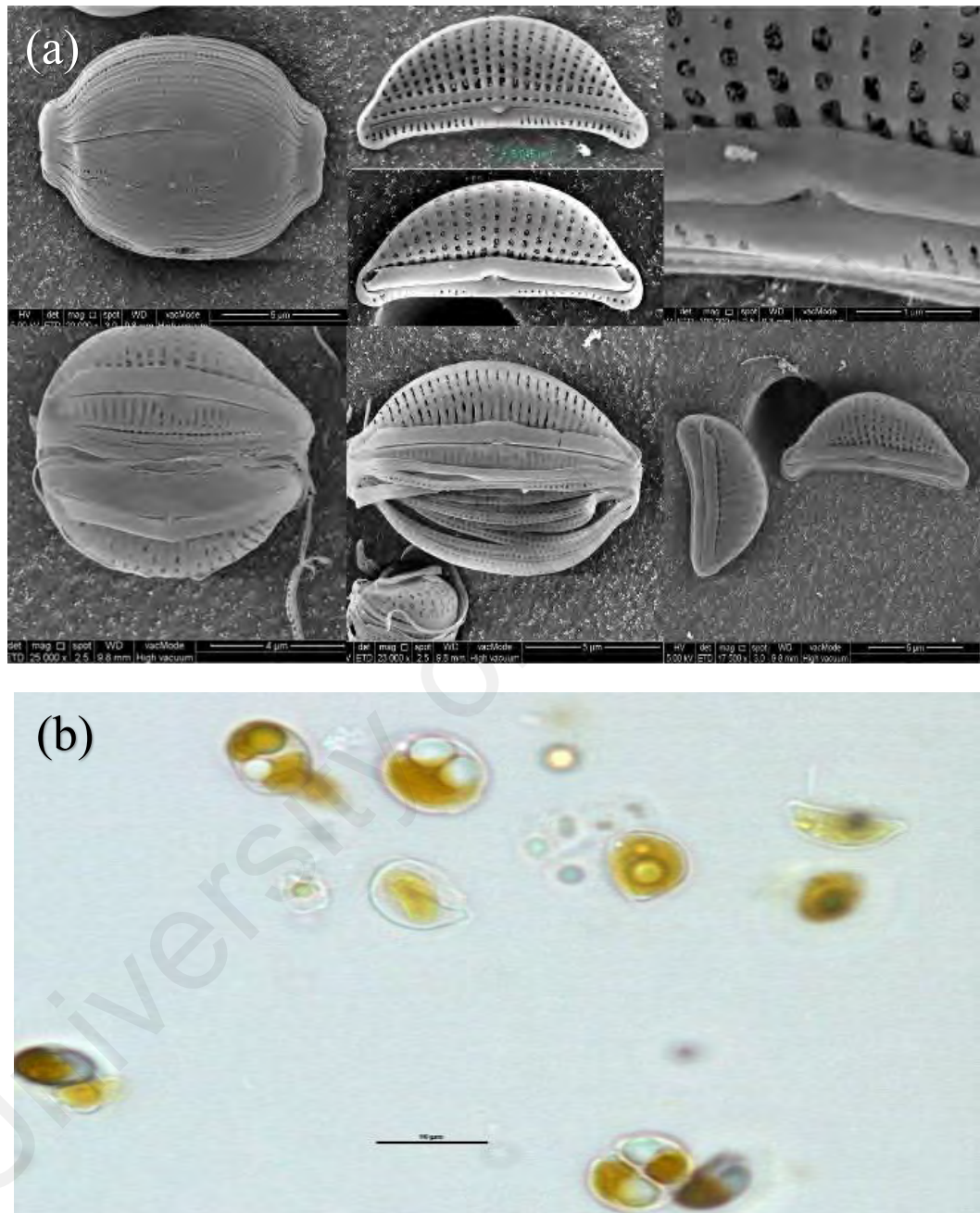
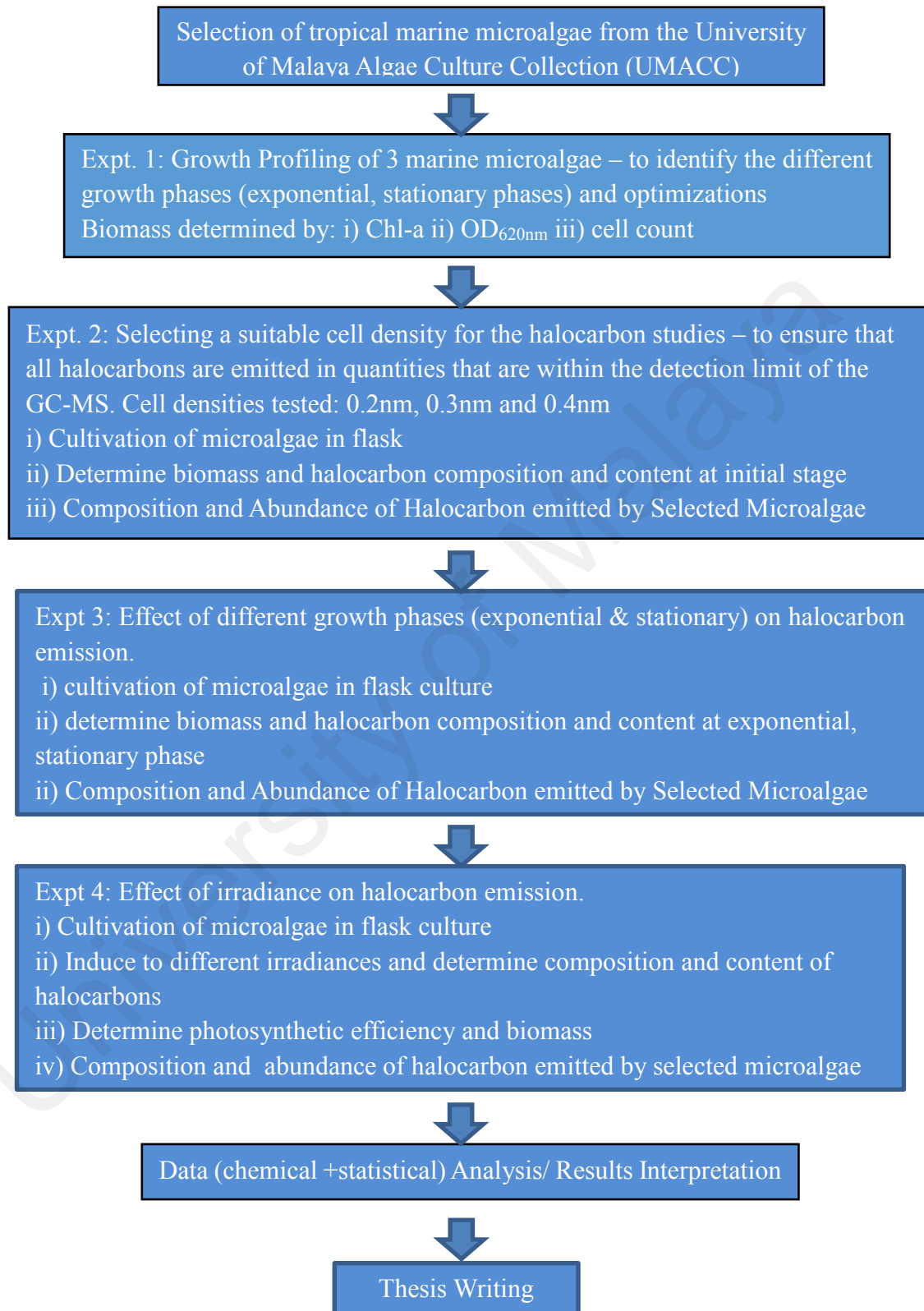


Figure 3.3: *Amphora* sp. UMACC 370 under (a) FESEM using High vacuum mode (23 000x to 100 000x magnification) and (b) light microscope.

Figure 3.4: Flow-chart of research work



3.2 Experiment 1: Optimization of selected parameters for studies

3.2.1 Selection of suitable growth media

The objective was to select the suitable culture medium for the isolated microalgae. Three different growth media, Provasoli 50 (CCMP, 1996), F/2 (Guillard & Ryther, 1962) and Diatom Medium (Beakes *et al.*, 1988), were used to determine the most suitable medium for the growth of the three microalgae. The Optical Density (OD_{620nm}) of the cultures of the three microalgae were grown at 0.2 with 10% inoculum of exponential phase for a period of 12 days. The cultures of total volume of 150 mL in 250 mL conical flasks were incubated in the incubator shaker (100 rpm) at 25°C with irradiance of 40 $\mu\text{mol photons m}^{-2} \text{ s}^{-1}$ on a 12h light:12h dark cycle. OD_{620nm} readings were taken on a daily basis. This was done in triplicates.

3.2.2 Profiling algal growth

The objective was to profile the basic growth of the microalgae under laboratory conditions. The three local microalgal strains were grown in batch cultures of 150 ml in 250 mL conical flask with starting inoculum of 10% at OD_{620nm} 0.2 in Prov50 (CCMP, 1996) medium, with silicate ($\text{Na}_2\text{SiO}_3 \cdot 9\text{H}_2\text{O}$) supplemented at 0.01g dm^{-3} to the culture medium for *Amphora* sp. UMACC 370, for a growth period of 14 days. The starting pH and salinity of the medium at the beginning of the experiment were set at 8 and 30 ppt, respectively. The cultures were grown under a 12h light:12h dark cycle and at 25 ± 1 °C in an incubator shaker (Model: GC-1050) under axenic conditions. Irradiance level in the growth chamber was maintained 40 ± 5 $\mu\text{mol photons m}^{-2} \text{ s}^{-1}$ for all the cultures.

The biomass of the cultures were determined every 2 days from the growth based on OD_{620nm}, chlorophyll-a (Vello et al., 2014; Strickland & Parsons, 1968) and cell count was done using Bright-field Neubauer haemocytometer (Marienfeld-Superior, Germany) under a light microscope (Vello *et al.*, 2014). Readings from other responding variables such as the carotenoids and pH were determined and specific growth rates (μ) were calculated. F_v/F_m , the maximum quantum yield, was also measured as an indication of cells's health state.

3.2.3 Determination of incubation time

The objective was to determine the air-tight incubation time based on cells' state of health (F_v/F_m) using PAM (Pulmonary Amplitude Modulation) Fluorometry (Hughes et al., 2011; Keng *et al.*, 2013). Cultures of the three microalgae were grown in triplicates for a total of eight hours, with F_v/F_m measured every hour. The value of the maximum quantum efficiency of photosystem II, denoted as F_v/F_m (where F_v is the variable fluorescence measured as the difference between maximum (F_m) and minimum (F_o) fluorescence in dark-adapted culture), was estimated using a Water PAM Fluorometer (Walz, Model: WATER-ED, S/N:EDEE0238 Germany). Samples from each culture were dark-adapted for 15 minutes prior to F_v/F_m determination.

3.3 Experiment 2: Determining suitable cell density for halocarbon studies

A short-term experiment to determine the suitable cell density in the cultures was conducted prior to the growth cycle experiment. The objective was to ensure that the cell density in the cultures during the growth cycle studies was sufficient to emit detectable levels of a suite of halocarbons by the GC-MS system used. The optical density at 620nm (OD_{620 nm}) of the cultures of the three microalgae were adjusted to 0.2, 0.3 and 0.4 for a growth period of four days, prior to measurement of the halocarbons. The cultures of total volume of 150 mL in 250 mL conical flasks were incubated in the incubator shaker (100

rpm) at 25°C with irradiance of 40 $\mu\text{mol photons m}^{-2} \text{s}^{-1}$ on a 12h light:12h dark cycle. The procedure for halocarbon determination is given below (Section 3.4.1).

3.4 Experiment 3: Effects of algal growth cycle on halocarbon emission

The objective of this experiment was to study how the emissions of halocarbons were affected by the difference in growth stages, specifically the exponential and stationary phase.

3.4.1 Experimental design

All three microalgal cultures were grown in batch culture with an inoculum size of 10% of a log phase culture, standardized at an optical density of 0.4 at 620nm ($\text{OD}_{620\text{nm}}$). The cultures of 150 mL total volume, were grown in 250 mL conical flasks in an incubator shaker (100 rpm) at 25°C with irradiance of 40 $\mu\text{mol photons m}^{-2} \text{s}^{-1}$ on a 12h light:12h dark cycle. The experiments with each microalga was conducted in triplicates, with measurements done every two days. The experiment was completed after 12 days of growth. A control with culture medium but no microalgal inoculum was set up in triplicate for each microalga.

Every two days, 60 mL of cultures were removed from each triplicate flask and centrifuged (3000 rpm for 10 min) and replenished with fresh medium, then drawn out into a 100 mL glass syringe to be incubated air-tight for 4 hours. Incubation time was set to 4 hours to achieve sufficient amount of halocarbons trapped in the medium while minimizing cell stress. The amount of concentration for each halocarbon was obtained by subtracting the concentration of the sample to the control. Samples were also collected at the same time for biomass estimation using various parameters as described below (Section 3.4.5). This was to allow calculation of the emission rate through normalization of real-time biomass to the concentration of each compound emitted by microalgae over the culture period.

Emission rates were calculated by normalizing emission of halocarbons to the real-time biomass, both chlorophyll-a ($\text{pmol mg}^{-1} \text{ day}^{-1}$) and cell density ($\text{pmol cell}^{-1} \text{ day}^{-1}$). The formula to determine emission rate for this study is as follows:

$$\text{Emission rate} = \frac{\text{Emission}}{\text{Biomass}} \div \left(\text{Incubation time} \times \frac{1 \text{ day}}{24 \text{ hour}} \right)$$

where,

Emission = the concentration of halocarbon emitted at pmol L^{-1}

Biomass = chlorophyll-a content (mg L^{-1}) or cell density (cell mL^{-1})

Incubation time = 4 hours

The state of the cells was determined using PAM Fluorometry (Hughes *et al.*, 2011; Keng *et al.*, 2013). The value of the maximum quantum efficiency of photosystem II, denoted as F_v/F_m (where F_v is the variable fluorescence measured as the difference between maximum (F_m) and minimum (F_o) fluorescence in dark-adapted culture), was estimated using a Water PAM (Pulmonary Amplitude Modulation) (Walz, Model: WATER-ED, S/N:EDDE0238 Germany) before and after the gas-tight incubation period to indicate the cells' health. Samples from each culture were dark-adapted for 15 minutes prior to F_v/F_m determination.

After 4 hours of incubation, the culture from the incubation syringes was gently swirled and extracted into 100 mL glass syringes through a two-syringe ($0.2 \mu\text{m}$ Merck filter unit) closed filter system to ensure no ingress of air into the syringe. Figure 3.4 shows the transfer of culture-filtered medium through an enclosed system.

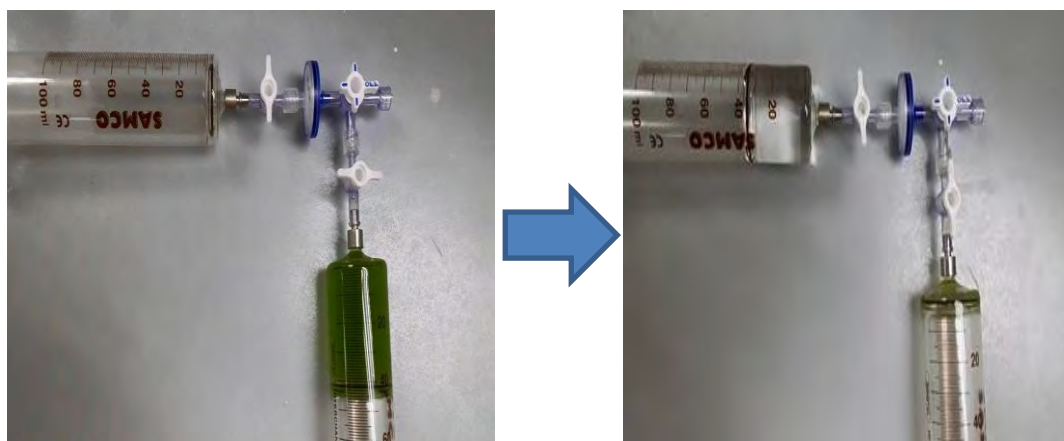


Figure 3.5: Two-syringe collection system

The medium subsample left in the syringe was then ready for halocarbon analysis. The experiments were repeated for all three marine tropical microalgae.

All cultures were kept and maintained under axenic conditions using standard aseptic techniques; glassware and growth media were sterilized by autoclaving (15 min at 121°C) before use. Lysogenic broth (LB) agar plate was used to test and ensure the axenicity of the inoculum cultures.

3.4.2 Analysis for halocarbons

All halocarbon analyses were carried out using a purge-and-trap system developed by the University of East Anglia (UEA), UK (Hughes *et al.*, 2006) equipped with an Agilent Technologies 7890A gas chromatograph (GC). The GC was fitted with a J&W 60 m DB-VRX capillary column (film thickness 1.40 μm ; internal diameter 0.25 mm).



Figure 3.6: Gas-Chromatography Mass-Spectrometry (left) and Purge-&-Trap System (right)

The extracted medium subsamples that had been injected into the system were purged for 15 minutes using oxygen-free nitrogen (OFN) at a flow rate of 40 mL min^{-1} . Any aerosols or particles in the bypassing purged gas would be removed through the stuffed glass wool held in a glass tubing. Water vapor in the bypassing of the purged gas was removed through a molecular sieve followed by a counter-flow Nafion dryer (Perma-Pure) using OFN at a rate of 100 mL min^{-1} . The targeted compounds were then trapped and cryogenically focused synchronously purging in a stainless-steel tubing coil immersed in liquid nitrogen at a temperature of -150°C , aided by a thermostated heating device for a total of 15 minutes.

Then to allow sample desorption, liquid nitrogen was quickly swapped with boiling water in a flow of high-purity Helium at 1 mL min^{-1} via a heated (95°C) transfer line to the GC. As the run starts, the oven was initially held at 36°C for 5 min, followed by heating up to 200°C at $20^{\circ}\text{C min}^{-1}$, and lastly heated up to 240°C at a rate of $40^{\circ}\text{C min}^{-1}$. The quantification and identification of the compounds were determined by an Agilent 5975C mass-selective detector (MSD), operated in Single Ion Mode. Data was collected between 4 and 18 min. Calibrations for all compounds were done using gravimetrically

prepared liquid standards (Sigma-Aldrich) mixed in high-performance liquid chromatography-grade methanol (Fischer Scientific) injected into medium samples.

3.4.3 Calibration of halocarbon standards

Calibrations for all compounds (CH_3I , CHBr_3 , CHCl_3 , CH_2Br_2 , CHBr_2Cl) were done using gravimetrically prepared liquid standards (Sigma-Aldrich) mixed in high-performance liquid chromatography-grade methanol (Fischer Scientific) injected into medium samples. The amount of halocarbon concentration from samples and phytoplankton-free controls were calculated based on a five-point calibration curve that plots concentration against peak area. The regression coefficient (r^2) for the linear calibration curve was above 0.95. Deuterated-iodomethane (CD_3I) (ARMAR chemicals) and deuterated-diiodomethane (CD_2I_2) (Sigma-Aldrich) were injected into every medium sample before the halocarbon analysis as a way to monitor and correct for drift in the detector sensitivity (Hughes *et al.*, 2006). A loss of peak area from the internal standards due to the drift was corrected and equated to the original peak area as initially detected. Peak areas originated from analyte of interest, which was the halocarbons detected from the samples or controls, were also corrected following the same ratio as the surrogate standards did. The relative response, halocarbon concentration, was then obtained from the calibration that plots concentration against integrated peak area.

3.4.4 Detection limit and precision of the system

All halocarbon compounds were identified with their individual quantifying ions (Table 3.1) under the single ion mode (SIM) selected under the GCMS software programme run.

Table 3.1: Summary of halocarbons extracted by purge-and-trap and analyzed using GC-MSD and their associated quantifying ion, retention time, detection limit and precision.

Compounds	Quantifying Ion (m/z)	Retention time (min)	Detection Limit (pmol L ⁻¹)	Precision (%) (n=6)
CHBr ₃	173	15.61	0.30	10.3
CH ₃ I	142	8.18	0.20	5.9
CHCl ₃	83	10.33	0.50	7.3
CHBr ₂ Cl	129	14.09	0.05	9.8
CH ₂ Br ₂	174	12.19	0.30	7.9

3.4.5 Cell biomass determination

The biomass was determined based on cell number, which was counted using haemocytometer (Vello *et al.*, 2014). The chlorophyll-a content (chl-a) was determined by harvesting the microalgal cells by Millipore filtration using filter paper (Whatmann GF/C, 0.45 µm). The chl-a of the microalgae were extracted using acetone and left overnight 4°C in the dark (Vello *et al.*, 2014; Strickland & Parsons, 1968). The absorption of the extract was measured at 665nm, 645nm and 630nm. Chl-a was calculated using the formula as follows:

$$Chl\ a\ (mg\ m^{-3}) = (Ca \times Va) / Va$$

$$\text{where, } Ca = 11.6 (OD_{665nm}) - 1.31(OD_{645nm}) - 0.14(OD_{630nm})$$

Va = Volume of acetone (mL) used for extraction

Vc = Volume of culture (L)

$$Chl\ a\ (mg\ L^{-1}) = Chl\ a\ (mg\ m^{-3}) / 1000$$

The specific growth rate (μ , day⁻¹) for all cultures were based on calculated real-time biomass (chl-a and cell number) using the formula as follows:

$$\mu, day^{-1} = \frac{\ln(N_2/N_1)}{(t_2 - t_1)}$$

where N_2 , is OD_{620nm} at t_2 , N_1 , is real-time biomass at t_1 , and t_2 , t_1 are time periods within log phase (Strickland & Parsons, 1968).

To obtain dry weight, a pre-weighed glass fiber filter was used to filter 30.0 mL of culture. The filter paper was then dried in the oven at 100 °C for 24 hours, cooled in a dessicator before weighing. Dry weight (DW) was calculated as follows:

$$DW (mg L^{-1}) = \frac{(wt\ of\ filter\ paper\ \&\ algae) - wt\ of\ filter\ paper}{Volume\ of\ algal\ culture\ (L)}$$

3.5 Experiment 4: Effects of varying irradiance on halocarbon emission

The objective of this experiment was to study how the emission of halocarbons and photosynthetic performance (F_v/F_m) of the microalgae were affected when exposed to a range of irradiance.

3.5.1 Experimental set-up

Three microalgal cultures, *Synechococcus* sp. UMACC 371, *Amphora* sp. UMACC 370 and *Parachlorella* sp. UMACC 245 were grown in batch culture with a starting inoculum size of 10% of a log phase culture, standardized at an optical density of 0.4 at OD_{620nm} . The cultures of 150 mL total volume, were grown in 250 mL conical flasks in an incubator shaker (100 rpm) at 25°C with irradiance of 40 $\mu mol\ photons\ m^{-2}\ s^{-1}$ on a 12h light:12h dark cycle using F30T8/D HITACHI Fluorescent lamps 28W for up to 4 days to achieve exponential phase. On Day 4 during its light cycle, the cultures were exposed to 0, 40 (control) and 120 $\mu mol\ photons\ m^{-2}\ s^{-1}$ for 12 hours. Light source was adjusted higher by adding the number of fluorescent tubes onto the incubator. Prior (t_0) and post (t_1) of the light-exposure period, samples were removed from each triplicate flasks and centrifuged (3000 rpm for 10 min) and replenished with fresh medium, drawn

out into a 100 mL glass syringe to be incubated air-tight for 4 hours. After 4 hours of incubation, the culture from the incubation syringes was gently swirled and extracted into 100 mL glass syringes through a two-syringe (0.2 µm Merck filter unit) closed filter system to ensure no ingress of air into the syringe. The medium subsample left in the syringe was then ready for halocarbon analysis. Experiments were repeated for all three marine tropical microalgae.

3.5.2 Analysis and calibration of halocarbons

The procedure of analysis of halocarbon using GCMS equipped with Purge-and-Trap System was described in section 3.4.2.

3.5.3 Cell biomass determination

Samples were also collected at the same time for biomass estimation using various parameters, including chlorophyll-a and cell number as described in section 3.4.5. This was to allow calculation of the emission rate before and after 12hr of light-exposure through normalization of biomass to the emission of each compound emitted by microalgae.

3.5.4 Determination of photosynthetic parameter, F_v/F_m

The photosynthetic parameter, F_v/F_m was estimated by using a Water PAM (Pulmonary Amplitude Modulation) (Walz, Model: WATER-ED, S/N:EDEE0238 Germany) to indicate the changes of stress level before and after the light exposure, as well as before and after the gas-tight incubation period to indicate cells' health. Samples from each culture were dark-adapted for 15 minutes prior to F_v/F_m determination. A control with culture medium but no microalgal inoculum was set up in triplicate for each microalga.

3.6 Statistical Analysis

One-Way ANOVA was used to test the significance ($p < 0.05$) of emission of all five compounds detected at early growth stage of the three microalgae at different OD_{620nm}.

Repeated Measures-ANOVA was used to test the significance ($p < 0.05$) of emissions of all the five compounds by the three different microalgae within the culture period. Pearson Product-Moment correlation coefficient (r) was used to analyze the emission rate of the five detected compounds in term of chlorophyll-a, cell density and both.

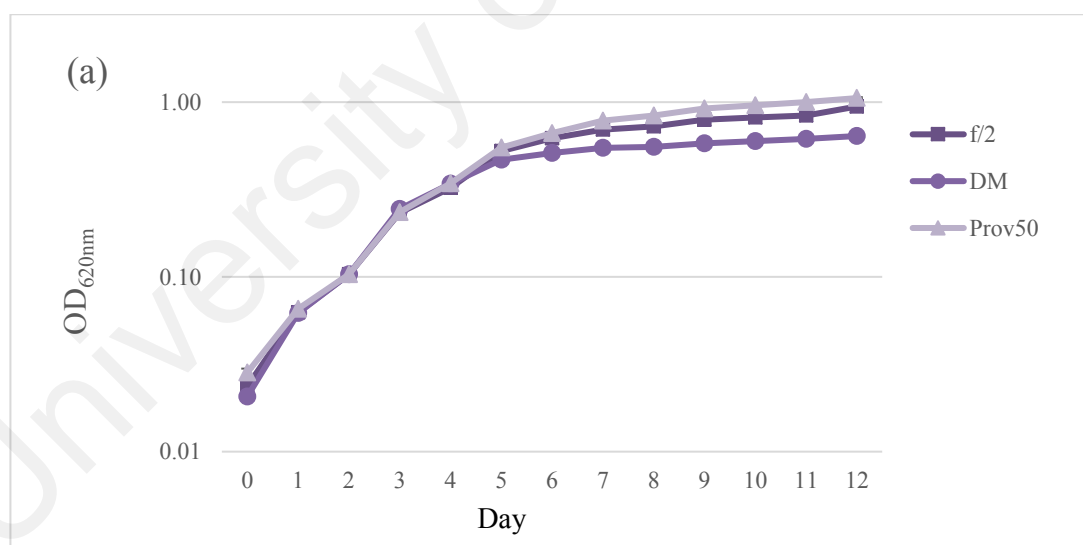
Factorial-ANOVA was used to test the significance ($p < 0.05$) of the means of F_v/F_m through homogenous grouping for the three microalgae. Pearson Product-Moment correlation coefficient (r) was used to analyze the emission rates of the five compounds in terms of chlorophyll-a, cell density and both, as well as the correlation between F_v/F_m and halocarbon emission rates of the three taxa with irradiance. Pairwise comparison through Bonferroni adjustment was used to analyze the relationship between irradiance and halocarbon emission rates across the microalgae. Statistical analyses were done using the Statistica 8.0 and IBM SPSS Statistics software ($p < 0.05$). Data prior to data analyses were subject to the normality test using the skewness and kurtosis and results indicated that all data were distributed normally.

CHAPTER 4: RESULTS

4.1 Experiment 1: Optimization for halocarbon studies

4.1.1 Growth curves of microalgae in different culture media

Figure 4.1 show the growth curves of three tropical marine microalgae, (a) *Parachlorella* sp. UMACC 245, (b) *Synechococcus* sp. UMACC 371 and (c) *Amphora* sp. UMACC 370 grown in three media, namely f/2, Diatom (DM) and Prosavoli 50 (Prov 50) medium at OD_{620nm} 0.2. The three microalgae showed clear trends of higher biomass when grown in Prov50 based on OD_{620nm} as compared to the other two media, though the trend of growth under f/2 medium came close with Prov50 for *Parachlorella* sp. UMACC 245 and *Synechococcus* sp. UMACC 371. There were more clumpings observed in DM in comparisons with Prov50 and f/2 as the diatom cultures proceeded from exponential to stationary phase.



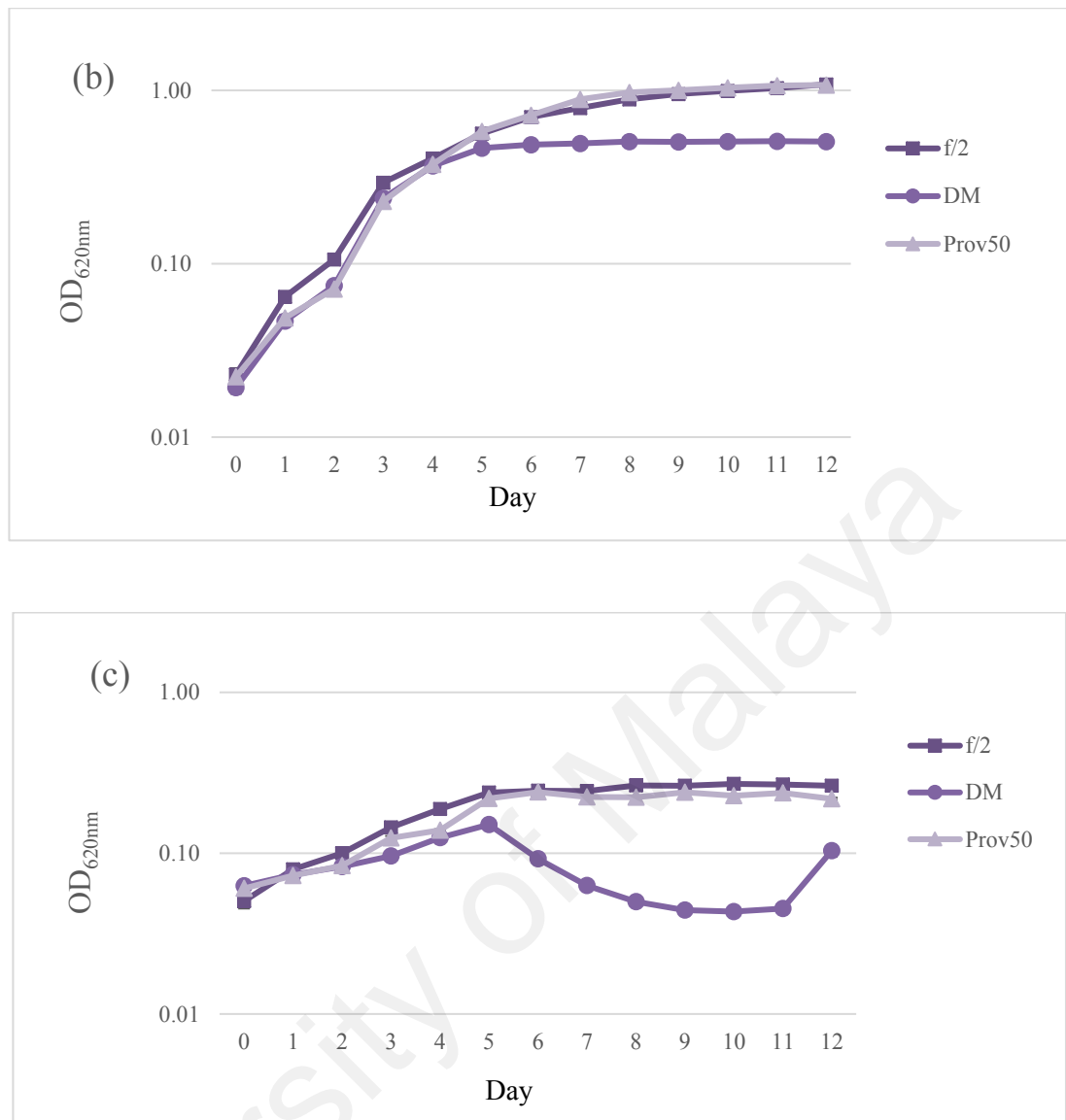


Figure 4.1: Growth curves based on Optical Density (OD_{620nm}) of three tropical marine microalgae, (a) *Parachlorella* sp. UMACC 245, (b) *Synechococcus* sp. UMACC 371 and (c) *Amphora* sp. UMACC 370 under different growth media over a period of 12 days. $n = 3$

Specific growth rates, μ (day^{-1}) of the microalgae under all three different growth media were calculated and summarized in Table 4.1. Based on the results, all microalgae had the highest specific growth rate when grown under Prov50 medium as compared to other media, F/2 and Diatom media. Hence, Prov50 medium was selected as the most suitable medium for all microalga culture.

Table 4.1: Specific growth rate, μ (day^{-1}) of three tropical marine microalgae based on exponential phase under different growth media. $n = 3$.

Medium	<i>Parachorella</i> sp. UMACC 245	<i>Synechococcus</i> sp. UMACC 371	<i>Amphora</i> sp. UMACC 370
F/2	0.657 (± 0.034)	1.019 (± 0.001)	0.288 (± 0.008)
Diatom	0.685 (± 0.020)	1.159 (± 0.042)	0.189 (± 0.026)
Provasoli 50	0.705 (± 0.019)	1.163 (± 0.022)	0.320 (± 0.012)

4.1.2 Basic growth profile of the selected microalgae

Three selected tropical marine microalgae were grown for 14 days to obtain respective growth curve profiles, from lag phase to stationary phase, through the measurements of chlorophyll-a (Figure 4.2), cell density (Figure 4.3), optical density (Figure 4.4) and carotenoids (Figure 4.5). Maximum quantum yield, F_v/F_m , for all three microalgae were recorded as shown in Figure 4.6 to be observed as cell stress indicator.

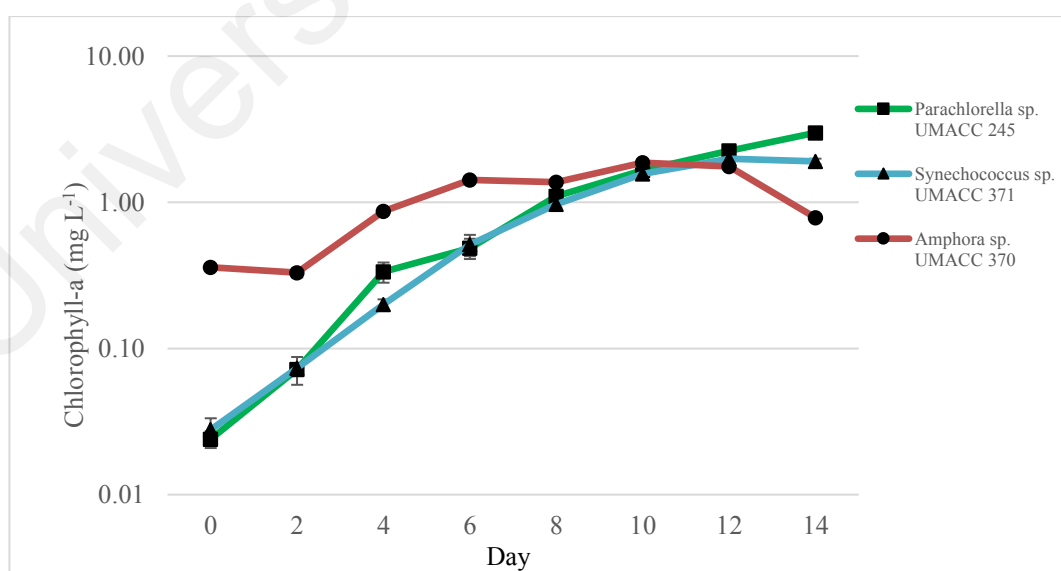


Figure 4.2: Growth curves of three tropical marine microalgae over a growth period of 14 days determined by chlorophyll-a. $n = 3$

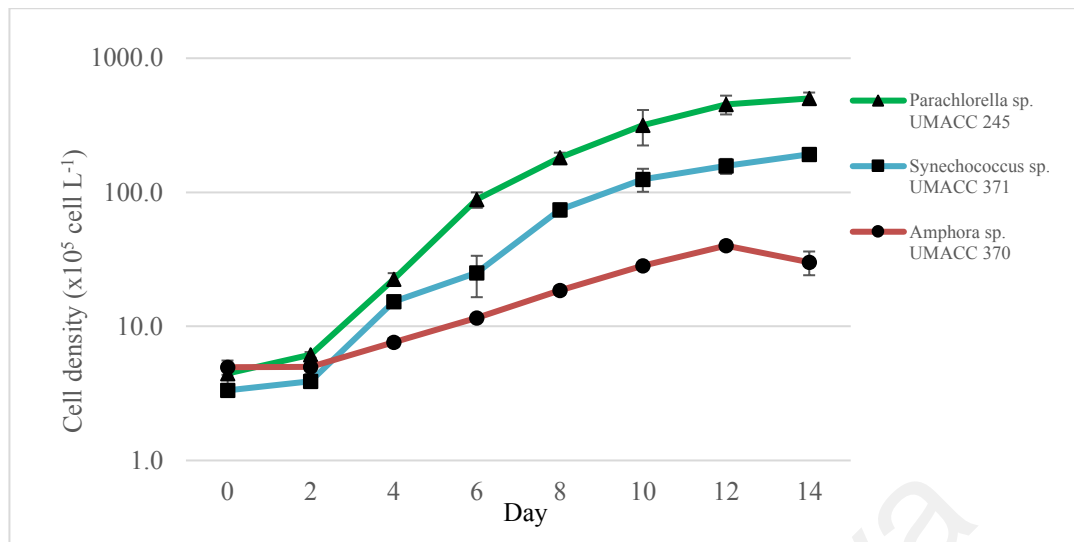


Figure 4.3: Growth curves of three tropical marine microalgae over a growth period of 14 days determined by cell density. $n = 3$

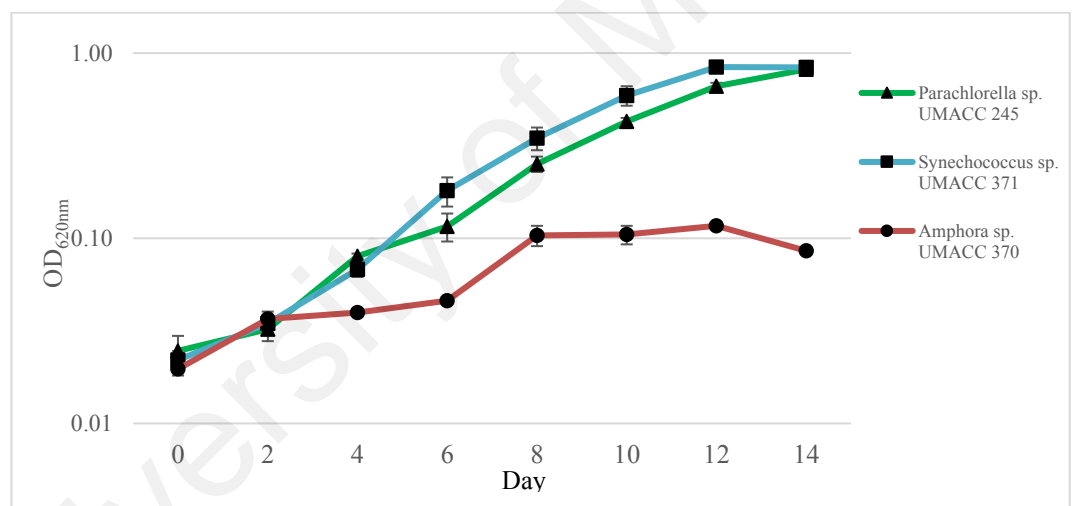


Figure 4.4: Growth curve of three tropical marine microalgae over a growth period of 14 days determined by Optical Density (OD_{620nm}). $n = 3$

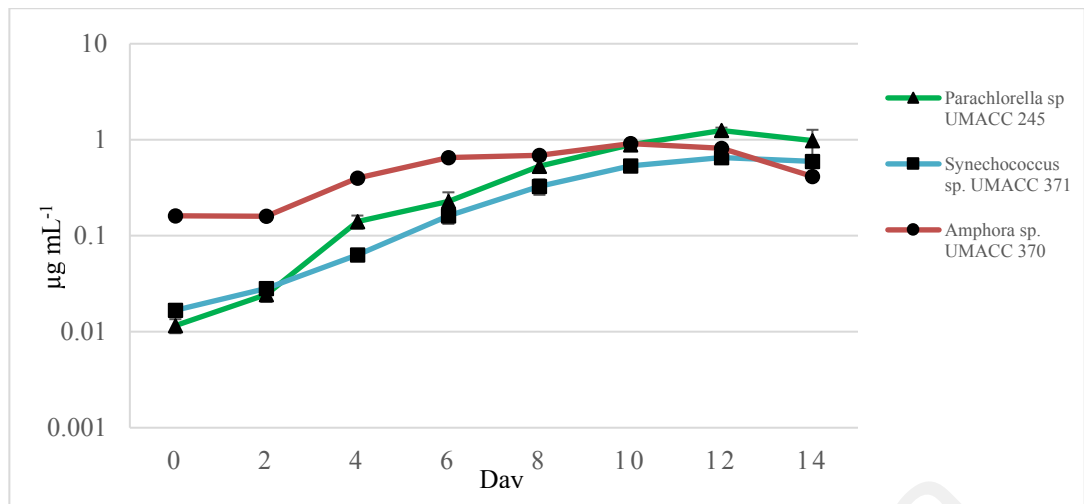


Figure 4.5: Carotenoids of three tropical microalgae over a growth period of 14 days.
n = 3

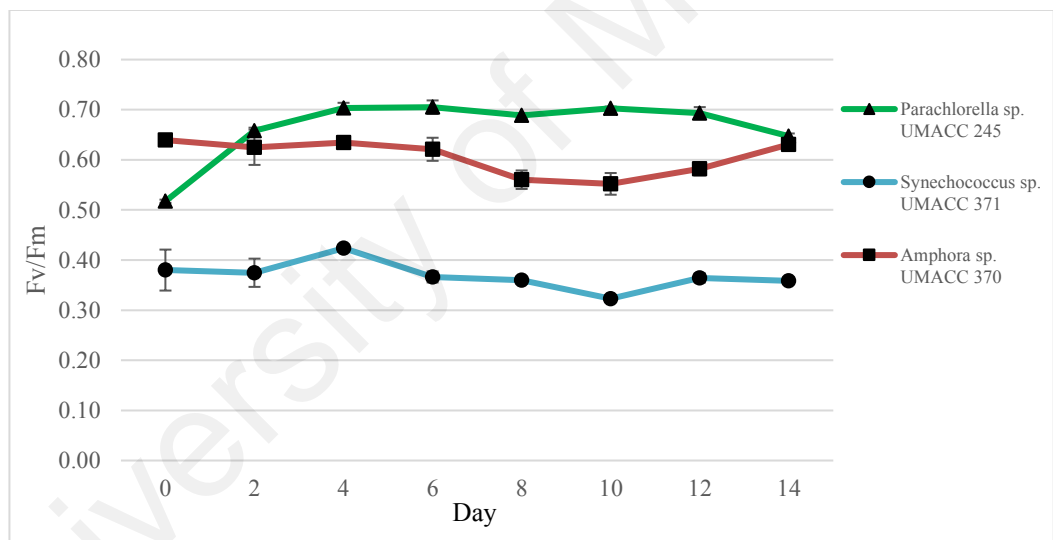


Figure 4.6: Maximum quantum yield, F_v/F_m of three tropical marine microalgae over a growth period of 14 days. n = 3

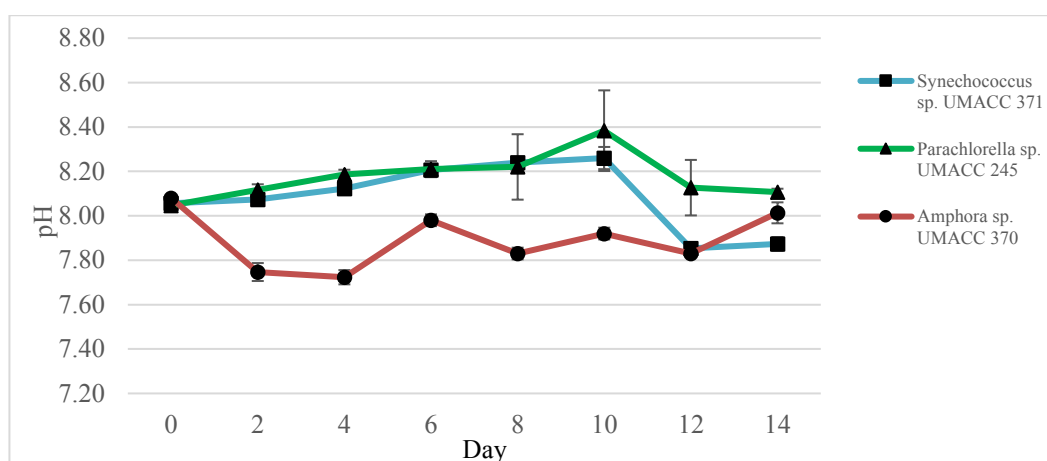


Figure 4.7: pH of three tropical marine microalgae over a growth period of 14 days.
n =3

Parachlorella sp. UMACC 245 and *Synechococcus* sp. UMACC 371 showed consistent trends of higher biomass in exponential phase as compared to *Amphora* sp. UMACC 370 based on chlorophyll-a, cell density, OD_{620nm} and carotenoids. Over the 14-day of culture period, the range of F_v/F_m falls between 0.5-0.7, 0.3-0.4 and 0.5-0.6 for *Parachlorella* sp. UMACC 245, *Synechococcus* sp. UMACC 371 and *Amphora* sp. UMACC 370 respectively. The starting pH for the culture on Day 0 was 8.0. Over the 14 day growth period, the pH trend for *Parachlorella* sp. UMACC 245 and *Synechococcus* sp. UMACC 371 increased but decreased for *Amphora* sp. UMACC 370 during the exponential phase.

4.1.3 Selection of suitable air-tight incubation hours

The aim of this test was to determine the most suitable air-tight incubation time for the three microalgae so as to maximize the production of halocarbons while minimizing cells' physiological stress. Based on the F_v/F_m results as shown in Table 4.2, there was an indication of stress from the decrease of F_v/F_m starting 5th hour onwards for all three microalgae. Hence, 4 hours was the longest possible period for air-tight incubation. Whilst the F_v/F_m were slightly higher on the first three hours as compared to the 4th hour across all three taxa, 4 hours was ultimately selected as the most suitable incubation time

as one of the two aims in this test was to trap more halocarbons within the fixed incubation time. The cells were generally under non-stress condition after 4 hours of air-tight process.

Table 4.2: Comparison of F_v/F_m across 8 hours of air-tight incubation for *Parachlorella* sp. UMACC 245, *Synechococcus* sp. UMACC 371 and *Amphora* sp. UMACC 370.

Time	Air-Tight Hours	Maximum Quantum Efficiency (F_v/F_m), n=3		
		<i>Parachlorella</i> sp. UMACC 245	<i>Synechococcus</i> sp. UMACC 371	<i>Amphora</i> sp. UMACC 370
9.50am	0 (control)	0.62 (± 0.00)	0.38 (± 0.01)	0.63 (± 0.00)
10.50am	1	0.63 (± 0.00)	0.36 (± 0.00)	0.62 (± 0.00)
11.50am	2	0.61 (± 0.00)	0.37 (± 0.01)	0.62 (± 0.00)
12.50am	3	0.61 (± 0.00)	0.38 (± 0.00)	0.60 (± 0.00)
1.50pm	4	0.61 (± 0.00)	0.37 (± 0.00)	0.60 (± 0.00)
2.50pm	5	0.59 (± 0.00)	0.32 (± 0.01)	0.59 (± 0.00)
3.50pm	6	0.60 (± 0.00)	0.29 (± 0.01)	0.56 (± 0.00)
4.50pm	7	0.60 (± 0.00)	0.29 (± 0.01)	0.52 (± 0.00)
5.50pm	8	0.59 (± 0.01)	0.27 (± 0.01)	0.49 (± 0.01)

4.2 Experiment 2: Emission of halocarbons at different cell densities

Only five halocarbons were detected in the emissions from the three microalgae. Table 4.3 shows the concentration (pmol L^{-1}) of halocarbons emitted by the three microalgae of different cell densities ($\text{OD}_{620\text{nm}}$)*. a) *Synechococcus* UMACC 371; b) *Amphora* UMACC 370; c) *Parachlorella* UMACC 245. n= 3.

Synechococcus sp. UMACC 371 showed no emission at $\text{OD}_{620\text{nm}}$ 0.2 for all five compounds except CH_3I and CHBr_3 on Day 4. At $\text{OD}_{620\text{nm}}$ 0.3, all compounds showed no emission except CH_3I on Day 0, 2 and 4, and CHBr_3 on Day 4. At $\text{OD}_{620\text{nm}}$ 0.4, emissions for all compounds were detected except on Day 0 and 4 for CHCl_3 , Day 0 and 4 for CH_2Br_2 and Day 0 and 2 for CHBr_2Cl . $\text{OD}_{620\text{nm}}$ 0.4 produced the highest ($p < 0.05$)

emission for all five compounds on Day 0, 2 and 4 as compared to OD_{620nm} 0.2 and 0.3. The inoculum of OD_{620nm} 0.4 was selected to be the starting inoculum for halocarbon emission study for *Synechococcus* sp. UMACC 371.

At OD_{620nm} of 0.2, there was no emission from *Amphora* sp. UMACC 370 except for CH₂Br₂ on Day 4 and CH₃I. At OD_{620nm} 0.3, emissions of all compounds were detected but were inconsistent from Day 0 to 4 as no emission was observed in some compounds. Higher emission (at least 1x and above) was detected at OD_{620nm} 0.4 across all five compounds from Day 0 to 4, except for CHBr₂Cl at Day 0. OD_{620nm} 0.4 produced the highest ($p<0.05$) emission compared to OD_{620nm} 0.2 and 0.3. The inoculum of OD_{620nm} 0.4 was selected for *Amphora* sp. UMACC 370 as the starting inoculum.

Parachlorella sp. UMACC 245 showed no emission at OD_{620nm} 0.2 for all five compounds across the 4-day experiment period and no emission at OD_{620nm} 0.3 except for two brominated compounds, CHBr₃ on Day 2 and CH₂Br₂ on Day 4. Emissions were detected for all compounds at OD_{620nm} 0.4, but not detected from Day 0 to 4. The inoculum of OD_{620nm} 0.4 produced the highest ($p<0.05$) emission amongst the three OD_{620nm} tested, and was selected to be the starting inoculum for the halocarbon emission studies.

Tables 4.3: Emission of five halocarbons emitted by cultures of different OD_{620nm}. Concentration (pmol L⁻¹) of halocarbons emitted by three microalgae of different cell densities (OD_{620nm})*. a) *Synechococcus* UMACC 371; b) *Amphora* UMACC 370; c) *Parachlorella* UMACC 245. n= 3. Different letters denote standard deviation (SD) homogenous group ($p<0.05$) according to post-hoc Tukey's test.

(a)			
CH ₃ I	0.2*	0.3*	0.4*
Day 0	0.00 ^b	0.18 (±0.03) ^b	1.02 (±0.23) ^a
Day 2	0.00 ^b	0.04 (±0.03) ^b	0.11 (±0.02) ^b
Day 4	0.20 (±0.10) ^b	0.07 (±0.03) ^b	0.18 (±0.06) ^b
CHCl ₃	0.2*	0.3*	0.4*
Day 0	0.00 ^b	0.00 ^b	0.00 ^b
Day 2	0.00 ^b	0.00 ^b	0.00 ^b
Day 4	0.00 ^b	0.00 ^b	1.03 (±0.19) ^a
CHBr ₃	0.2*	0.3*	0.4*
Day 0	0.00 ^c	0.00 ^c	0.02 (±0.01) ^b
Day 2	0.00 ^c	0.00 ^c	0.01 (±0.00) ^{b,c}
Day 4	0.03(±0.00) ^b	0.02 (±0.00) ^b	0.05 (±0.01) ^a
CH ₂ Br ₂	0.2*	0.3*	0.4*
Day 0	0.00 ^b	0.00 ^b	0.00 ^b
Day 2	0.00 ^b	0.00 ^b	0.04 (±0.03) ^a
Day 4	0.00 ^b	0.00 ^b	0.00 ^b
CHBr ₂ Cl	0.2*	0.3*	0.4*
Day 0	0.00 ^b	0.00 ^b	0.00 ^b
Day 2	0.00 ^b	0.00 ^b	0.00 ^b
Day 4	0.00 ^b	0.00 ^b	0.01 (±0.00) ^a

(b)			
CH ₃ I	0.2*	0.3*	0.4*
Day 0	0.09 (±0.04) ^d	0.28 (±0.03) ^d	0.67 (±0.10) ^{b,c}
Day 2	0.12 (±0.04) ^d	0.27 (±0.06) ^d	0.87 (±0.06) ^{a,b}
Day 4	0.24 (±0.04) ^d	0.56 (±0.12) ^c	1.07 (±0.08) ^a
CHCl ₃	0.2*	0.3*	0.4*
Day 0	0.00 ^d	0.28 (±0.13) ^{b,c}	0.78 (±0.14) ^a
Day 2	0.00 ^d	0.00 ^d	0.37 (±0.08) ^b
Day 4	0.00 ^d	0.00 ^d	0.11 (±0.03) ^{c,d}
CHBr ₃	0.2*	0.3*	0.4*
Day 0	0.00 ^c	0.00 ^c	0.15 (±0.04) ^b
Day 2	0.00 ^c	0.00 ^c	0.09 (±0.01) ^b
Day 4	0.00 ^c	0.02 (±0.00) ^c	0.22 (±0.06) ^a
CH ₂ Br ₂	0.2*	0.3*	0.4*
Day 0	0.00 ^b	0.00 ^b	0.03 (±0.02) ^b
Day 2	0.00 ^b	0.01 (±0.00) ^b	0.14 (±0.06) ^a
Day 4	0.00 ^b	0.02 (±0.01) ^b	0.04 (±0.02) ^b
CHBr ₂ Cl	0.2*	0.3*	0.4*
Day 0	0.00 ^c	0.00 ^c	0.00 ^c
Day 2	0.00 ^c	0.00 ^c	0.02 (±0.00) ^a
Day 4	0.00 ^c	0.01 (±0.00) ^{a,b}	0.01 (±0.00) ^b

(c)			
CH ₃ I	0.2*	0.3*	0.4*
Day 0	0.00 ^c	0.00 ^c	0.12 (±0.03) ^a
Day 2	0.00 ^c	0.00 ^c	0.05 (±0.03) ^b
Day 4	0.00 ^c	0.00 ^c	0.00 ^c
CHCl ₃	0.2*	0.3*	0.4*
Day 0	0.00 ^b	0.00 ^b	0.36 (±0.17) ^a
Day 2	0.00 ^b	0.00 ^b	0.00 ^b
Day 4	0.00 ^b	0.00 ^b	0.00 ^b
CHBr ₃	0.2*	0.3*	0.4*
Day 0	0.00 ^c	0.00 ^c	0.00 ^c
Day 2	0.00 ^c	0.01 (±0.03) ^b	0.00 ^c
Day 4	0.00 ^c	0.00 ^c	0.01 (±0.00) ^a
CH ₂ Br ₂	0.2*	0.3*	0.4*
Day 0	0.00 ^c	0.00 ^c	0.00 ^c
Day 2	0.00 ^c	0.00 ^c	0.03 (±0.01) ^a
Day 4	0.00 ^c	0.01 (±0.00) ^b	0.01 (±0.00) ^b
CHBr ₂ Cl	0.2*	0.3*	0.4*
Day 0	0.00 ^b	0.00 ^b	0.00 ^b
Day 2	0.00 ^b	0.00 ^b	0.00 ^b
Day 4	0.00 ^b	0.00 ^b	0.02 (±0.01) ^a

4.3 Experiment 3: Halocarbon emission at different life-cycle stage

4.3.1 Growth curves of microalgae

The growth curves in terms of chlorophyll-a are shown in Figure 4.8 (a-c) and cell density as shown in Figure 4.9 (a-c), indicating the exponential and stationary phases for all three taxa (Table 4.4), and allowing the calculation of the specific growth rates (Table 4.5).

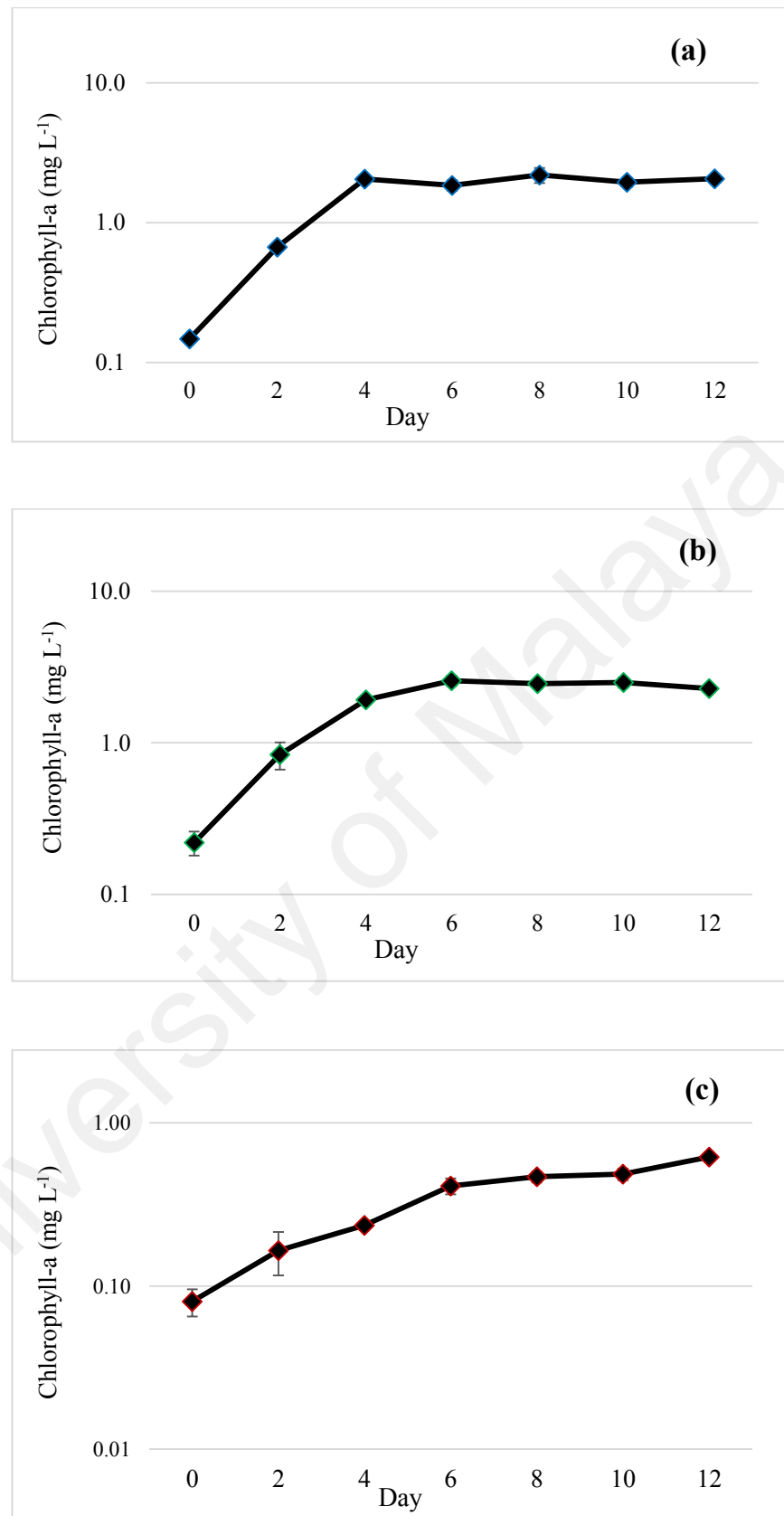


Figure 4.8: Growth curves based on chlorophyll-a. Cell growth phases of three tropical marine microalgae, (a) *Synechococcus* sp. UMACC 371; (b) *Parachlorella* sp. UMACC 245; (c) *Amphora* sp. UMACC 370 based on real-time biomass, chlorophyll-a (mg L⁻¹) over 12 days of culture period. n = 3

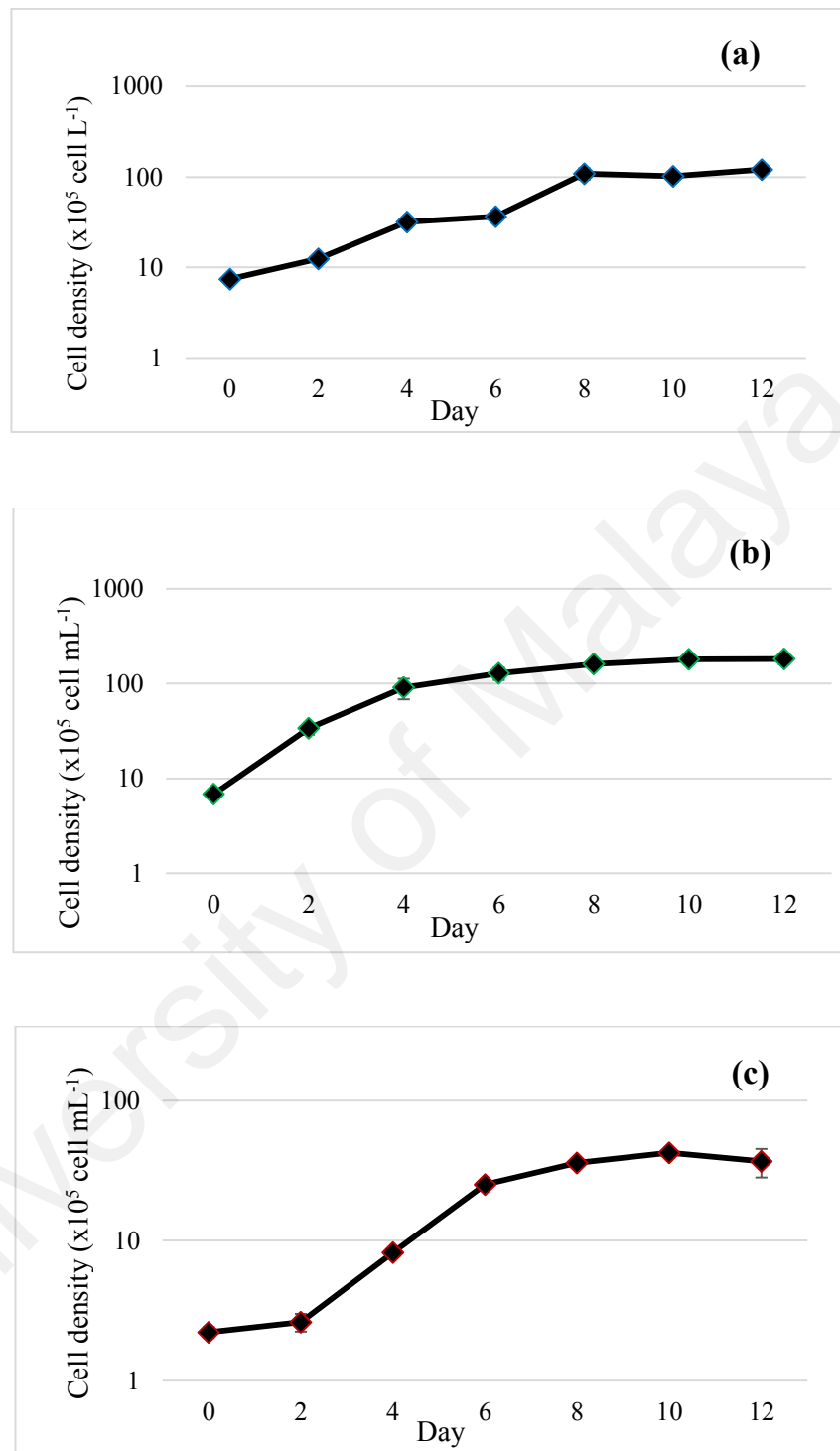


Figure 4.9: Growth curves based on cell density. Cell growth phases of three tropical marine microalgae, (a) *Synechococcus* sp. UMACC 371; (b) *Parachlorella* sp. UMACC 245; (c) *Amphora* sp. UMACC 370 based on real-time biomass, cell density (cell mL^{-1}) over 12 days of culture period. $n = 3$

Table 4.4: Algal growth stages determined by chlorophyll-a and cell density. Selected range and representative points of exponential and stationary phases for the three tropical marine microalgae are shown.

Taxa	Exponential phase		Stationary phase	
	Phase range	Representative point	Phase range	Representative point
<i>Synechococcus</i> sp. UMACC 371	Day 0—4	Day 4	Day 4—12	Day 8
<i>Parachlorella</i> sp. UMACC 245	Day 0—4		Day 4—12	
<i>Amphora</i> sp. UMACC 370	Day 0—6 Day 2 – 6#		Day 6—12	

For *Amphora*, the exponential phase ranged from day 2 to day 6.

Table 4.5: Specific growth rate. The mean of specific growth rate, μ (day^{-1}) of the three tropical marine microalgae based on their exponential growth phase of chlorophyll-a and cell density. $n = 3$.

Taxa	Specific Growth Rate (μ)	
	Chlorophyll-a	Cell density
<i>Synechococcus</i> sp. UMACC 371	0.66 (± 0.01)	0.36 (± 0.04)
<i>Parachlorella</i> sp. UMACC 245	0.54 (± 0.06)	0.64 (± 0.07)
<i>Amphora</i> sp. UMACC 370	0.27 (± 0.04)	0.74 (± 0.05)

4.3.2 Photosynthetic performance as an indication of cells' health state

Figure 4.10 (a-c) show the maximum quantum yield (F_v/F_m) of three tropical marine microalgae across a period of 12 days before and after the 4-hour air-tight incubation. F_v/F_m values shown prior to air-tight incubation act as control level. The smallest difference in F_v/F_m before and after air-tight incubation ensured the production of halocarbons trapped during the incubation from cell culture was maximized while the cells remained healthy or minimally affected by the physiological stress created from an air-tight environment. Under ambient laboratory conditions, the healthy range of F_v/F_m for *Synechococcus* sp. UMACC 371, *Parachlorella* sp.245 and *Amphora* sp.370 were

within 0.3-0.4, 0.5-0.7 and 0.5-0.7 respectively. In general, the cells for all cultures were in the healthy F_v/F_m range. Hence, the emission of halocarbons were not under the influence of cell stress from the air-tight incubation.

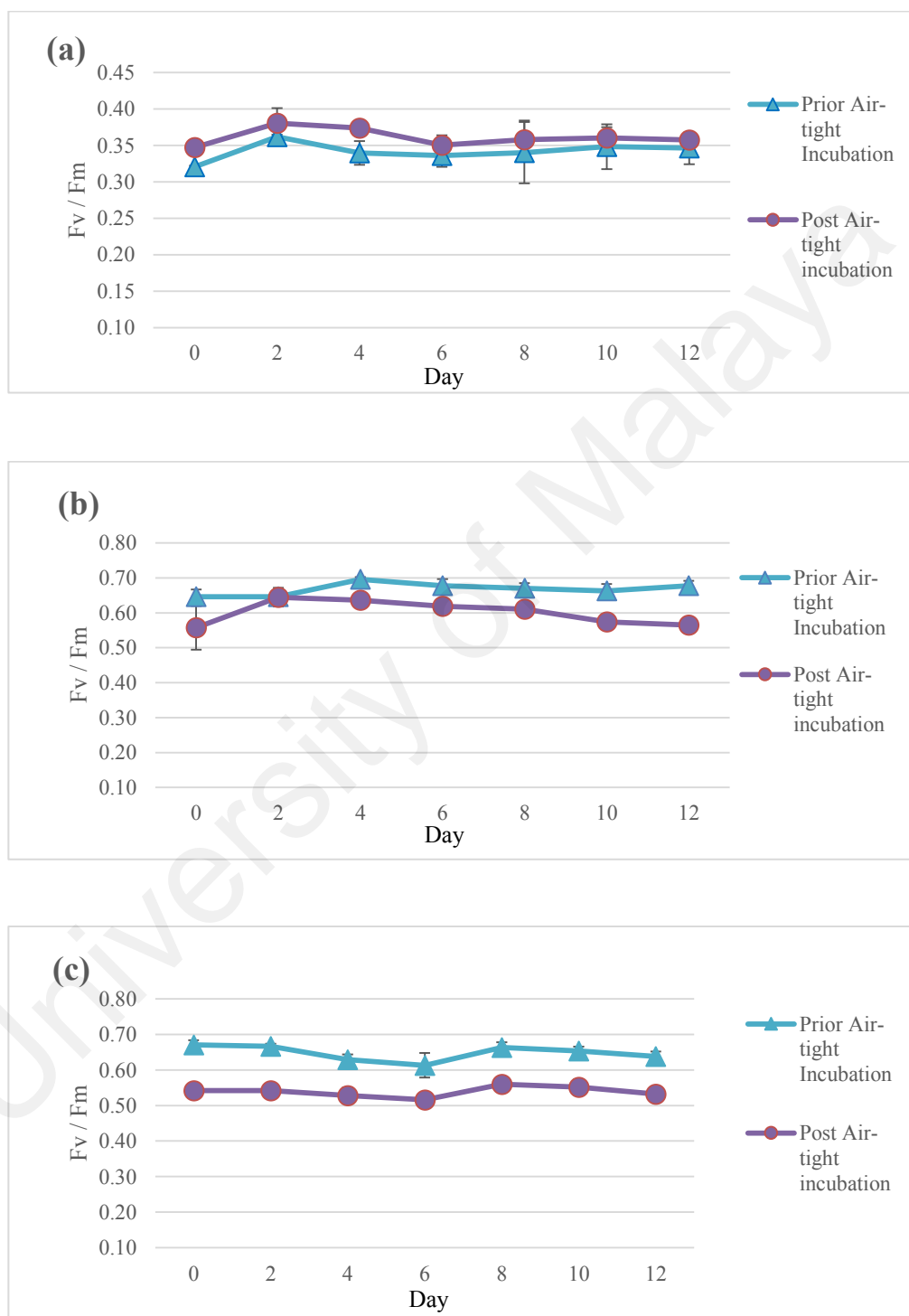
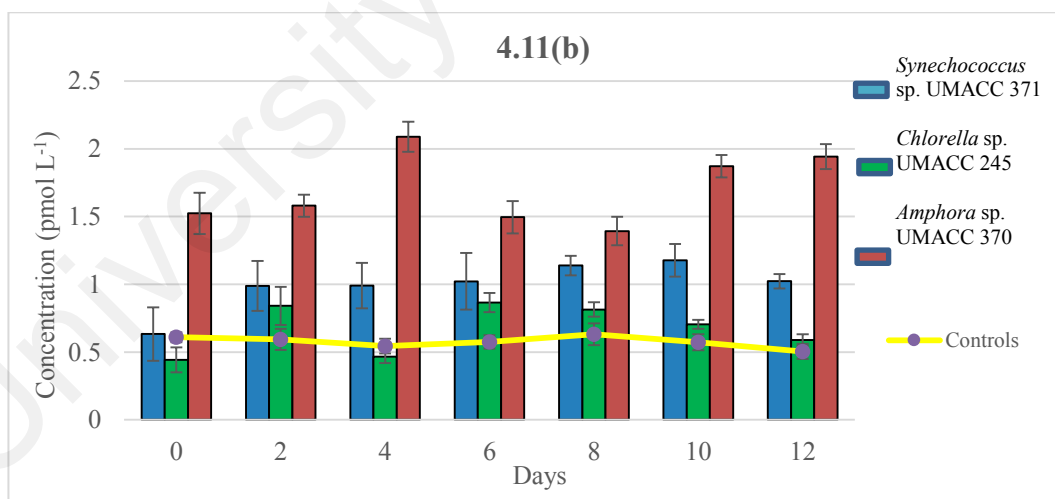
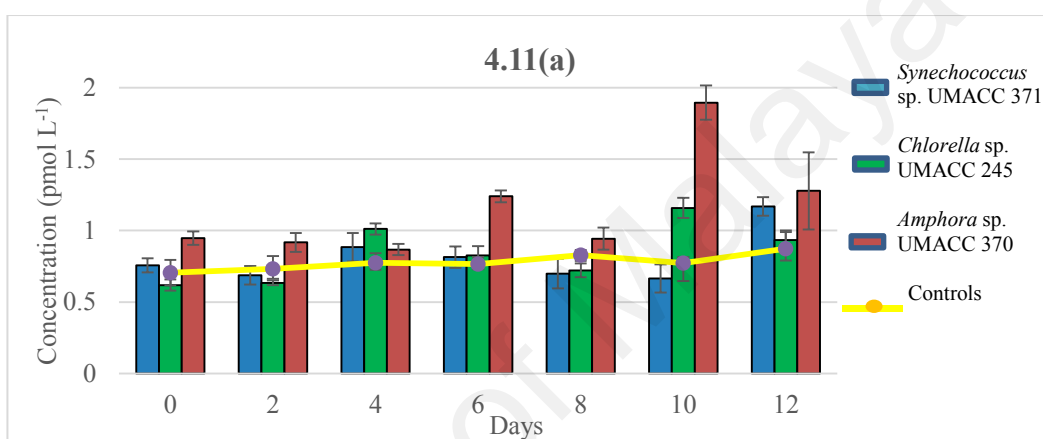


Figure 4.10: Maximal quantum efficiency, F_v/F_m . The mean of F_v/F_m for (a) *Synechococcus* sp. UMACC 371; (b) *Parachlorella* sp. UMACC 245; (c) *Amphora* sp. UMACC 370 before and after incubation over 12-day culture period. $n = 3$.

4.3.3 Emission of halocarbons

Figure 4.11 (a-e) show the changes of concentration of the five halocarbons from the three microalgae cultures and Prov50 medium over the 12 experimental days. The halocarbon concentrations above the control level were the emission while concentrations below the control level were the consumption or loss of the halocarbons. In case of present study, the aim focused on the emission of the halocarbons from the three microalgae.



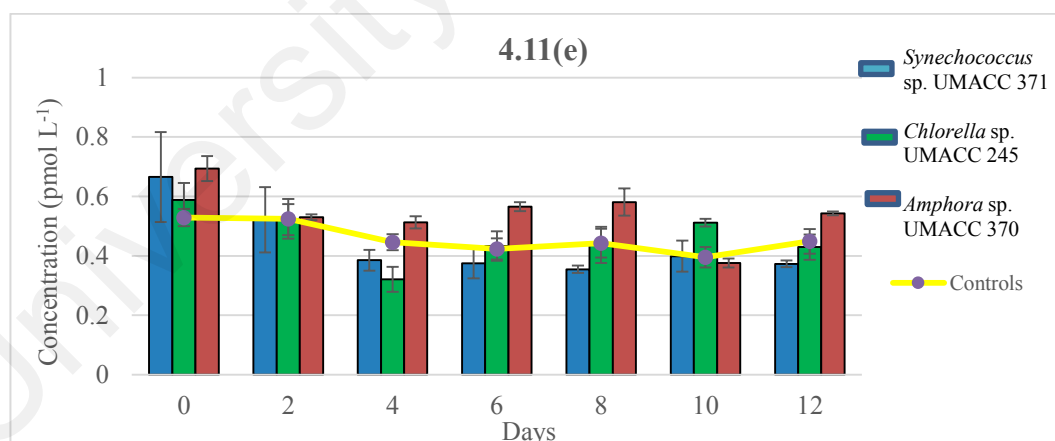
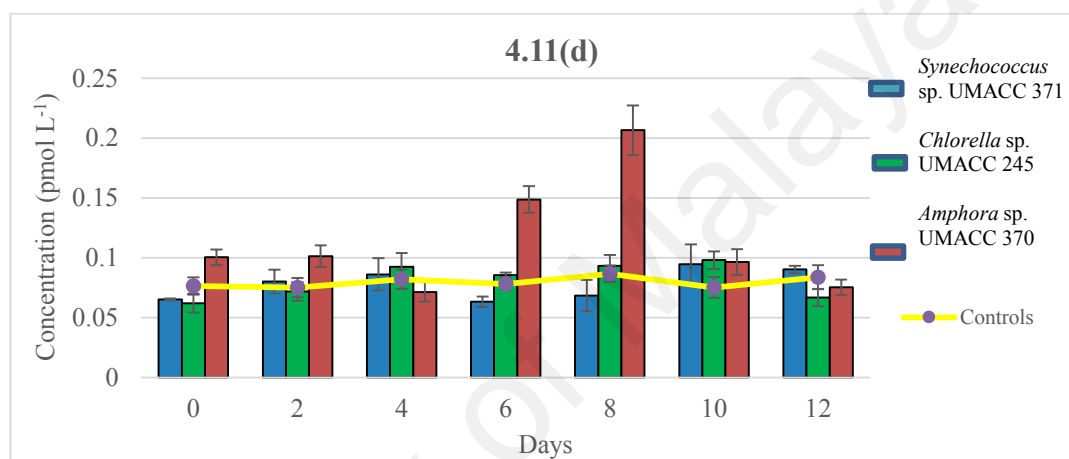
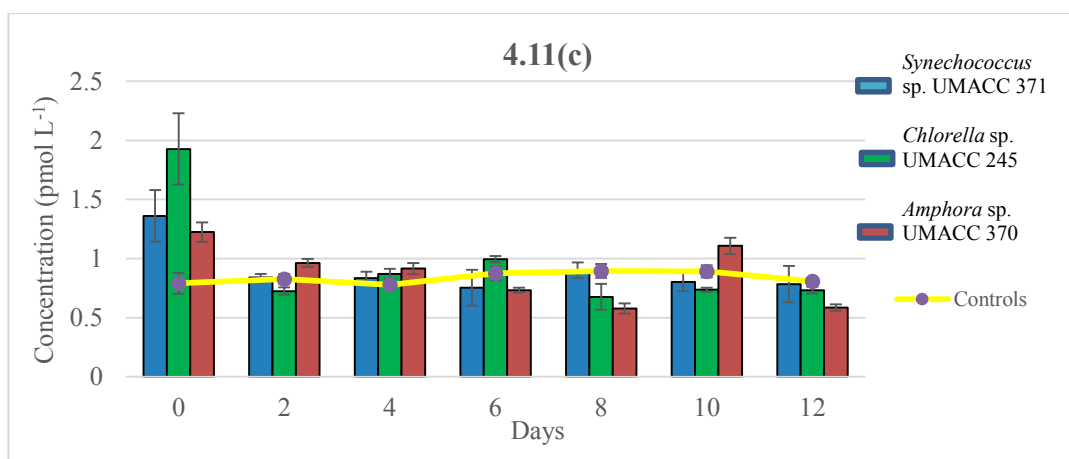
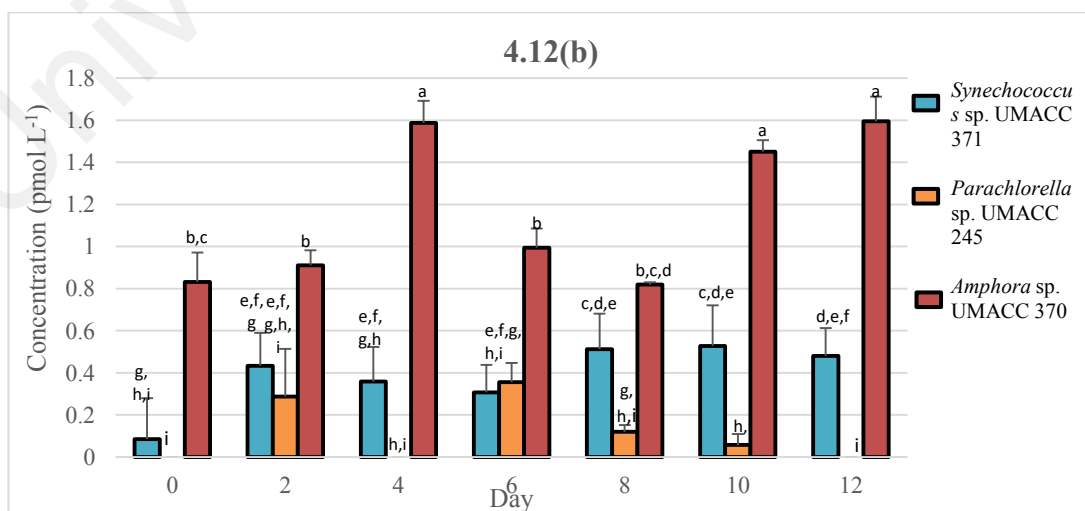
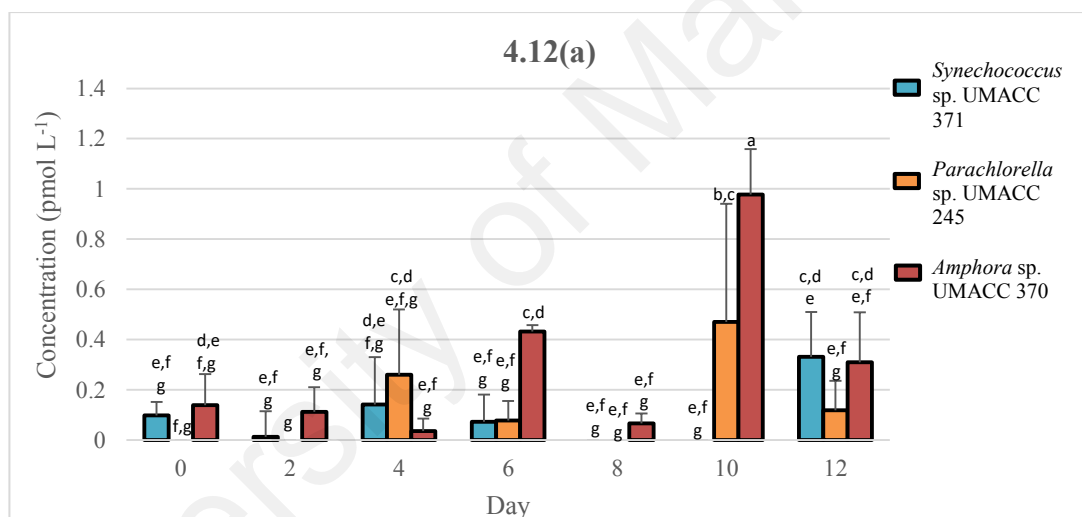


Figure 4.11: Changes of concentration of halocarbons detected from the three microalgae and Prov50 medium (controls) over a growth period of 12 days for compound (a) CHBr₃, (b) CH₃I, (c) CHCl₃, (d) CHBr₂Cl, and (e) CH₂Br₂. n = 3.

To obtain the amount of halocarbons emitted, the concentration of halocarbons from the Prov50 medium (controls) were subtracted from the concentration of halocarbons emitted from the microalgae. Figure 4.12 (a-e) show the concentrations of the five emitted

halocarbons from the three tropical marine microalgae. The concentration of CH₃I was the highest at 1.6 pmol L⁻¹ from both stationary and exponential phases. *Amphora* sp. UMACC 370 showed significantly ($p<0.05$) higher concentration of CHBr₃, CH₃I, CHBr₂Cl during the stationary phase and CH₂Br₂ during the late exponential phase. *Synechococcus* sp. UMACC 371 in general emitted higher amount of CH₃I during both exponential and stationary phases, as compared to other detected compounds. *Parachlorella* sp. UMACC 245 emitted low concentration across all compounds except CHBr₃ and CH₂Br₂ in both exponential and stationary phases and CH₃I during the exponential phase.



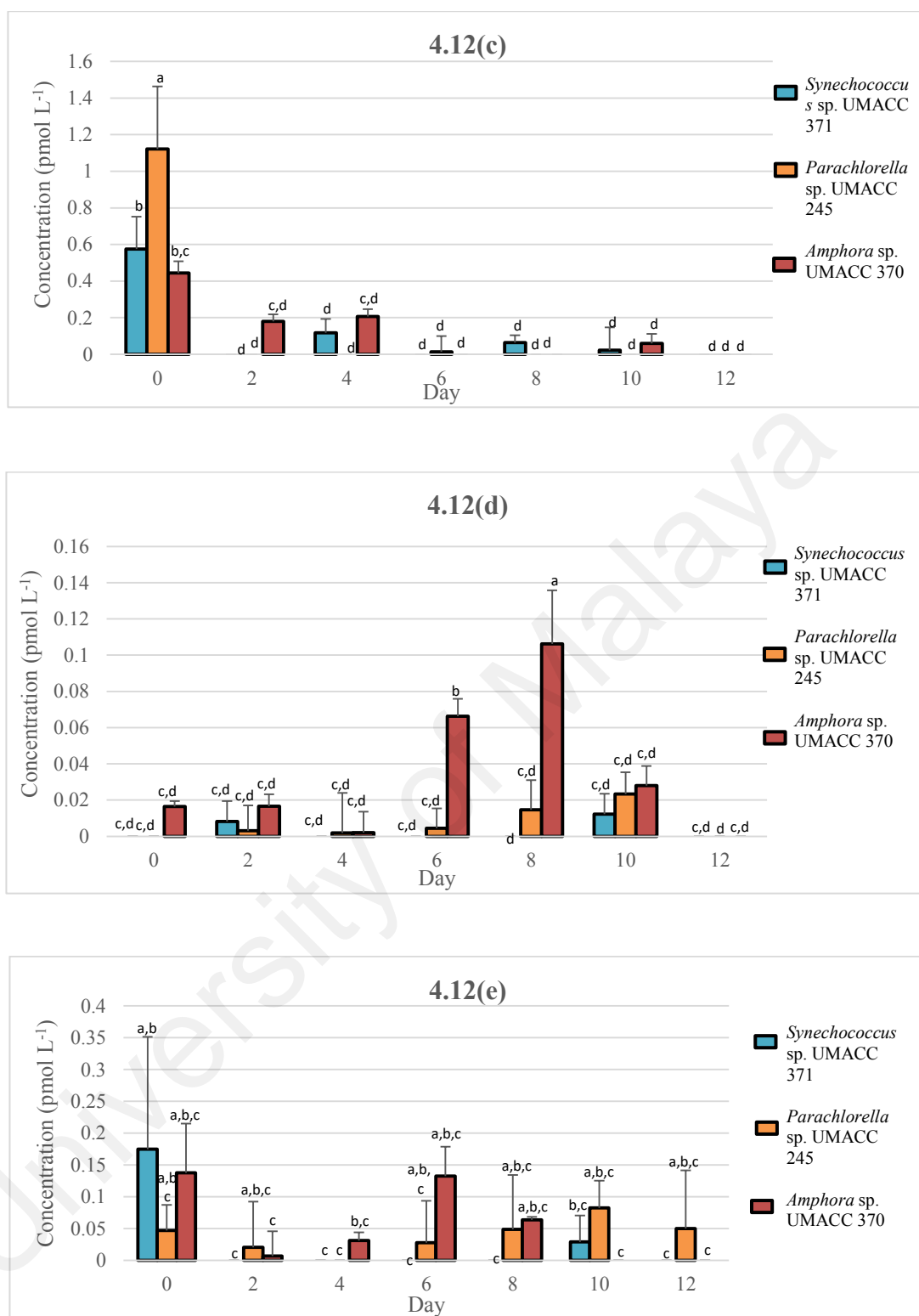
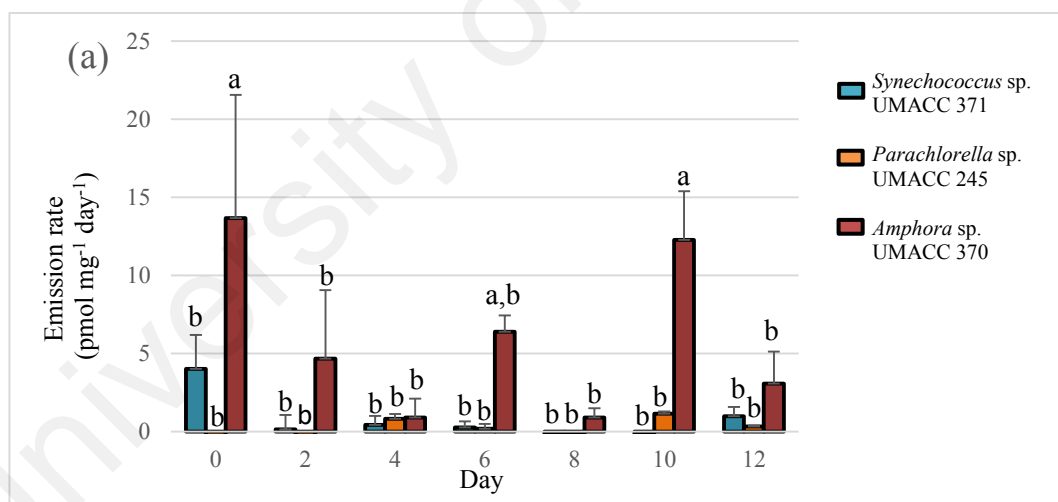


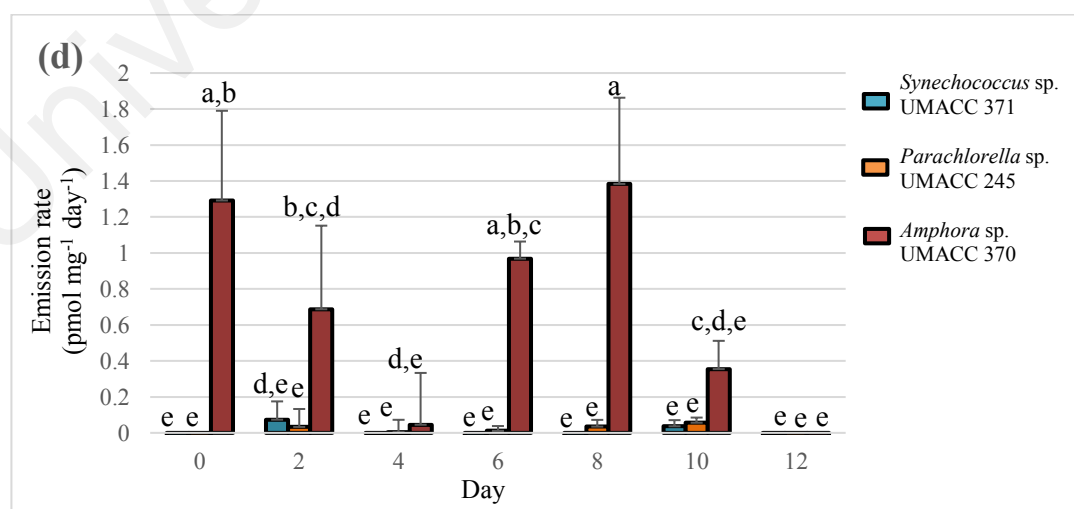
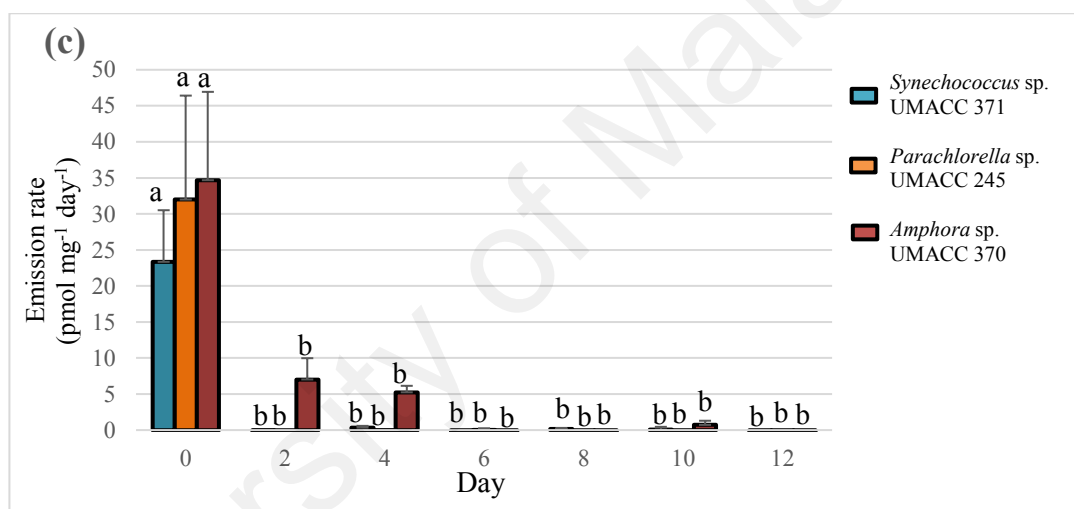
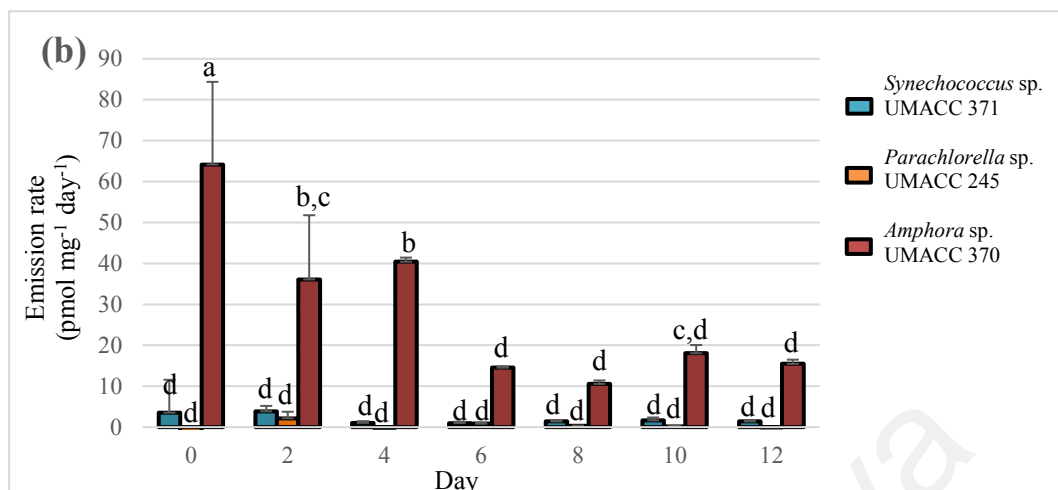
Figure 4.12: Emission of short-lived halocarbons. Concentration of halocarbon emitted by the three tropical marine microalgae across 12 experimental days for compound (a) CHBr_3 , (b) CH_3I , (c) CHCl_3 , (d) CHBr_2Cl and (e) CH_2Br_2 . Bar charts which contain different alphabets denote significant difference at ($p < 0.05$). $n = 3$

4.3.4 Emission rates of halocarbons

The concentration of the five detected halocarbons were used to normalize to chlorophyll-a (Figure 4.13) and cell density (Figure 4.14) to determine emission rate. Both chlorophyll-a and cell density normalized emission rates for all five compounds across the three microalgae were in good agreement. *Amphora* sp. UMACC 370 showed significantly ($p<0.05$) higher emission rate of CH_3I , CHCl_3 and CH_2Br_2 in the exponential phase. In addition, emission rates of CHBr_3 and CHBr_2Cl were significantly higher ($p<0.05$) than other halogenated compounds during exponential and stationary phase. The emission rates of all five compounds for *Synechococcus* sp. UMACC 371 and *Parachlorella* sp. UMACC 245 were significantly ($p<0.05$) lower as compared to *Amphora* sp. UMACC 370.

4.3.4.1 Normalization to chlorophyll-a





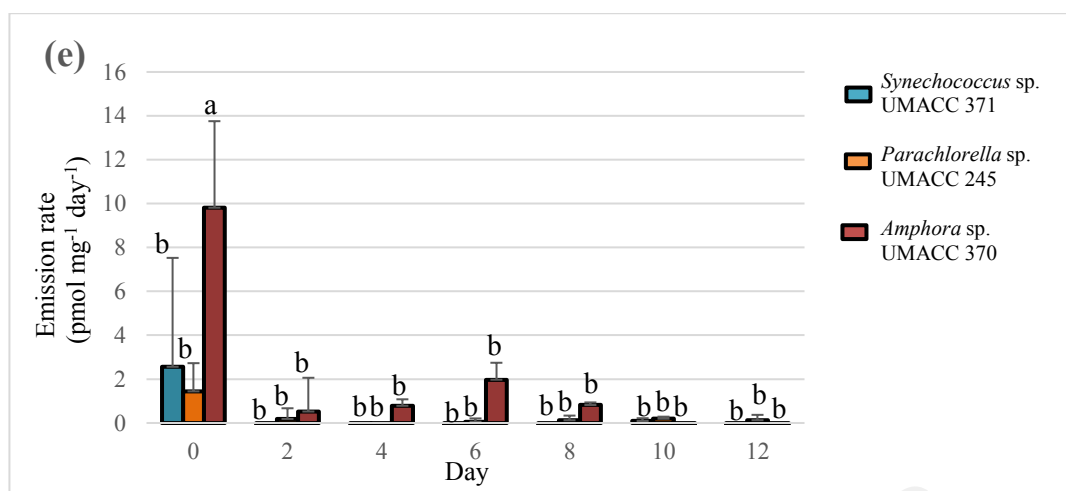
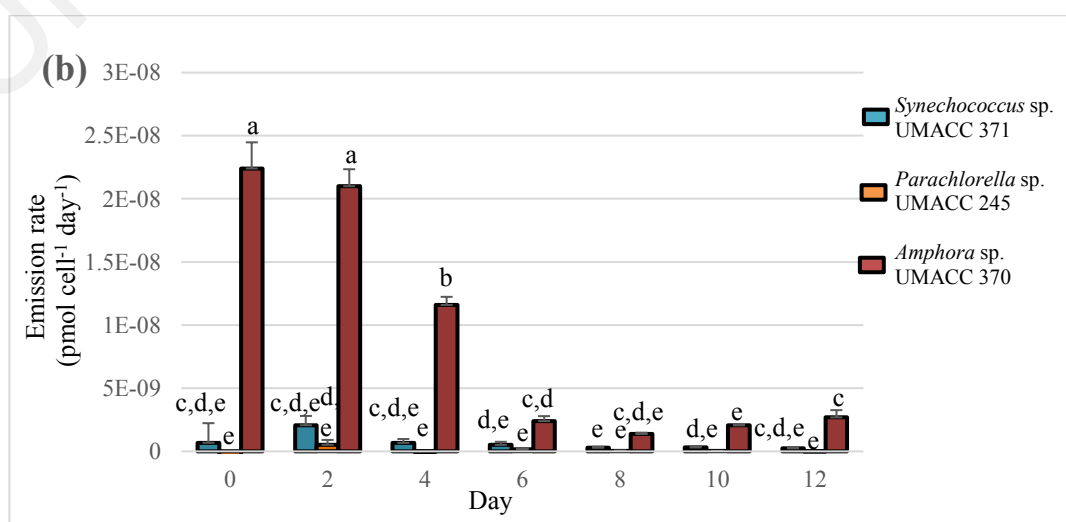
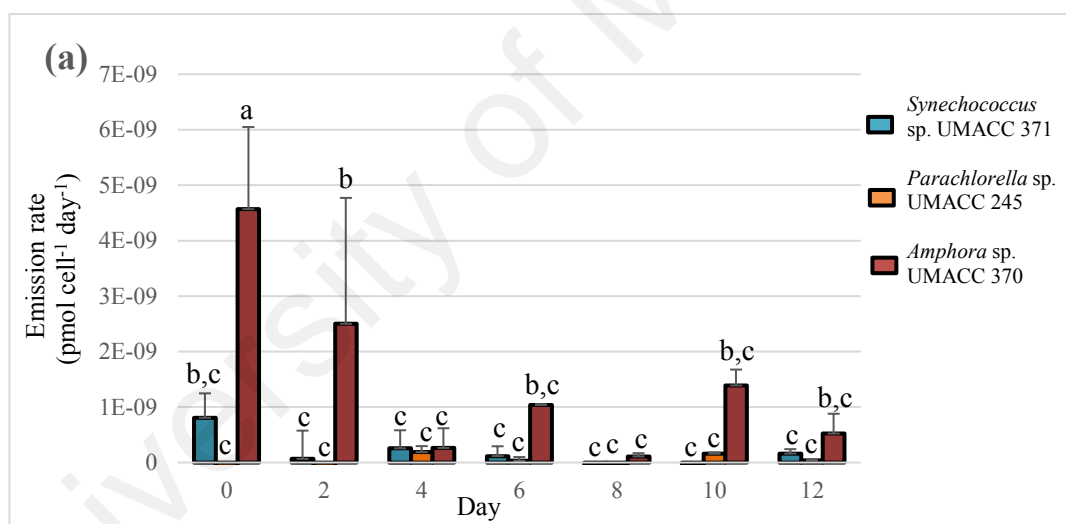


Figure 4.13: Emission rate normalized to chlorophyll-a. Concentration of compound (a) CHBr₃, (b) CH₃I, (c) CHCl₃, (d) CHBr₂Cl and (e) CH₂Br₂ normalized to real-time chlorophyll-a for the three tropical microalgae across 12 experimental days. Bar charts which contain different alphabets denote significant difference at ($p < 0.05$). $n = 3$

4.3.4.2 Normalization to cell density



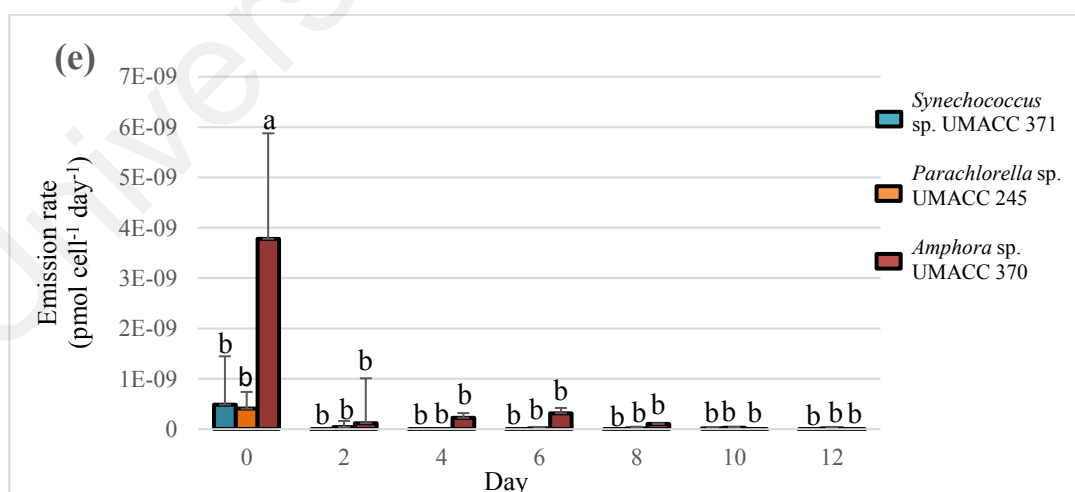
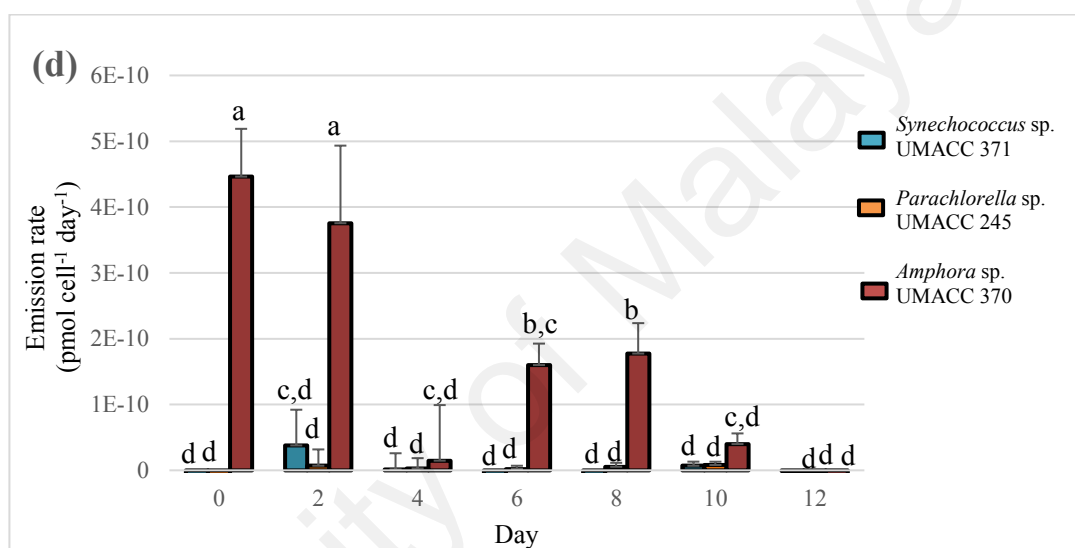
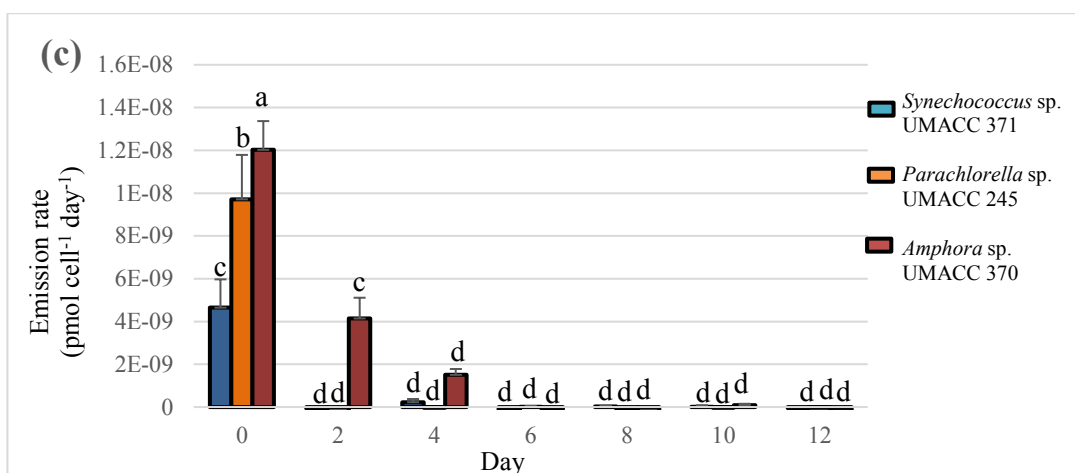


Figure 4.14: Emission rate normalized to cell density. Concentration of compound (a) CHBr_3 , (b) CH_3I , (c) CHCl_3 , (d) CHBr_2Cl and (e) CH_2Br_2 normalized to cell density for the three tropical microalgae across 12 experimental days. Bar charts which contain different alphabets denote significant difference at ($p < 0.05$). $n = 3$

4.3.5 Comparison of emission rates of halocarbons by growth phases

Table 4.6 (a-c) show the estimated (upper and lower limits) emission rate of measured halocarbons under conditions of the experiments by the three tropical marine microalgae. *Amphora* sp. UMACC 370 showed the highest emission rates for methyl iodide (CH_3I) in both exponential and stationary phases, reporting $14.18 - 86.79 \text{ pmol (mg chl-a)}^{-1} \text{ day}^{-1}$ and $10.02 - 18.08 \text{ pmol (mg chl-a)}^{-1} \text{ day}^{-1}$ respectively when normalized to chlorophyll-a, and $2.05 - 24.05 \text{ pmol (10}^9 \text{ cell)}^{-1} \text{ day}^{-1}$ (exponential) and $1.29 - 3.16 \text{ pmol (10}^9 \text{ cell)}^{-1} \text{ day}^{-1}$ (stationary) when normalized to cell density, as compared to *Synechococcus* sp. UMACC 370 and *Parachlorella* sp. UMACC 245. Estimated emission rates of CH_3I for *Amphora* sp. UMACC 370, *Synechococcus* sp. UMACC 371 and *Parachlorella* sp. UMACC 245 based on chlorophyll-a and cell density were higher in exponential phase than in stationary phase, except in case of *Synechococcus* sp. UMACC 371 where the emission of CH_3I was lower in exponential phase as compared to its stationary phase.

Table 4.6: Emission rate at different growth phases. Concentrations of five halocarbons normalized to chlorophyll-a ($\text{pmol mg chl-a}^{-1} \text{ day}^{-1}$) and cell density ($\text{pmol (10}^9 \text{ cell)}^{-1} \text{ day}^{-1}$) at exponential and stationary phase for (a) *Synechococcus* sp. UMACC 371, (b) *Parachlorella* sp. UMACC 245 and (c) *Amphora* sp. UMACC 370.

(a)				
Compound	Exponential phase		Stationary Phase	
	$\text{pmol (mg chl-a)}^{-1} \text{ day}^{-1}$	$\text{pmol (10}^9 \text{ cell)}^{-1} \text{ day}^{-1}$	$\text{pmol (mg chl-a)}^{-1} \text{ day}^{-1}$	$\text{pmol (10}^9 \text{ cell)}^{-1} \text{ day}^{-1}$
CHBr_3	0.00 – 5.97	0.00 – 1.18	0.00 – 1.58	0.00 - 0.32
CH_3I	0.00 – 12.27	0.00 – 2.70	0.74 – 2.23	0.16 – 0.79
CHCl_3	0.00 – 30.96	0.00 – 5.95	0.00 – 0.37	0.00 - 0.07
CHBr_2Cl	0.00 -- 0.13	0.00 - 0.07	0.00 - 0.07	0.00 - 0.01
CH_2Br_2	0.00 – 8.23	0.00 – 1.58	0.00 - 0.21	0.00 - 0.04

(b)				
Compound	Exponential phase		Stationary Phase	
	pmol (mg chla) ⁻¹ day ⁻¹	pmol (10 ⁹ cell) ⁻¹ day ⁻¹	pmol (mg chla) ⁻¹ day ⁻¹	pmol (10 ⁹ cell) ⁻¹ day ⁻¹
CHBr ₃	0.00 – 1.16	0.00 – 0.30	0.00 – 1.28	0.00 - 0.19
CH ₃ I	0.00 – 3.36	0.00 – 0.83	0.00 – 1.02	0.00 - 0.23
CHCl ₃	0.00 – 48.68	0.00 – 12.11	0.00 – 0.26	0.00 – 0.05
CHBr ₂ Cl	0.00 - 0.22	0.00 - 0.05	0.00 - 0.08	0.00 - 0.01
CH ₂ Br ₂	0.00 – 2.63	0.00 - 0.66	0.00 - 0.33	0.00 - 0.04

(c)				
Compound	Exponential phase		Stationary Phase	
	pmol (mg chla) ⁻¹ day ⁻¹	pmol (10 ⁹ cell) ⁻¹ day ⁻¹	pmol (mg chla) ⁻¹ day ⁻¹	pmol (10 ⁹ cell) ⁻¹ day ⁻¹
CHBr ₃	0.00 – 22.46	0.00 – 5.97	0.45 – 8.81	0.09 – 1.59
CH ₃ I	14.18 – 86.79	2.05 – 24.05	10.02 – 18.08	1.29 – 3.16
CHCl ₃	0.00 – 48.51	0.00 – 12.90	0.00 – 1.27	0.00 – 0.15
CHBr ₂ Cl	0.00 – 1.84	0.00 - 0.49	0.00 – 1.89	0.00 - 0.21
CH ₂ Br ₂	0.00 – 14.04	0.00 – 5.85	0.00 – 2.77	0.00 – 0.44

The estimated emission rates of CHBr₃, CH₂Br₂, CHCl₃, CH₃I and CHBr₂Cl for *Amphora* sp. UMACC 370 were all higher in exponential phase than in stationary phase, except the emission rate based on chlorophyll-a for CHBr₂Cl during exponential phase (1.84 pmol (mg chla)⁻¹ day⁻¹) was lower than in stationary phase (1.89 pmol (mg chla)⁻¹ day⁻¹). *Synechococcus* sp. UMACC 370 reported higher range of CH₃I and CHCl₃ emission rates in log phase than in stationary phase based on chlorophyll-a, whereas higher range of emission rates for CH₃I, CHBr₃, CHCl₃ and CH₂Br₂ based on cell density. *Parachlorella* sp. UMACC 245 reported lower estimated emission rates for CHBr₃, CHCl₃, CH₂Br₂ and CHBr₂Cl during exponential phase as compared to its stationary phase.

Estimated emission rate of CHCl_3 was higher in exponential phase as compared to stationary phase; $30.96 \text{ pmol (mg chl-a)}^{-1} \text{ day}^{-1}$ and $0.37 \text{ pmol (mg chl-a)}^{-1} \text{ day}^{-1}$ respectively for *Synechococcus* sp. UMACC 371, $48.51 \text{ pmol (mg chl-a)}^{-1} \text{ day}^{-1}$ and $1.27 \text{ pmol (mg chl-a)}^{-1} \text{ day}^{-1}$, respectively for *Amphora* sp. UMACC 370. *Parachlorella* sp. UMACC 245 had higher emission rates during the exponential phase as compared to its stationary phase based on chlorophyll-a and cell density.

Out of the three brominated compounds, estimated emission rates for CHBr_3 was higher than CH_2Br_2 and CHBr_2Cl during stationary phase based on chlorophyll-a across all three tropical marine microalgae. The estimated emission rates of CHBr_3 , CH_2Br_2 and CHBr_2Cl by *Synechococcus* sp. UMACC 371 based on chlorophyll-a and cell density during exponential phase were higher as compared to their stationary phase. Higher estimated emission rates based on chlorophyll-a during stationary phase than in exponential phase was observed for CHBr_3 and CHBr_2Cl both by *Parachlorella* sp. UMACC 245 and *Amphora* sp. UMACC 370, except for CH_2Br_2 where emission rate during exponential phase was higher than its stationary phase. *Amphora* sp. UMACC 370 had at least two times higher of CH_2Br_2 , CHBr_3 and CHBr_2Cl emission rates during both exponential and stationary phases based on chlorophyll-a. *Chlorella* sp. UMACC 245 showed the least emission rates of all three brominated compounds during exponential phase as compared to *Synechococcus* sp. UMACC 371. Higher emission rates based on chlorophyll-a for the three brominated compounds during stationary phase than exponential phase was observed.

4.3.6 Emission rate as a whole in percentage

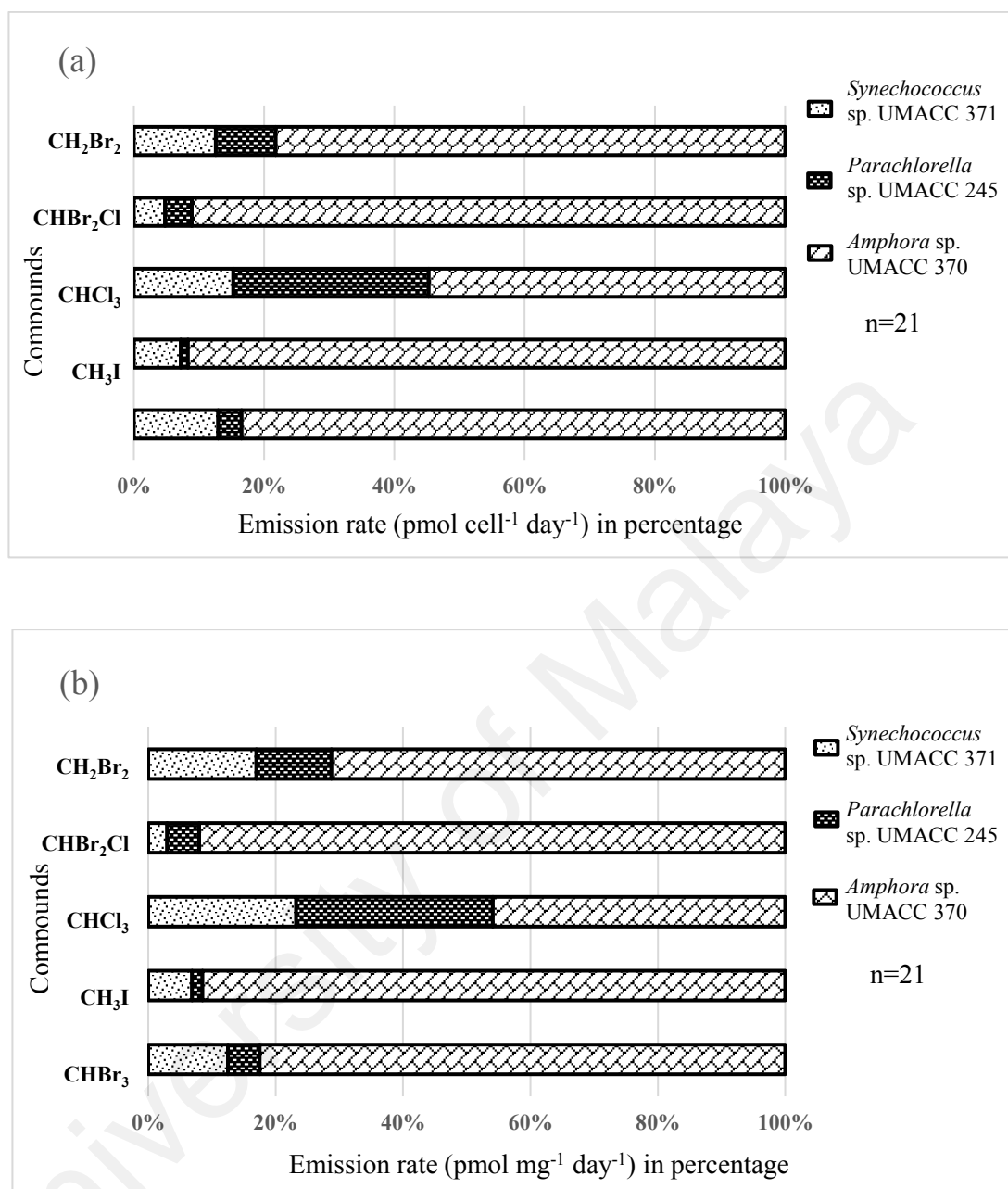


Figure 4.15: Total emission rate in percentage. Total rate of emission (%) of every five halocarbons in comparison amongst the three tropical marine microalgae based on (a) cell number and (b) chlorophyll-a.

Data for emission rate for all 12 days of cultures were combined (n=21) and were expressed and compared in percentage in terms of five compounds amongst the three microalgae. In Figure 4.15, *Amphora* sp. UMACC 370, consisting the majority of emission rate percentage for all five compounds, showed higher emission rate percentage as compared to *Synechococcus* sp. UMACC 371 and *Parachlorella* sp. UMACC 245. In

other words, *Amphora* sp. UMACC 370 was clearly a stronger emitter of the five halogenated compounds as compared to the other two taxa based on chlorophyll-a and cell density.

4.3.7 Correlation of detected halocarbons

The emission rates for all five compounds based on chlorophyll-a, cell density and both as summarized in Table 4.7 (a-c) were highly ($p < 0.01$) correlated.

Table 4.7: Correlation of the halocarbons. Pearson Product-Moment correlation coefficient (r) of the emission rate from the five detected compounds in term of (a) chlorophyll-a, (b) cell density, (c) chlorophyll-a and cell density.

(a)	CHBr ₃	CH ₃ I	CHCl ₃	CHBr ₂ Cl	CH ₂ Br ₂
CHBr ₃	1.0000	0.7122**	0.4224**	0.6016**	0.4642**
CH ₃ I	0.7122**	1.0000	0.4828**	0.6390**	0.6195**
CHCl ₃	0.4224**	0.4828**	1.0000	0.3081*	0.6543**
CHBr ₂ Cl	0.6016**	0.6390**	0.3081*	1.0000	0.4659**
CH ₂ Br ₂	0.4642**	0.6195*	0.6543**	0.4659**	1.0000

Number of replicates (n) = 63, ** = (p) < 0.01; * = (p) < 0.05

(b)	CHBr ₃	CH ₃ I	CHCl ₃	CHBr ₂ Cl	CH ₂ Br ₂
CHBr ₃	1.0000	0.7864**	0.6176**	0.8391**	0.6266**
CH ₃ I	0.7864**	1.0000	0.5964**	0.8489**	0.6430**
CHCl ₃	0.6176**	0.5964**	1.000	0.5872**	0.6872**
CHBr ₂ Cl	0.8391**	0.8489**	0.5872**	1.0000	0.6070**
CH ₂ Br ₂	0.6266**	0.6430**	0.6872**	0.6070**	1.0000

Number of replicates (n) = 63, ** indicates significance level (p) < 0.01

(c)	CHBr ₃ ^a	CH ₃ I ^a	CHCl ₃ ^a	CHBr ₂ Cl ^a	CH ₂ Br ₂ ^a
CHBr ₃ ^b	0.8390**	0.5278**	0.4296*	0.6061**	0.4269**
CH ₃ I ^b	0.8018**	0.8969**	0.5593*	0.7816**	0.6087**
CHCl ₃ ^b	0.5228**	0.4419**	0.9511*	0.4412**	0.5715**
CHBr ₂ Cl	0.6152**	0.5217**	0.3628*	0.8200**	0.4114**
CH ₂ Br ₂ ^b	0.6254**	0.6003**	0.7117*	0.5977**	0.9610**

Number of replicates (n) = 126, ** indicates significance level (p) < 0.01, ^a denotes chlorophyll a-normalized compounds; ^b denotes cell density-normalized compounds

4.3.8 Axenicity of cultures

All cultures were checked by culture on nutrient agar prior to start of experiment, and shown to be free of bacterial contamination, hence the net production of halocarbons observed relative to the subtraction of the controls are ascribed to the microalgal cultures.

4.4 Experiment 4: Effects of different irradiances on halocarbon emission

4.4.1 Growth response and pH changes

The changes of chlorophyll-a and cell density, specifically the increase of chlorophyll a and cell density as observed in Figure 4.16 and Figure 4.17 shown in percentage, were used to normalize with the emission before and after 12-hour light-exposure, which will be shown in this chapter later, in order to determine the emission rates of halocarbons from the three tropical marine microalgae.

With 40 $\mu\text{mol photons m}^{-2} \text{ s}^{-1}$ serving as the control of the irradiance experiments, chlorophyll-a decreased when exposed to higher irradiance (120 $\mu\text{mol photons m}^{-2} \text{ s}^{-1}$) for *Synechococcus* sp. UMACC 371 and *Parachlorella* sp. UMACC 245 as compared to *Amphora* sp. UMACC 370 (Figure 4.16) that increased. The opposite was observed when measured with cell density (Figure 4.17).

The percentage change in chlorophyll a and cell density decreased for *Amphora* sp. UMACC 370 and *Parachlorella* sp. but increased for *Synechococcus* sp. UMACC 371 when exposed to complete darkness (0 $\mu\text{mol photons m}^{-2} \text{ s}^{-1}$) as compared to the control experiment (40 $\mu\text{mol photons m}^{-2} \text{ s}^{-1}$).

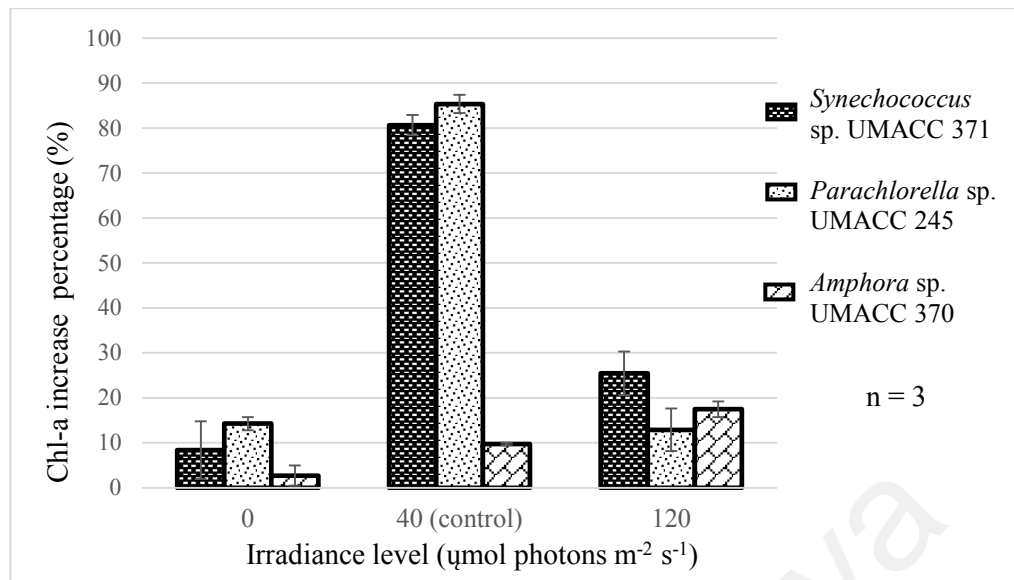


Figure 4.16: Changes (%) in chlorophyll-a before and after 12-hour of light-exposure of the three microalgae under three different irradiance levels.

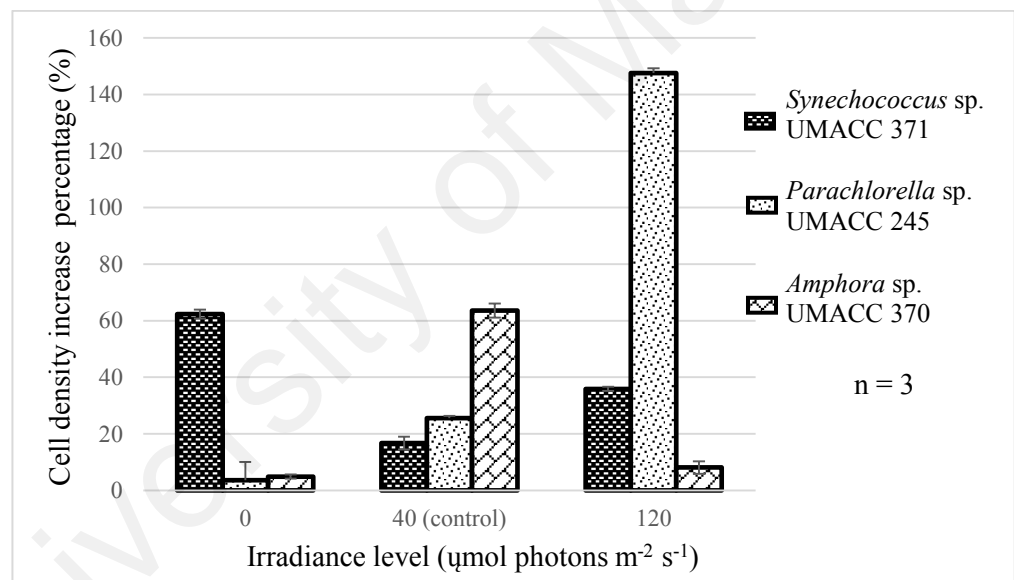


Figure 4.17: Changes (%) in cell density before and after 12-hour light-exposure of the three microalgae under three different irradiance levels.

To further assess the growth of the microalgae for all three different irradiances, other growth parameters were taken into account and recorded such as dry weight (Figure 4.18), Optical Density, $\text{OD}_{620\text{nm}}$ (Figure 4.19), and carotenoid content (Figure 4.20).

The increase or decrease of the biomass varied amongst different algal species. For instance, no more than 15% of a change in biomass was observed for dry weight, except a large percentage increase for *Parachlorella* sp. UMACC 245 from 0 $\mu\text{mol photons m}^{-2}$

s^{-1} to $120 \mu\text{mol photons m}^{-2} s^{-1}$, and large decrease and increase of other biomasses ranging as low as 2% to more than 100% in chlorophyll-a, cell density and $OD_{620\text{nm}}$ and carotenoids.

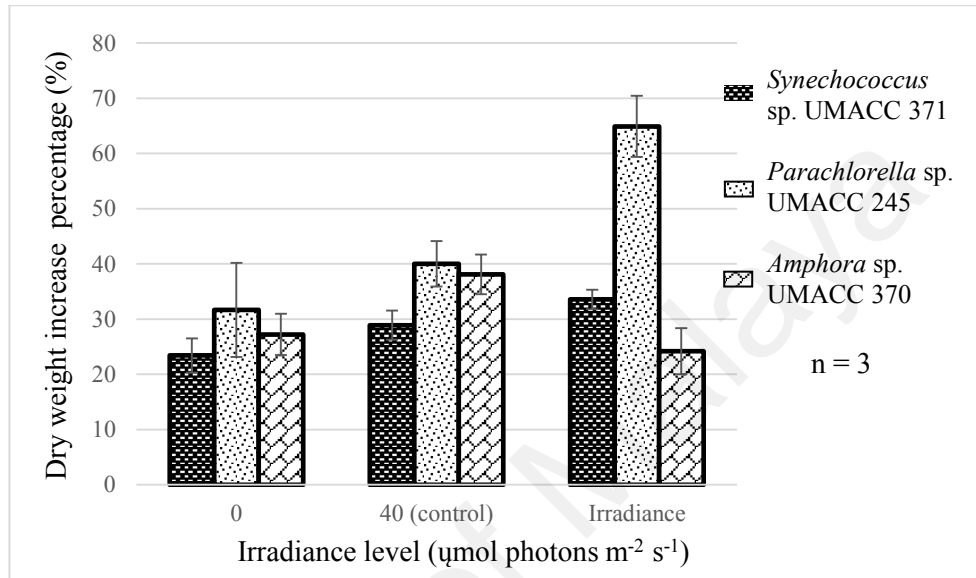


Figure 4.18: Changes (%) in dry weight before and after 12-hour light-exposure of the three microalgae under three different irradiance levels.

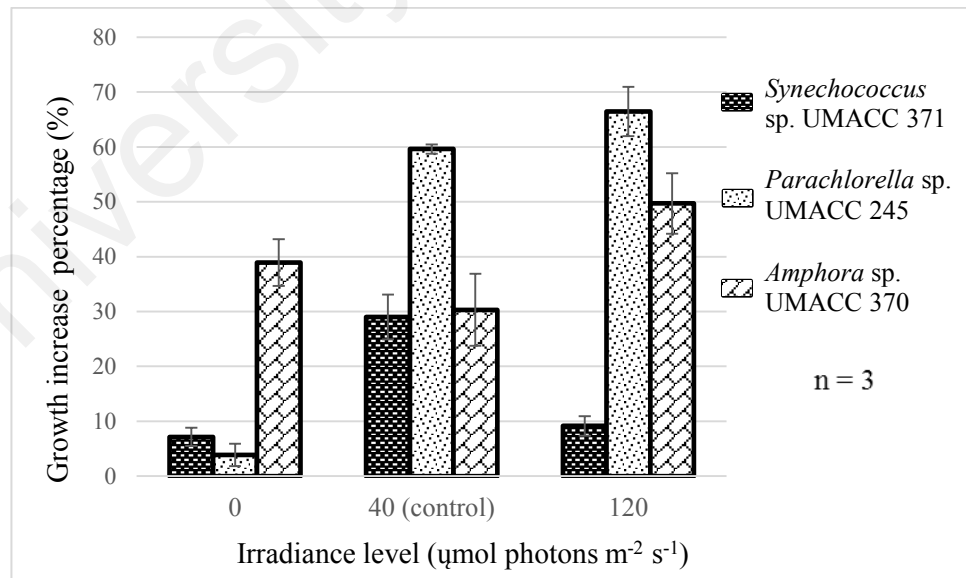


Figure 4.19: Changes (%) in $OD_{620\text{nm}}$ before and after 12-hour light-exposure of the three microalgae under different irradiance levels.

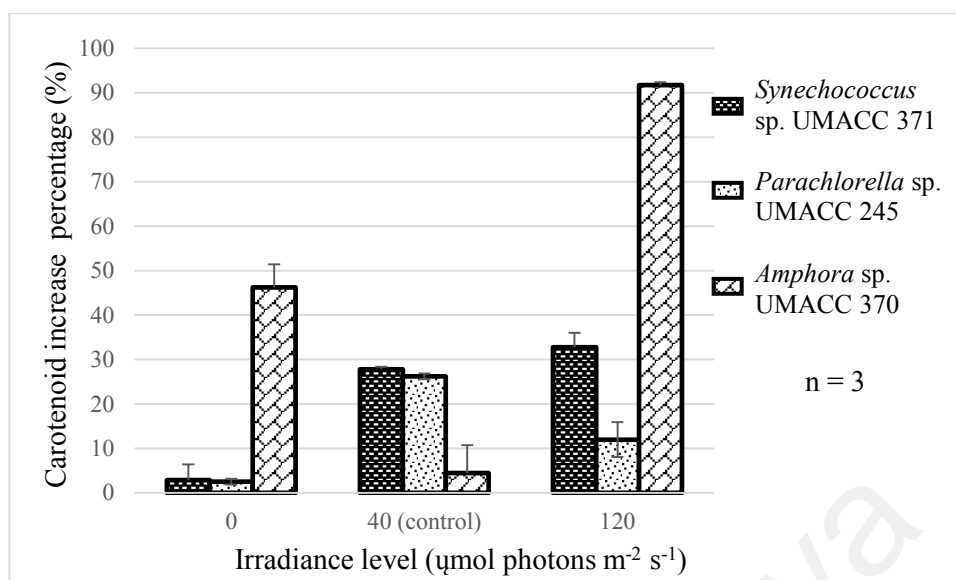


Figure 4.20: Changes (%) in carotenoids before and after 12-hour light-exposure of the three microalgae under different irradiance levels.

The pH of the culture medium was measured in triplicates as pH before and after the light-exposure as shown in Figure 4.21 to allow interpretation of cell physiological changes with its surroundings with regards to halocarbon emissions. All three microalgae in general showed a decrease in pH after exposure to 12-hour of complete darkness and an increase in pH after exposure to higher irradiance ($120 \mu\text{mol photons m}^{-2} \text{s}^{-1}$) for the same amount of time. When exposed to the control level of irradiance ($40 \mu\text{mol photons m}^{-2} \text{s}^{-1}$), all three microalgae also showed an increase in pH, though the increased pH in $120 \mu\text{mol photons m}^{-2} \text{s}^{-1}$ was higher than the control irradiance level.

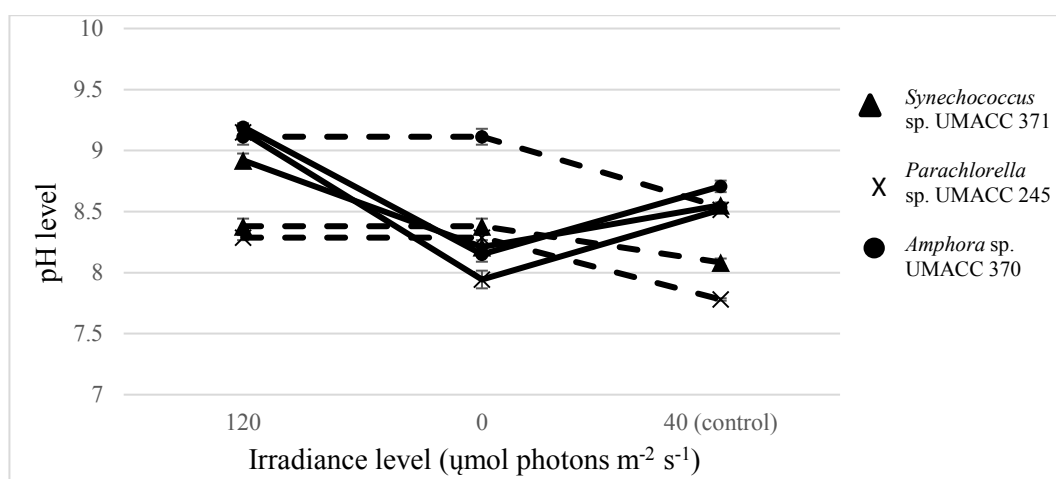


Figure 4.21: Changes of pH before (dashed lines) and after (solid lines) 12-hour light-exposure of the three microalgae under three different irradiance levels. $n = 3$.

4.4.2 Changes of F_v/F_m as algal cell stress indicator

The maximum quantum yield, F_v/F_m , was measured as an indication of physiological state (health) of the cells (Hughes *et al.* 2006; Keng *et al.*, 2013). It is thus a good biological tool that can be used to explain the relationship between cell stress and halocarbon emission or production.

Figure 4.22 shows the F_v/F_m measured before and after 12-hour light-exposure acclimatization for all three microalgae in triplicates. A decrease in F_v/F_m after 12 hour of acclimatization under all three different irradiances, 0, 40 and $120 \mu\text{mol photons m}^{-2} \text{s}^{-1}$ was observed for all microalgae, except an increase by *Amphora* sp. UMACC 370 at 0 $\mu\text{mol photons m}^{-2} \text{s}^{-1}$ and $40 \mu\text{mol photons m}^{-2} \text{s}^{-1}$. At $120 \mu\text{mol photons m}^{-2} \text{s}^{-1}$, the decrease in F_v/F_m was larger as compared to other irradiances.

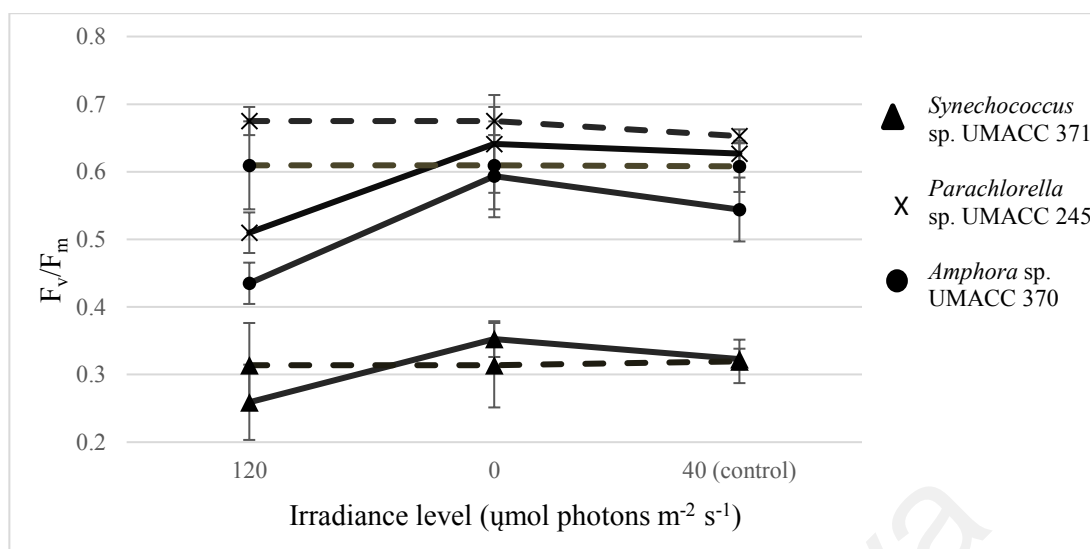


Figure 4.22: Changes of maximum quantum yield, F_v/F_m , before (dashed lines) and after (solid lines) 12-hour light-exposure under three different irradiance levels for the three microalgae. $n = 3$.

When compared amongst taxa using mean F_v/F_m as shown in Table 4.8, there was a decrease in F_v/F_m across all three microalgae when comparing the control irradiance ($40 \mu\text{mol photons m}^{-2} \text{s}^{-1}$) and the higher irradiance ($120 \mu\text{mol photons m}^{-2} \text{s}^{-1}$). When cultures were exposed to complete darkness, *Synechococcus* sp. UMACC 371 and *Parachlorella* sp. UMACC 245 showed an increase in F_v/F_m , 0.32 to 0.334 and 0.64 to 0.66 respectively while *Amphora* sp. UMACC 370 showed a decrease in F_v/F_m , from 0.576 to 0.558.

Table 4.8: Mean $F_v/F_m \pm \text{S.D.}$ values of the microalgae measured under different irradiance levels. Data was statistically analyzed using Factorial ANOVA. Data presented are mean values of F_v/F_m from a total of 36 replicates ($n = 36$). Different letters denote standard deviation (S.D.) homogenous group ($p < 0.01$) according to post hoc Tukey's test.

Irradiance ($\mu\text{mol photons m}^{-2} \text{s}^{-1}$)	<i>Synechococcus</i> sp. UMACC 371	<i>Parachlorella</i> sp. UMACC 245	<i>Amphora</i> sp. UMACC 370
0	0.334 (± 0.021) ^b	0.658(± 0.020) ^{c,d}	0.558(± 0.010) ^{c,d}
40	0.320 (± 0.007) ^b	0.640 (± 0.021) ^c	0.576(± 0.037) ^{a,d}
120	0.288 (± 0.029) ^b	0.592(± 0.087) ^{a,c,d}	0.522(± 0.094) ^a

4.4.3 Comparison of halocarbon emissions amongst microalgae

Data acquired for the five halocarbon emission were used to normalize to biomass, chlorophyll-a and cell density to obtain emission rates. Figures 4.23 to 4.25 (chlorophyll-a normalized) and Figure 4.26 to 4.28 (cell density normalized) show the increase and decrease (indicated by positive and negative values respectively) of five halocarbon emission rates in percentage (%) after 12-hour exposure to different irradiances. This was assessed and grouped by taxa.

4.4.3.1 Normalization to chlorophyll-a

In Figure 4.23, *Synechococcus* sp. UMACC 371 showed an increase in emission rate for CH_3I , CHBr_3 and CH_2Br_2 when exposed to both complete darkness ($0 \mu\text{mol photons m}^{-2} \text{ s}^{-1}$) and higher irradiance ($120 \mu\text{mol photons m}^{-2} \text{ s}^{-1}$) as compared to the control irradiance ($40 \mu\text{mol photons m}^{-2} \text{ s}^{-1}$). CHBr_2Cl emission rate increased when exposed to 0 and $120 \mu\text{mol photons m}^{-2} \text{ s}^{-1}$ as compared to $40 \mu\text{mol photons m}^{-2} \text{ s}^{-1}$. The emission rate of CHBr_3 and CH_2Br_2 decreased when exposed to $40 \mu\text{mol photons m}^{-2} \text{ s}^{-1}$.

The emission rates of all five compounds, CHBr_3 , CH_3I , CHCl_3 , CHBr_2Cl and CH_2Br_2 for *Parachlorella* sp. UMACC 245 as shown in Figure 4.24 decreased when exposed to $40 \mu\text{mol photons m}^{-2} \text{ s}^{-1}$. All compounds except CH_3I showed an increase in emission rates when exposed to $120 \mu\text{mol photons m}^{-2} \text{ s}^{-1}$. All compounds except CH_2Br_2 showed an increase in emission rate when exposed to $0 \mu\text{mol photons m}^{-2} \text{ s}^{-1}$.

CHBr_3 emitted by *Amphora* sp. UMACC 370 in Figure 4.25 showed a decrease in emission rates when exposed to 40 and $120 \mu\text{mol photons m}^{-2} \text{ s}^{-1}$. When exposed to $120 \mu\text{mol photons m}^{-2} \text{ s}^{-1}$, the emission rate for CH_3I and CH_2Br_2 increased. The emission rate of CHBr_2Cl remained relatively unchanged when exposed to $120 \mu\text{mol photons m}^{-2} \text{ s}^{-1}$. When exposed to 0 and $120 \mu\text{mol photons m}^{-2} \text{ s}^{-1}$ as compared to $40 \mu\text{mol photons m}^{-2} \text{ s}^{-1}$, the emission rates of CH_3I increased, except for *Parachlorella* sp. UMACC 245 that

showed a decrease in emission when exposed to 120 $\mu\text{mol photons m}^{-2} \text{s}^{-1}$. All five compounds showed an increase in emission rates when exposed to 0 $\mu\text{mol photons m}^{-2} \text{s}^{-1}$.

1.

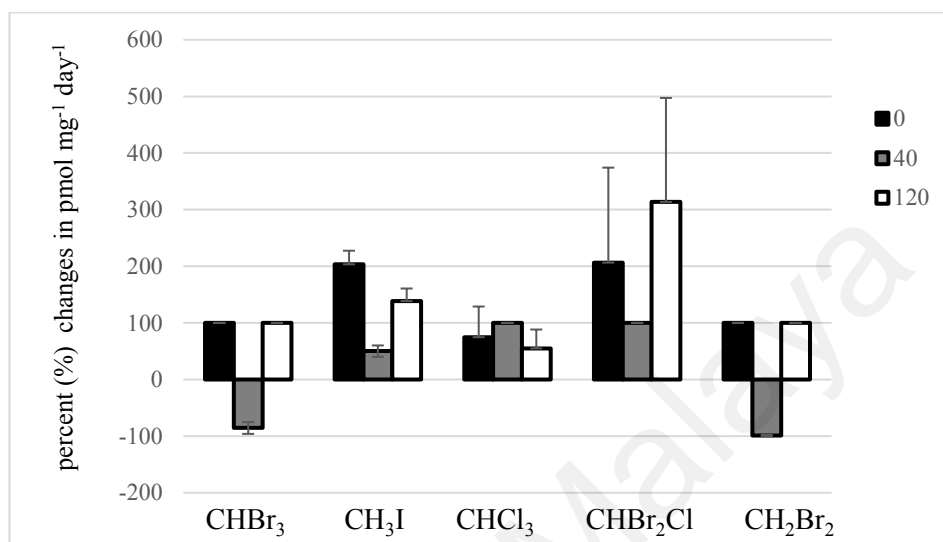


Figure 4.23: Percent changes of the five halocarbon emission rates normalized to chlorophyll-a by *Synechococcus* sp. UMACC 371 under three different irradiance levels, 0, 40, 120 $\mu\text{mol photons.m}^{-2} \text{s}^{-1}$.

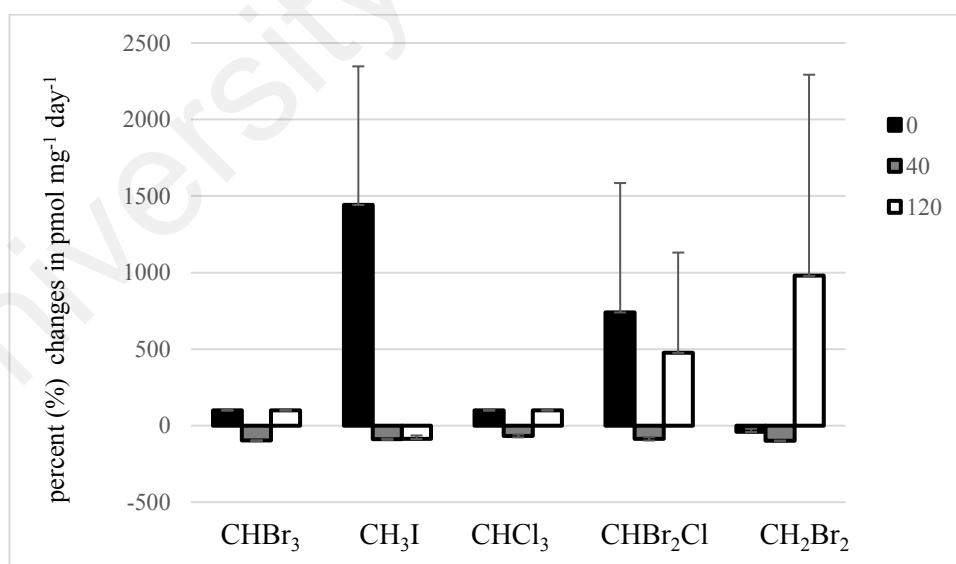


Figure 4.24: Percent changes of the five halocarbon emission rates normalized to chlorophyll-a by *Parachlorella* sp. UMACC 245 under three different irradiance levels, 0, 40, 120 $\mu\text{mol photons.m}^{-2} \text{s}^{-1}$.

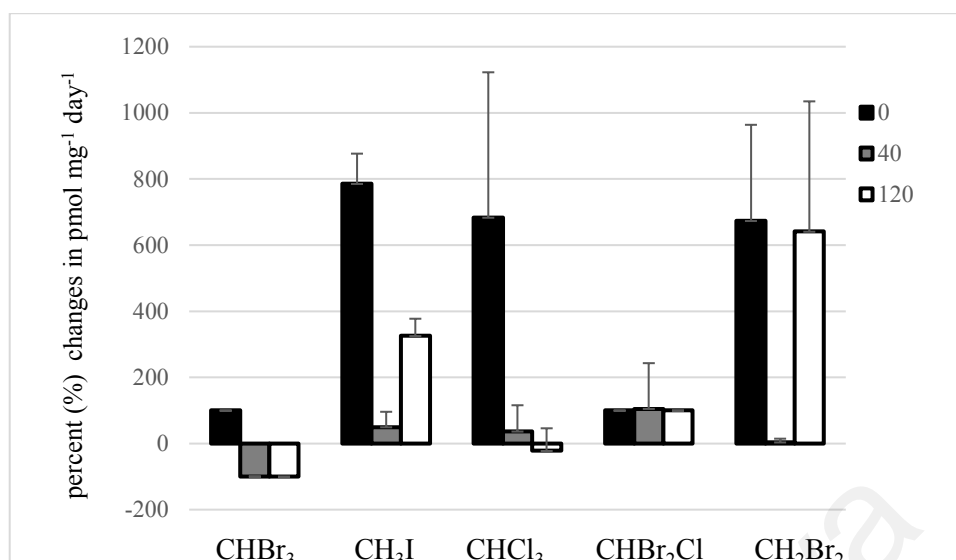


Figure 4.25: Percent changes of the five halocarbon emission rates normalized to chlorophyll-a by *Amphora* sp. UMACC 370 under three different irradiance levels, 0, 40, 120 $\mu\text{mol photons.m}^{-2}\text{s}^{-1}$.

4.4.3.2 Normalization to cell density

For *Synechococcus* sp. UMACC 371, the increase and decrease of emission rates for CHBr₃, CHCl₃, CHBr₂Cl and CH₂Br₂ normalized to cell density as observed in Figure 4.26 were similar to the emission rates normalized to chlorophyll-a. The emission rates for all five short-lived halocarbons normalized to cell density as observed in Figure 4.27 was consistent with the emission rates normalized to chlorophyll-a by *Parachlorella* sp. UMACC 245.

In Figure 4.28, the emission rate for all five compounds by *Amphora* sp. UMACC 370 increased when exposed to 0 $\mu\text{mol photons m}^{-2}\text{s}^{-1}$. When exposed to 120 $\mu\text{mol photons m}^{-2}\text{s}^{-1}$, the emission rate of CH₃I, CHBr₂Cl and CH₂Br₂ increased. The emission rate of CH₃I increased when exposed to both 0 and 120 $\mu\text{mol photons m}^{-2}\text{s}^{-1}$ as compared to 40 $\mu\text{mol photons m}^{-2}\text{s}^{-1}$.

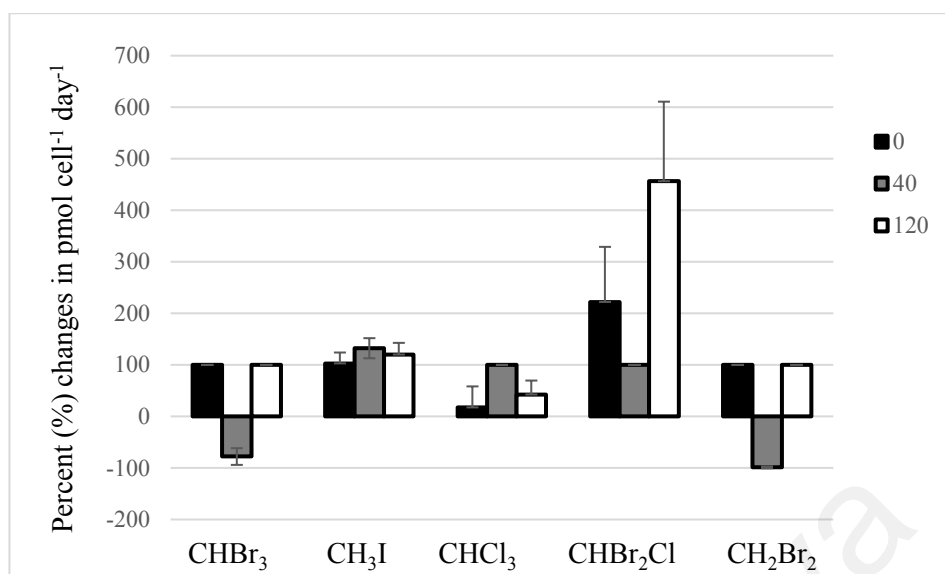


Figure 4.26: Percent changes of the five halocarbon emission rates normalized to cell density by *Synechococcus* sp. UMACC 371 under three different irradiance levels, 0, 40, 120 $\mu\text{mol photons.m}^{-2} \text{s}^{-1}$.

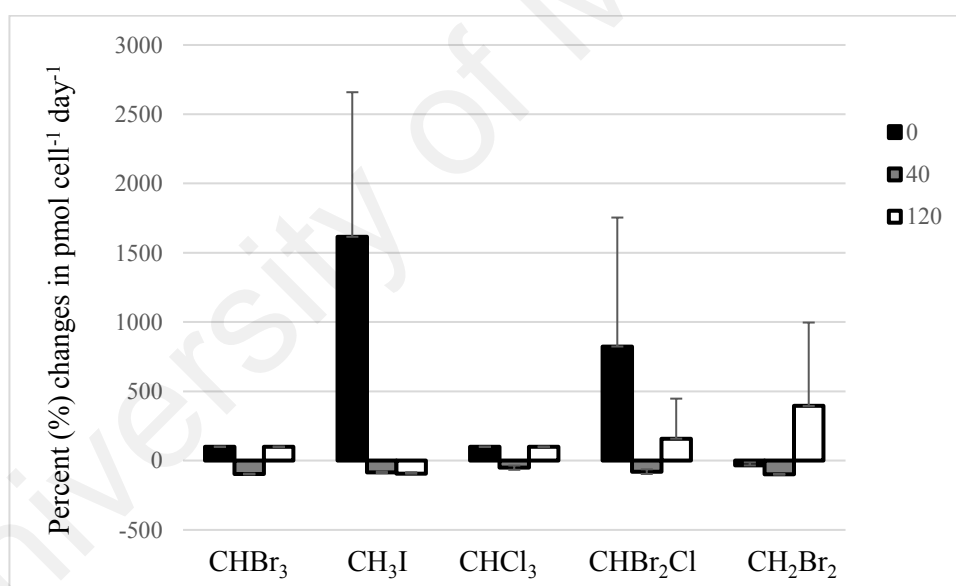


Figure 4.27: Percent changes of the five halocarbon emission rates normalized to cell density by *Parachlorella* sp. UMACC 245 under three different irradiance levels, 0, 40, 120 $\mu\text{mol photons.m}^{-2} \text{s}^{-1}$.

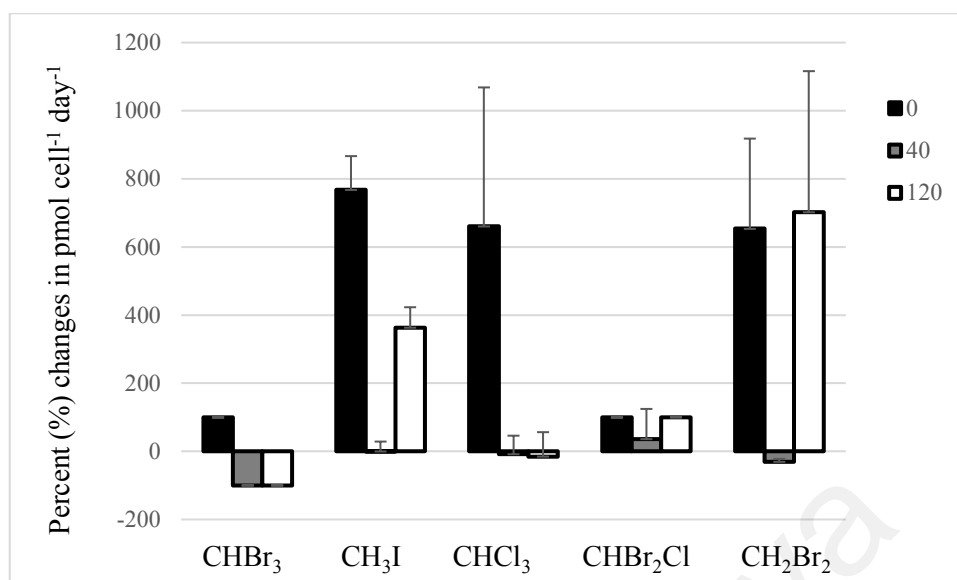


Figure 4.28: Percent changes of the five halocarbon emission rates normalized to cell density by *Amphora* sp. UMACC 370 under three different irradiance levels, 0, 40, 120 $\mu\text{mol photons.m}^{-2} \text{s}^{-1}$.

4.4.4 Comparisons between irradiance and F_v/F_m amongst microalgae

Figure 4.29 shows significant ($p < 0.05$) decrease and increase in F_v/F_m of the three microalgae after 12-hour of irradiance exposure to 0, 40 and 120 $\mu\text{mol photons m}^{-2} \text{s}^{-1}$. Cultures that were exposed to higher irradiance (120 $\mu\text{mol photons m}^{-2} \text{s}^{-1}$) as compared to control irradiance (40 $\mu\text{mol photons m}^{-2} \text{s}^{-1}$) showed a decrease (negative values) in the F_v/F_m across all three microalgae. *Parachlorella* sp. UMACC 245 showed a significant ($p < 0.05$) decrease, indicating the largest decrease in F_v/F_m as compared to the other two taxa. After exposure to 12-hour of complete darkness, the F_v/F_m for *Synechococcus* sp. UMACC 371 and *Amphora* sp. UMACC 370 increased but decreased for *Parachlorella* sp. UMACC 245.

Table 4.9 shows multiple comparisons of the effect of irradiance on the changes in F_v/F_m for each microalgae. The changes in F_v/F_m were significant ($p < 0.05$) for all pairwise (Bonferroni) interactions at all levels of irradiance by the three microalgae, except the comparison of F_v/F_m between irradiance 0 and 40 $\mu\text{mol photons m}^{-2} \text{s}^{-1}$ by *Parachlorella* sp. UMACC 245.

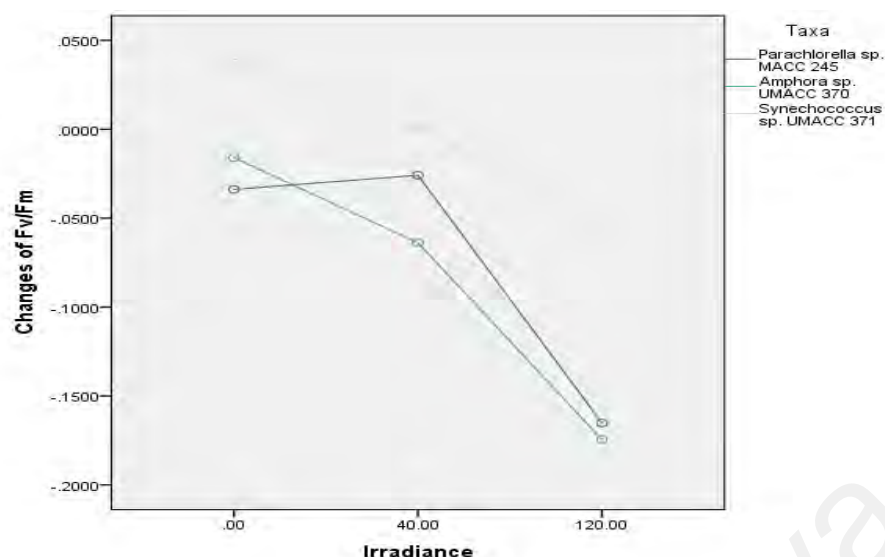


Figure 4.29: Changes of maximum quantum yield, F_v/F_m , across three different irradiance levels (0, 40, 120 $\mu\text{mol photons m}^{-2} \text{ s}^{-1}$) by the three microalgae. $n=9$.

Table 4.9: Pairwise comparisons of the F_v/F_m at different irradiances (0, 40, 120 $\mu\text{mol photons m}^{-2} \text{ s}^{-1}$) amongst the three microalgae. $n = 27$.

Pairwise Comparisons Dependent Variable: F_v/F_m					
Taxa	(I) Light	(J) Light	Mean Difference (I – J)	Std. Error	Sig. ^b
<i>Parachlorella</i> sp. UMACC 245	0	40	-.008	.005	.447
		120	.131*	.005	.000
	40	0	.008	.005	.447
		120	.139*	.005	.000
	120	0	-.131*	.005	.000
		40	-.139*	.005	.000
<i>Amphora</i> sp. UMACC 370	0	40	.048*	.005	.000
		120	.159*	.005	.000
	40	0	-.048*	.005	.000
		120	.111*	.005	.000
	120	0	-.159*	.005	.000
		40	-.111*	.005	.000
<i>Synechococcus</i> sp. UMACC 371	0	40	.038*	.005	.000
		120	.091*	.005	.000
	40	0	-.038*	.005	.000
		120	.054*	.005	.000
	120	0	-.091*	.005	.000
		40	-.054*	.005	.000

Based on estimated marginal means.

*. The mean difference is significant at the 0.05 level.

b. Adjustment for multiple comparisons: Bonferroni.

4.4.5 Correlation of halocarbon emission rates

The correlation of the emission rates for all five compounds are summarized in Table 4.10 based on chlorophyll-a, cell density and both, respectively. Emission rates normalized to chlorophyll-a were highly-correlated ($p < 0.01$) for all compounds. Emission rates normalized to cell density were non-significant. When pooled together to correlate the emission rates normalized to cell density and chlorophyll-a, CH_3I , CHCl_3 and CH_2Br_2 were highly positive correlated ($p < 0.01$), CHBr_2Cl was correlated ($p < 0.05$) while CHBr_3 was not significantly ($p < 0.05$) correlated. The correlation implies that emission rates normalized to chlorophyll a were independent of those normalized to cell density.

Table 4.10: Correlation of the halocarbons. Pearson Product-Moment correlation coefficient (r) of the emission rate from the five detected compounds in term of (a) chlorophyll-a, (b) cell density, (c) chlorophyll-a and cell density produced by the three microalgae with irradiance.

(a)	CHBr_3	CH_3I	CHCl_3	CH_2Br_2	CHBr_2Cl
CHBr_3	1.000	0.621**	0.698**	0.846**	0.808**
CH_3I	0.621**	1.000	0.456*	0.650**	0.579**
CHCl_3	0.698**	0.456*	1.000	0.615**	0.694**
CH_2Br_2	0.846**	0.650**	0.615**	1.000	0.678**
CHBr_2Cl	0.808**	0.579**	0.694**	0.678**	1.000

** indicates significance level ($p < 0.01$); * = ($p < 0.05$). n = 27

(b)	CHBr_3	CH_3I	CHCl_3	CH_2Br_2	CHBr_2Cl
CHBr_3	1.000	-0.166 ^{NS}	0.059 ^{NS}	-0.152 ^{NS}	-0.063 ^{NS}
CH_3I	-0.166 ^{NS}	1.000	0.317 ^{NS}	0.488**	0.804**
CHCl_3	0.059 ^{NS}	0.317 ^{NS}	1.000	0.225 ^{NS}	0.278 ^{NS}
CH_2Br_2	-0.152 ^{NS}	0.488**	0.225 ^{NS}	1.000	0.308 ^{NS}
CHBr_2Cl	-0.063 ^{NS}	0.804**	0.278 ^{NS}	0.308 ^{NS}	1.000

^{NS} Non-significant emission rate data were pooled from triplicates for three irradiance levels. ** indicates significance level ($p < 0.01$). n = 27

(c)	CHBr ₃ ^a	CH ₃ I ^a	CHCl ₃ ^a	CH ₂ Br ₂ ^a	CHBr ₂ Cl ^a
CHBr ₃ ^b	0.379 ^{NS}	0.160 ^{NS}	0.255 ^{NS}	0.470*	0.340 ^{NS}
CH ₃ I ^b	0.051 ^{NS}	0.548**	0.339 ^{NS}	0.715**	0.550**
CHCl ₃ ^b	0.028 ^{NS}	0.161 ^{NS}	0.621*	0.360 ^{NS}	0.312 ^{NS}
CH ₂ Br ₂ ^b	0.047 ^{NS}	0.125 ^{NS}	0.157 ^{NS}	0.712**	0.225 ^{NS}
CHBr ₂ Cl ^b	0.080 ^{NS}	0.125 ^{NS}	0.279 ^{NS}	0.371 ^{NS}	0.419*

NS Non-significant emission rate data were pooled from triplicates for three irradiance levels. ** indicates significance level (p) < 0.01; * = (p) < 0.05. n = 54. ^a denotes cell density-normalized compounds; ^b denotes chlorophyll a-normalized compounds

4.4.6 Pairwise comparisons between halocarbon emission rates and irradiances amongst microalgae

Pairwise comparisons showed a specific relationship of significant (p <0.05) changes in halocarbon emission rates compared amongst different irradiances for every taxa, as well as the significant (p <0.05) changes in halocarbon emission rates compared amongst different taxa for each irradiance level, chlorophyll-a and cell density-normalized emissions.

4.4.6.1 Normalization to chlorophyll-a

The pairwise comparisons of changes in halocarbon emission rates normalized to chlorophyll-a are summarized by compound, namely CHBr₃ (Figure 4.30), CH₃I (Figure 4.31), CHCl₃ (Figure 4.32), CH₂Br₂ (Figure 4.33) and CHBr₂Cl (Figure 4.34) for all three microalgae under three irradiances. Pairwise comparisons with significant (p <0.05) changes in halocarbon emission rates involving two factors, irradiances and taxa, are summarized in tables based on all five compounds, namely CHBr₃ (Table 4.11), CH₃I (Table 4.12), CHCl₃ (Table 4.13), CH₂Br₂ (Table 4.14) and CHBr₂Cl (Table 4.15). The increase and decrease of halocarbon emission rates after 12-hour exposure to different irradiances for all three microalgae are indicated with positive and negative values in figures and tables.

Figure 4.30 and Table 4.11 showed significant ($p<0.05$) changes in halocarbon emission rates at 0, 40 and 120 $\mu\text{mol photons m}^{-2} \text{ s}^{-1}$ for *Parachlorella* sp. UMACC 245 but not *Synechococcus* sp. UMACC 371 and *Amphora* sp. UMACC 370. All three taxa showed significant ($p<0.05$) changes in CH_3I emission rates when exposed to all three different irradiances. The emission rates of CH_3I at 40 $\mu\text{mol photons m}^{-2} \text{ s}^{-1}$ as shown in Figure 4.31 and Table 4.12 were the lowest as compared to other irradiances. In Figure 4.32 and Table 4.13, significant ($p<0.05$) changes in emission rates for CHCl_3 were observed for *Parachlorella* sp. UMACC 245 when exposed to all three irradiances, but not *Synechococcus* sp. UMACC 371 and *Amphora* sp. UMACC 370. Significant ($p<0.05$) changes in CH_2Br_2 emission rates (Figure 4.33 and Table 4.14) were observed across all three different irradiances for *Parachlorella* sp. UMACC 245 and *Synechococcus* sp. UMACC 2371. Significant ($p<0.05$) changes in CHBr_2Cl emission rates (Figure 4.34 and Table 4.15) were observed only for *Parachlorella* sp. UMACC 245 across all irradiances except the changes between 0 and 120 $\mu\text{mol photons m}^{-2} \text{ s}^{-1}$.

Parachlorella sp. UMACC 245 showed the biggest change in emissions of all five halocarbons as compared to *Synechococcus* sp. UMACC 371 and *Amphora* sp. UMACC 370 under 120 $\mu\text{mol photons m}^{-2} \text{ s}^{-1}$ and chlorophyll-a normalized condition. CH_3I showed the biggest in emission changes as compared to other halocarbons namely, CHBr_3 , CHCl_3 , CH_2Br_2 and CHBr_2Cl , while CH_2Br_2 was shown to be the second largest.

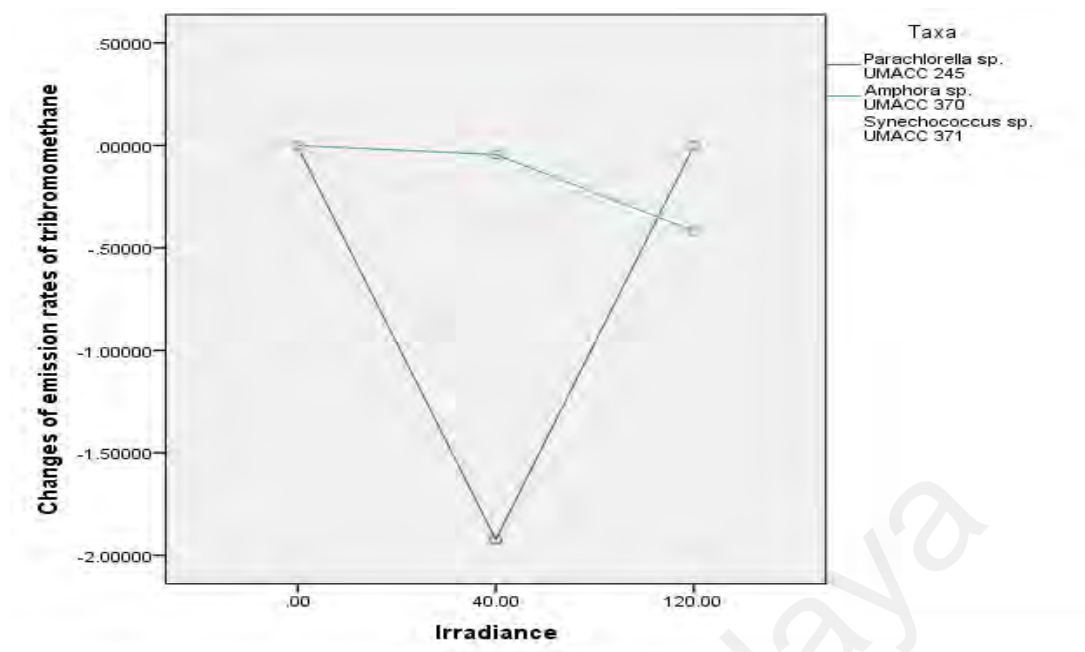


Figure 4.30: Changes of CHBr₃ emission rates normalized to chlorophyll-a from the microalgae under three irradiance levels (0, 40, 120 $\mu\text{mol photons m}^{-2} \text{s}^{-1}$). n= 27

Table 4.11: Pairwise comparisons of CHBr₃ at different irradiances (0, 40, 120 $\mu\text{mol photons m}^{-2} \text{s}^{-1}$) amongst the three microalgae. n = 27.

Pairwise Comparisons Dependent Variable: CHBr ₃					
Taxa	(I) Light	(J) Light	Mean Difference (I – J)	Std. Error	Sig. ^b
<i>Parachlorella</i> sp. UMACC 245	0	40	1.918*	.199	.000
		120	-.004	.199	1.000
	40	0	-1.918*	.199	.000
		120	-1.922*	.199	.000
<i>Amphora</i> sp. UMACC 370	120	0	.004	.199	1.000
		40	1.922*	.199	.000
	0	40	.045	.199	1.000
		120	.418	.199	.150
<i>Synechococcus</i> sp. UMACC 371	40	0	-.045	.199	1.000
		120	.373	.199	.231
	120	0	-.418	.199	.150
		40	-.373	.199	.231
<i>Parachlorella</i> sp. UMACC 245	0	40	.384	.199	.208
		120	.000	.199	1.000
	40	0	-.384	.199	.208
		120	-.384	.199	.208
<i>Amphora</i> sp. UMACC 370	120	0	-.000	.199	1.000
		40	-.384	.199	.208
<i>Synechococcus</i> sp. UMACC 371	0	40	.384	.199	.208
		120	.000	.199	1.000
	40	0	-.384	.199	.208
		120	-.384	.199	.208

Based on estimated marginal means.

*. The mean difference is significant at the 0.05 level.

b. Adjustment for multiple comparisons: Bonferroni.

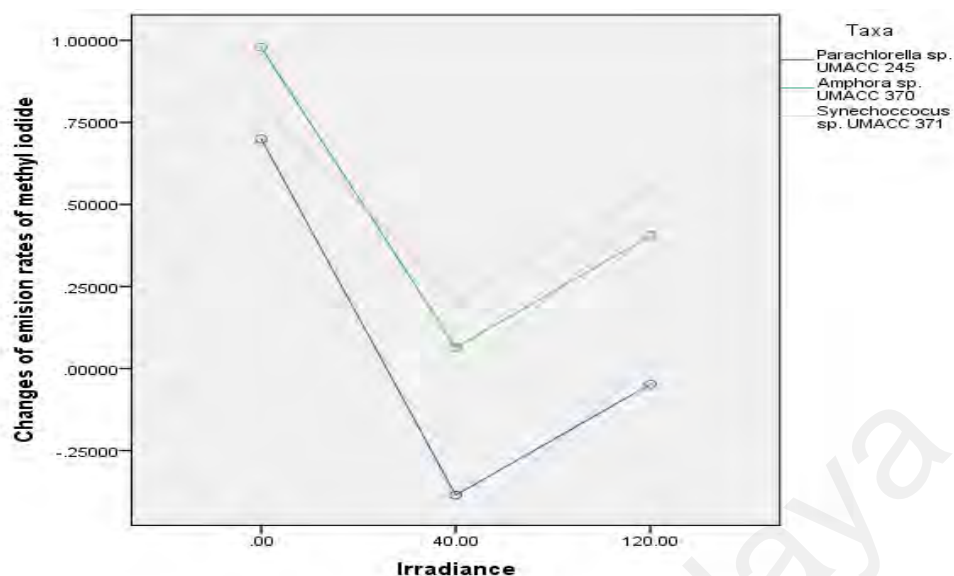


Figure 4.31: Changes of CH₃I emission rates normalized to chlorophyll-a from microalgae under three irradiance levels (0, 40, 120 $\mu\text{mol photons m}^{-2} \text{s}^{-1}$). n= 27.

Table 4.12: Pairwise comparisons of CH₃I at different irradiances (0, 40, 120 $\mu\text{mol photons m}^{-2} \text{s}^{-1}$) amongst the three microalgae. n = 27.

Pairwise Comparisons Dependent Variable: CH ₃ I					
Taxa	(I) Light	(J) Light	Mean Difference (I – J)	Std. Error	Sig. ^b
<i>Parachlorella</i> sp. UMACC 245	0	40	1.086*	.067	.000
		120	.748*	.067	.000
	40	0	-1.086*	.067	.000
		120	-.338*	.067	.000
<i>Amphora</i> sp. UMACC 370	0	40	.915*	.067	.000
		120	.574*	.067	.000
	40	0	-.915*	.067	.000
		120	-.341*	.067	.000
<i>Synechococcus</i> sp. UMACC 371	0	40	.594*	.067	.000
		120	.261*	.067	.003
	40	0	-.594*	.067	.000
		120	-.333*	.067	.000
	120	0	-.261*	.067	.003
		40	.333*	.067	.000

Based on estimated marginal means.

*. The mean difference is significant at the 0.05 level.

b. Adjustment for multiple comparisons: Bonferroni.

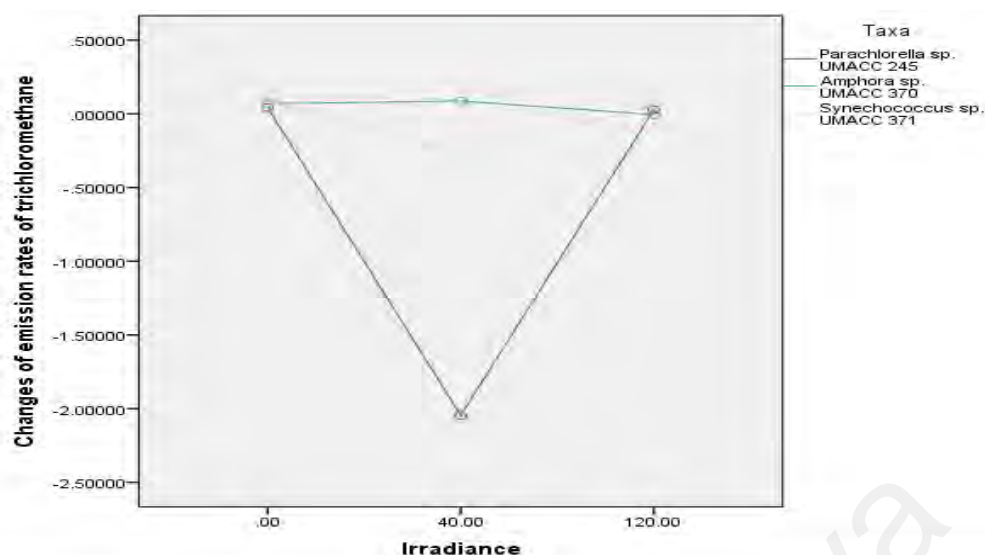


Figure 4.32: Changes of CHCl_3 emission rates normalized to chlorophyll-a from microalgae under three irradiance levels (0, 40, 120 $\mu\text{mol photons m}^{-2} \text{s}^{-1}$). $n = 27$.

Table 4.13: Pairwise comparisons of CHCl_3 at different irradiances (0, 40, 120 $\mu\text{mol photons m}^{-2} \text{s}^{-1}$) amongst the three microalgae. $n = 27$.

Pairwise Comparisons Dependent Variable: CHCl_3					
Taxa	(I) Light	(J) Light	Mean Difference (I – J)	Std. Error	Sig. ^b
<i>Parachlorella</i> sp. UMACC 245	0	40	2.089*	.639	.013
		120	.015	.639	1.000
	40	0	-2.089*	.639	.013
		120	-2.074*	.639	.013
	120	0	-.015	.639	1.000
		40	2.074*	.639	.013
<i>Amphora</i> sp. UMACC 370	0	40	-.019	.639	1.000
		120	.074	.639	1.000
	40	0	.019	.639	1.000
		120	.093	.639	1.000
	120	0	-.074	.639	1.000
		40	-.093	.639	1.000
<i>Synechococcus</i> sp. UMACC 371	0	40	.354	.639	1.000
		120	.020	.639	1.000
	40	0	-.354	.639	1.000
		120	-.334	.639	1.000
	120	0	-.020	.639	1.000
		40	.334	.639	1.000

Based on estimated marginal means.

*. The mean difference is significant at the 0.05 level.

b. Adjustment for multiple comparisons: Bonferroni.

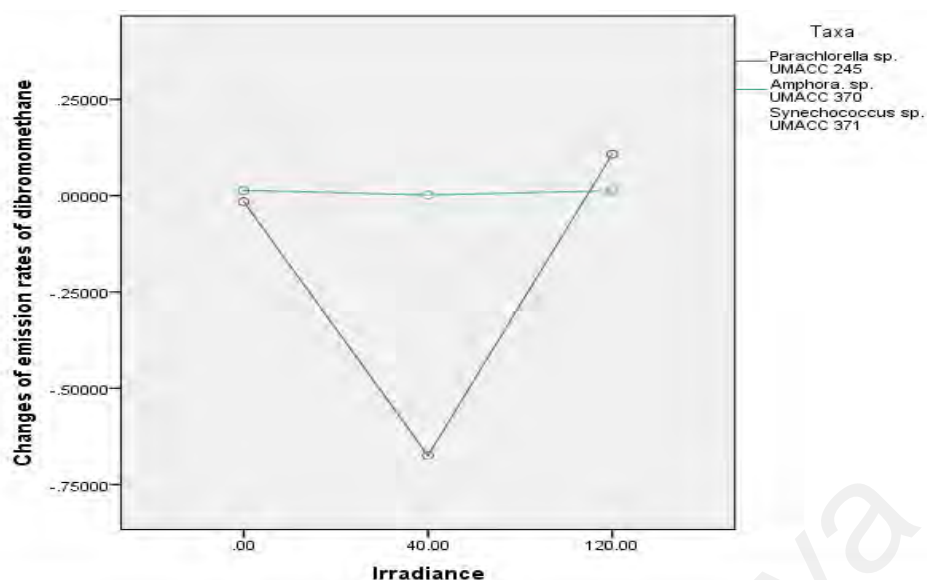


Figure 4.33: Changes of CH₂Br₂ emission rates normalized to chlorophyll-a from microalgae under three irradiance levels (0, 40, 120 $\mu\text{mol photons m}^{-2} \text{s}^{-1}$). n= 27.
Table 4.14: Pairwise comparisons of CH₂Br₂ at different irradiances (0, 40, 120 $\mu\text{mol photons m}^{-2} \text{s}^{-1}$) amongst the three microalgae. n = 27.

Pairwise Comparisons Dependent Variable: CH ₂ Br ₂					
Taxa	(I) Light	(J) Light	Mean Difference (I – J)	Std. Error	Sig. ^b
<i>Parachlorella</i> sp. UMACC 245	0	40	.659*	.031	.000
		120	-.123*	.031	.002
	40	0	-.659*	.031	.000
		120	-.782*	.031	.000
	120	0	.123*	.031	.002
		40	.782*	.031	.000
<i>Amphora</i> sp. UMACC 370	0	40	.012	.031	1.000
		120	.001	.031	1.000
	40	0	-.012	.031	1.000
		120	-.011	.031	1.000
	120	0	-.001	.031	1.000
		40	.011	.031	1.000
<i>Synechococcus</i> sp. UMACC 371	0	40	.543*	.031	.000
		120	.062	.031	.179
	40	0	-.543*	.031	.000
		120	-.481*	.031	.000
	120	0	-.062	.031	.179
		40	.481*	.031	.000

Based on estimated marginal means.

*. The mean difference is significant at the 0.05 level.

b. Adjustment for multiple comparisons: Bonferroni.

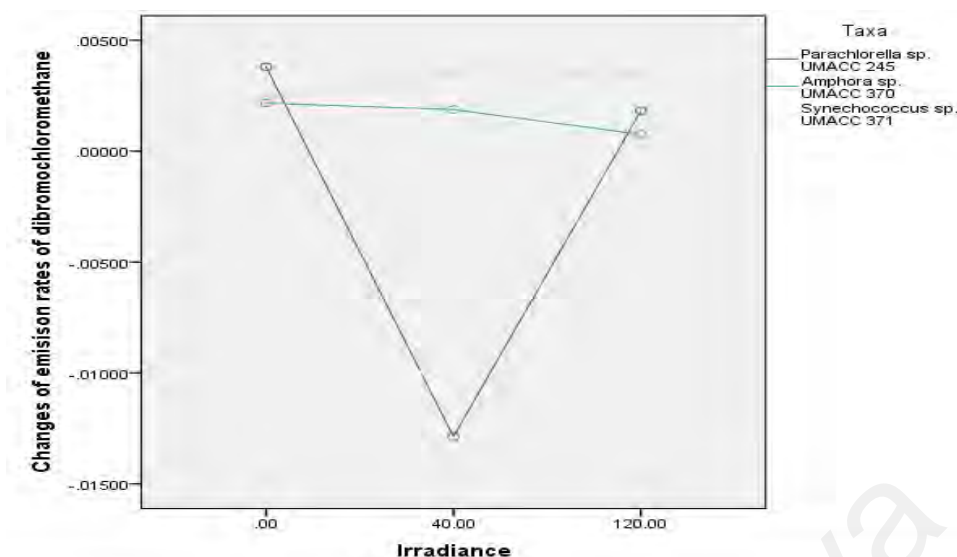


Figure 4.34: Changes of CHBr₂Cl emission rates normalized to chlorophyll-a from microalgae under three irradiance levels (0, 40, 120 μmol photons m⁻² s⁻¹). n = 27.

Table 4.15: Pairwise comparisons of CHBr₂Cl at different irradiances (0, 40, 120 μmol photons m⁻² s⁻¹) amongst the three microalgae. n = 27.

Pairwise Comparisons Dependent Variable: CHBr ₂ Cl					
Taxa	(I) Light	(J) Light	Mean Difference (I – J)	Std. Error	Sig. ^b
<i>Parachlorella</i> sp. UMACC 245	0	40	.017*	.002	.000
		120	-.002	.002	1.000
	40	0	-.017*	.002	.000
		120	-.015*	.002	.000
	120	0	-.002	.002	1.000
		40	.015*	.002	.000
<i>Amphora</i> sp. UMACC 370	0	40	.000	.002	1.000
		120	.001	.002	1.000
	40	0	.000	.002	1.000
		120	.001	.002	1.000
	120	0	-.001	.002	1.000
		40	-.001	.002	1.000
<i>Synechococcus</i> sp. UMACC 371	0	40	-.001	.002	1.000
		120	-.001	.002	1.000
	40	0	.001	.002	1.000
		120	.000	.002	1.000
	120	0	.001	.002	1.000
		40	.000	.002	1.000

Based on estimated marginal means.

*. The mean difference is significant at the 0.05 level.

b. Adjustment for multiple comparisons: Bonferroni.

4.4.6.2 Normalization to cell density

The pairwise comparisons of changes in halocarbon emission rates normalized to cell density are summarized by compound, namely CHBr_3 (Figure 4.35), CH_3I (Figure 4.36), CHCl_3 (Figure 4.37), CH_2Br_2 (Figure 4.38) and CHBr_2Cl (Figure 4.39) for all three microalgae under all three irradiances. Pairwise comparisons with significant ($p < 0.05$) changes in halocarbon emission rates involving the two factors, irradiances and taxa, are summarized in tables based on all five compounds, namely CHBr_3 (Table 4.16), CH_3I (Table 4.17), CHCl_3 (Table 4.18), CH_2Br_2 (Table 4.19) and CHBr_2Cl (Table 4.20). The increase and decrease of halocarbon emission rates after 12-hour exposure to different irradiances for all three microalgae are indicated with positive and negative values in figures and tables.

The changes in emission rates of CHBr_3 (Figure 4.35 and Table 4.16) were not significant when compared amongst all different irradiances for the three taxa. *Parachlorella* sp. UMACC 245 and *Amphora* sp. UMACC 370 showed significant ($p < 0.05$) changes in CH_3I emission rates (Figure 4.36 and Table 4.17). The changes of CHCl_3 emission rates were not significant (Table 4.18) across all irradiances but clear increase and decrease of halocarbon emission rate changes (Figure 4.37). Unlike the rest of other compounds, CH_2Br_2 normalized to cell density as shown in Table 4.19 and Figure 4.38 showed significant ($p < 0.05$) changes in emission rates across all different irradiances for *Parachlorella* sp. UMAC 245, *Synechococcus* sp. UMACC 371 and *Amphora* sp. UMACC 370. *Amphora* sp. UMACC 370 was the only taxa to show a significant ($p < 0.05$) change in CHBr_2Cl emission rates across all irradiances. Note that the mean differences obtained as shown in Table 4.16 to 4.20 were corrected to the power of 10^{11} for statistical analysis purpose and hence were not actual values.

The halocarbon emission normalized to cell density, by *Parachlorella* sp. UMAC 245 and *Synechococcus* sp. UMACC 371, was not significantly affected by exposure to higher irradiance ($120 \mu\text{mol photons m}^{-2} \text{s}^{-1}$). *Amphora* sp. UMACC 370 showed significance ($p < 0.05$) changes in all five halocarbon emission rate.

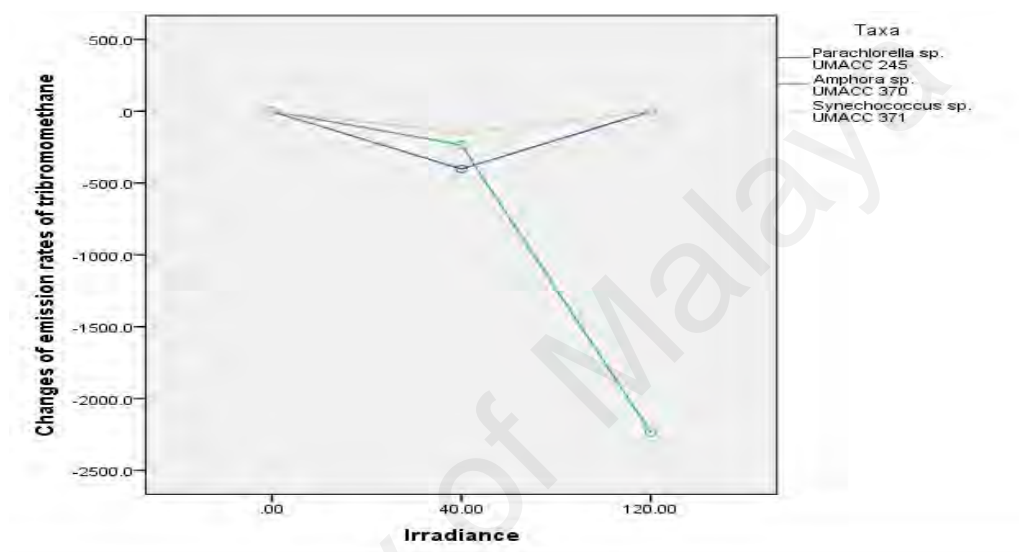


Figure 4.35: Changes of CHBr_3 emission rates normalized to cell density from microalgae under three irradiance levels (0, 40, $120 \mu\text{mol photons m}^{-2} \text{s}^{-1}$). $n = 27$.

Table 4.16: Pairwise comparisons of CHBr_3 at different irradiances (0, 40, 120 $\mu\text{mol photons m}^{-2} \text{s}^{-1}$) amongst the three microalgae. $n = 27$.

Pairwise Comparisons Dependent Variable: CHBr_3					
Taxa	(I) Light	(J) Light	Mean Difference (I – J)	Std. Error	Sig. ^b
<i>Parachlorella</i> sp. UMACC 245	0	40	400.700	1040.981	1.000
		120	-1.167	1040.981	1.000
	40	0	-400.700	1040.981	1.000
		120	-401.867	1040.981	1.000
	120	0	1.167	1040.981	1.000
		40	401.867	1040.981	1.000
<i>Amphora</i> sp. UMACC 370	0	40	235.767	1040.981	1.000
		120	2238.600	1040.981	.136
	40	0	-235.767	1040.981	1.000
		120	2002.833	1040.981	.211
	120	0	-2238.60	1040.981	.136
		40	-2002.83	1040.981	.211
<i>Synechococcus</i> sp. UMACC 371	0	40	145.200	1040.981	1.000
		120	.000	1040.981	1.000
	40	0	-145.200	1040.981	1.000
		120	-145.200	1040.981	1.000
	120	0	-.000	1040.981	1.000
		40	145.200	1040.981	1.000

Based on estimated marginal means.

*. The mean difference is significant at the 0.05 level.

b. Adjustment for multiple comparisons: Bonferroni.

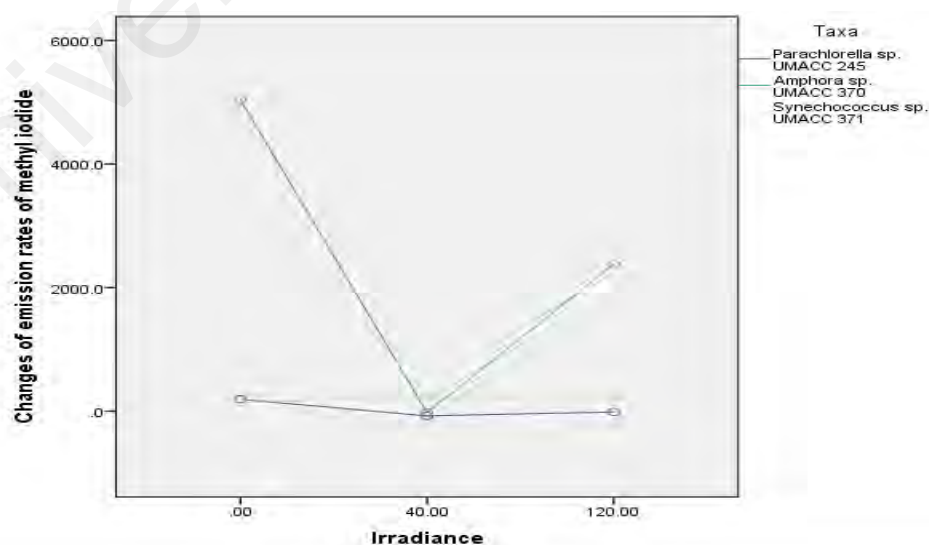


Figure 4.36: Changes of CH_3I emission rates normalized to cell density from microalgae under three irradiance levels (0, 40, 120 $\mu\text{mol photons m}^{-2} \text{s}^{-1}$). $n = 27$.

Table 4.17: Pairwise comparisons of CH₃I at different irradiances (0, 40, 120 $\mu\text{mol photons m}^{-2} \text{s}^{-1}$) amongst the three microalgae. n = 27.

Pairwise Comparisons Dependent Variable: CH ₃ I					
Taxa	(I) Light	(J) Light	Mean Difference (I – J)	Std. Error	Sig. ^b
<i>Parachlorella</i> sp. UMACC 245	0	40	268.700*	97.109	.038
		120	205.033	97.109	.147
	40	0	-268.700*	97.109	.038
		120	-63.667	97.109	1.000
	120	0	-205.033	97.109	.147
		40	63.667	97.109	1.000
<i>Amphora</i> sp. UMACC 370	0	40	5065.467*	97.109	.000
		120	2663.933*	97.109	.000
	40	0	-5065.47*	97.109	.000
		120	-2401.53*	97.109	.000
	120	0	-2663.93*	97.109	.000
		40	2401.533*	97.109	.000
<i>Synechococcus</i> sp. UMACC 371	0	40	-90.733	97.109	1.000
		120	-23.000	97.109	1.000
	40	0	90.733	97.109	1.000
		120	67.733	97.109	1.000
	120	0	23.000	97.109	1.000
		40	-67.733	97.109	1.000

Based on estimated marginal means.

*. The mean difference is significant at the 0.05 level.

b. Adjustment for multiple comparisons: Bonferroni.

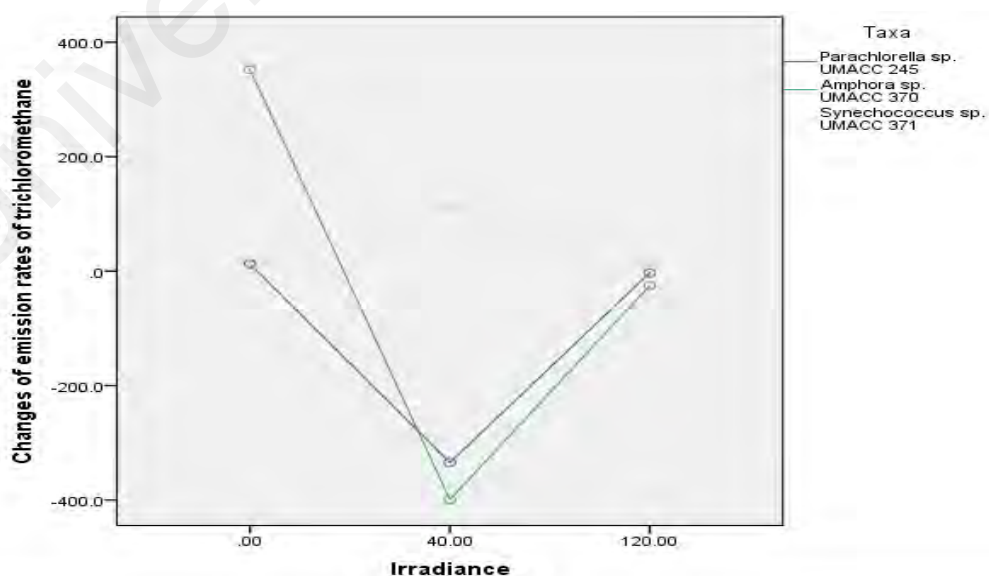


Figure 4.37: Changes of CHCl₃ emission rates normalized to cell density from microalgae under three irradiance levels (0, 40, 120 $\mu\text{mol photons m}^{-2} \text{s}^{-1}$). n = 27.

Table 4.18: Pairwise comparisons of CHCl_3 at different irradiances (0, 40, 120 $\mu\text{mol photons m}^{-2} \text{s}^{-1}$) amongst the three microalgae. $n = 27$.

Pairwise Comparisons Dependent Variable: CHCl_3					
Taxa	(I) Light	(J) Light	Mean Difference (I – J)	Std. Error	Sig. ^b
<i>Parachlorella</i> sp. UMACC 245	0	40	347.000	382.989	1.000
		120	15.233	382.989	1.000
	40	0	-347.000	382.989	1.000
		120	-331.767	382.989	1.000
	120	0	-15.233	382.989	1.000
		40	331.767	382.989	1.000
<i>Amphora</i> sp. UMACC 370	0	40	751.400	382.989	.196
		120	377.333	382.989	1.000
	40	0	-751.400	382.989	.196
		120	-374.067	382.989	.000
	120	0	-377.333	382.989	1.000
		40	374.067	382.989	1.000
<i>Synechococcus</i> sp. UMACC 371	0	40	-109.733	382.989	1.000
		120	-11.467	382.989	1.000
	40	0	109.733	382.989	1.000
		120	98.267	382.989	1.000
	120	0	11.467	382.989	1.000
		40	-98.267	382.989	1.000

Based on estimated marginal means.

*. The mean difference is significant at the 0.05 level.

b. Adjustment for multiple comparisons: Bonferroni.

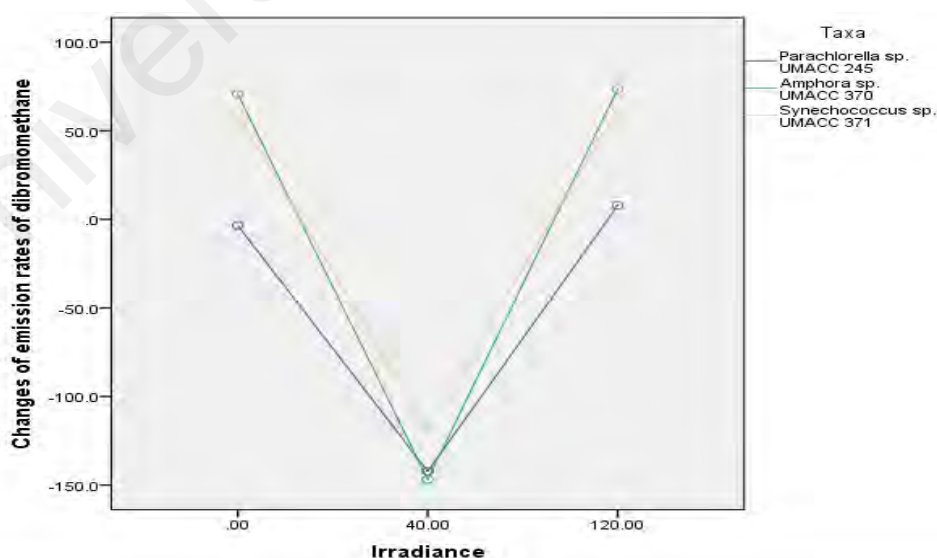


Figure 4.38: Changes of CH_2Br_2 emission rates normalized to cell density from microalgae under three irradiance levels (0, 40, 120 $\mu\text{mol photons m}^{-2} \text{s}^{-1}$). $n = 27$.

Table 4.19: Pairwise comparisons of CH₂Br₂ at different irradiances (0, 40, 120 $\mu\text{mol photons m}^{-2} \text{s}^{-1}$) amongst the three microalgae. n = 27.

Pairwise Comparisons Dependent Variable: CH ₂ Br ₂					
Taxa	(I) Light	(J) Light	Mean Difference (I – J)	Std. Error	Sig. ^b
<i>Parachlorella</i> sp. UMACC 245	0	40	137.767*	382.989	1.000
		120	-11.367	382.989	1.000
	40	0	-138.77*	382.989	1.000
		120	-150.13*	382.989	1.000
	120	0	11.367	382.989	1.000
		40	150.133*	382.989	1.000
<i>Amphora</i> sp. UMACC 370	0	40	217.600*	382.989	.196
		120	-2.800	382.989	1.000
	40	0	-217.60*	382.989	.196
		120	-220.40*	382.989	.000
	120	0	-2.800	382.989	1.000
		40	220.400*	382.989	1.000
<i>Synechococcus</i> sp. UMACC 371	0	40	177.300*	382.989	1.000
		120	-2.967	382.989	1.000
	40	0	-177.30*	382.989	1.000
		120	-180.27*	382.989	1.000
	120	0	2.967	382.989	1.000
		40	180.267*	382.989	1.000

Based on estimated marginal means.

*. The mean difference is significant at the 0.05 level.

b. Adjustment for multiple comparisons: Bonferroni.

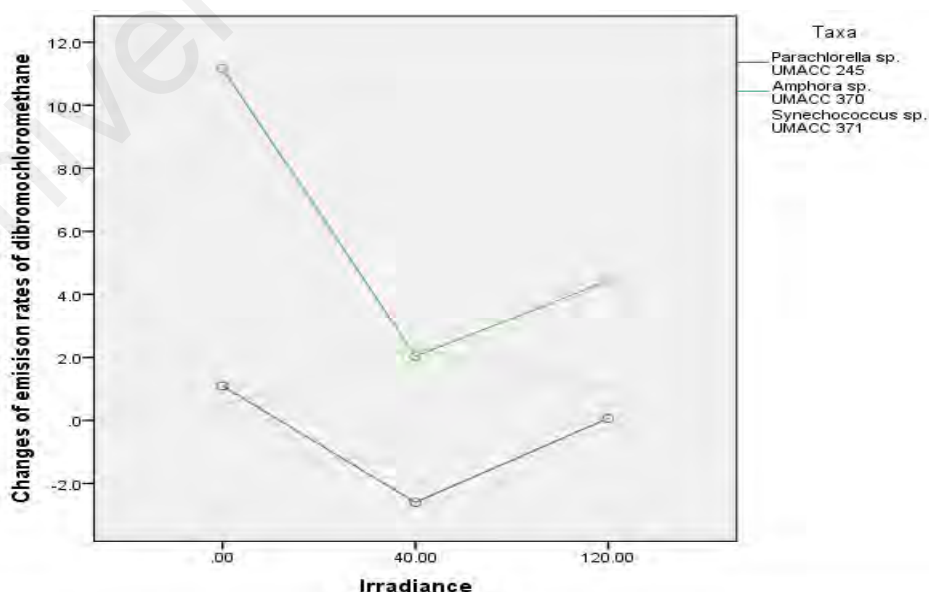


Figure 4.39: Changes of CHBr₂Cl emission rates normalized to cell density from microalgae under three irradiance levels (0, 40, 120 $\mu\text{mol photons m}^{-2} \text{s}^{-1}$). n= 27.

Table 4.20: Pairwise comparisons of CHBr₂Cl at different irradiances (0, 40, 120 $\mu\text{mol photons m}^{-2} \text{ s}^{-1}$) amongst the three microalgae. n = 27.

Pairwise Comparisons Dependent Variable: CHBr ₂ Cl					
Taxa	(I) Light	(J) Light	Mean Difference (I – J)	Std. Error	Sig. ^b
<i>Parachlorella</i> sp. UMACC 245	0	40	3.700	2.375	.410
		120	1.033	2.375	1.000
	40	0	-3.700	2.375	.410
		120	-2.667	2.375	.829
	120	0	-1.033	2.375	1.000
		40	2.667	2.375	.829
<i>Amphora</i> sp. UMACC 370	0	40	9.133*	2.375	.004
		120	6.733*	2.375	.033
	40	0	-9.133*	2.375	.004
		120	-2.400	2.375	.977
	120	0	-6.733*	2.375	.033
		40	2.400	2.375	.977
<i>Synechococcus</i> sp. UMACC 371	0	40	-1.833	2.375	1.000
		120	-.600	2.375	1.000
	40	0	1.833	2.375	1.000
		120	1.233	2.375	1.000
	120	0	.600	2.375	1.000
		40	-1.233	2.375	1.000

Based on estimated marginal means.

*. The mean difference is significant at the 0.05 level.

b. Adjustment for multiple comparisons: Bonferroni.

4.4.7 Correlation between F_v/F_m and halocarbon emission rates at different irradiances amongst microalgae

The correlation between halocarbon emission rates and maximum quantum yield, F_v/F_m , of the three microalgae under three different irradiances is summarized in Table 4.21 and Table 4.22, normalized to chlorophyll-a and cell density respectively.

Emission rate of all five compounds normalized to chlorophyll-a and cell density for *Parachlorella* sp. UMACC 245 and *Amphora* sp. UMAC 370 were negatively correlated to the changes in F_v/F_m , except CH₃I that showed the only positive correlation. Emission rates of CH₃I, CHCl₃ and CH₂Br₂ normalized to chlorophyll-a and emission rates of CHCl₃ normalized to cell density showed positive correlation to the F_v/F_m while the rest

showed negative correlations. The correlations between F_v/F_m and halocarbon emissions were non-significant.

Table 4.21: Pearson correlation coefficient (r) between net changes of maximum quantum yields (F_v/F_m) of the microalgae and their halocarbon emission rates normalized to chlorophyll-a.

Compounds	<i>Synechococcus</i> sp. UMACC 371	<i>Parachlorella</i> sp. UMACC 245	<i>Amphora</i> sp. UMACC 370
CHBr ₃	-0.089 ^{NS}	-.542 ^{NS}	.471 ^{NS}
CH ₃ I	0.298 ^{NS}	.157 ^{NS}	.430 ^{NS}
CHCl ₃	0.017 ^{NS}	-.523 ^{NS}	.273 ^{NS}
CH ₂ Br ₂	0.001 ^{NS}	-.653 ^{NS}	-.093 ^{NS}
CHBr ₂ Cl	-0.354 ^{NS}	-.383 ^{NS}	.557 ^{NS}

NS Non-significant emission rate data were pooled from three replicates for all F_v/F_m values; n = 27.

Table 4.22: Pearson correlation coefficient (r) between net changes of maximum quantum yields (F_v/F_m) of the microalgae and their halocarbon emission rates normalized to cell density.

Compounds	<i>Synechococcus</i> sp. UMACC 371	<i>Parachlorella</i> sp. UMACC 245	<i>Amphora</i> sp. UMACC 370
CHBr ₃	-0.085 ^{NS}	-.542 ^{NS}	.471 ^{NS}
CH ₃ I	-0.158 ^{NS}	.233 ^{NS}	.323 ^{NS}
CHCl ₃	0.025 ^{NS}	-.474 ^{NS}	.139 ^{NS}
CH ₂ Br ₂	-0.113 ^{NS}	-.592 ^{NS}	-.222 ^{NS}
CHBr ₂ Cl	-0.211 ^{NS}	-.240 ^{NS}	.386 ^{NS}

NS Non-significant emission rate data were pooled from three replicates for all F_v/F_m values; n = 27.

CHAPTER 5: DISCUSSION

5.1 Emission rates amongst the three tropical microalgae

5.1.1 Effect of different growth phases

The volatile short-lived halocarbons detected in the microalgae are CHBr_3 , CH_3I , CHCl_3 , CHBr_2Cl and CH_2Br_2 . *Amphora* sp. UMACC 371 emitted significantly ($p < 0.05$) higher concentrations of halogenated compounds, especially CH_3I as compared to *Synechococcus* sp. UMACC 371 and *Parachlorella* sp. UMACC 245. The emission of CH_3I is significantly ($p < 0.05$) higher compared to other detected compounds, CHBr_3 , CHCl_3 , CHBr_2Cl and CH_2Br_2 .

In this study, the estimated range of emission rates of each halocarbon that varied amongst the three microalgae suggested that the emission rates of each halogenated compound were species- dependent due to the different algal growth physiology at exponential and stationary phases. The higher emission rate for all five halocarbons during exponential phase than in stationary phase for *Synechococcus* sp. UMACC 371, *Amphora* sp. UMACC 370 and *Parachlorella* sp. UMACC 245 when normalized to chlorophyll-a (except CHBr_3 and CH_2Br_2 for the *Parachlorella*) and cell density, suggested that the emission of these halocarbons over 12 days of culturing were growth phase-dependent. None of the five halocarbons was found to be emitted in the same amount and concentration from the same microalgal species over the culture period, suggesting that the emissions of halocarbon may be compound-specific and strain-specific despite originating from the same microalgal species.

In this growth-cycle study, halocarbon emission rates were higher at exponential phase in general for the three microalgae. Exponential phase cells are actively growing and in a healthy state. As the culture proceed to stationary phase, the cell growth slows down and eventually stops due to chemical and physical changes such as nutrients,

irradiance and increase in inhibitory compounds in the medium. Consumption of the inorganic carbon source results in pH increase in the medium, which would influence algal activity. While it is often assumed that physiological stress does occur when microalgal cells transit from exponential to stationary phase due to limiting conditions and the stress would trigger haloperoxidase mechanism to produce more halocarbons (Moore *et al.*, 1996), the present study indicates otherwise. All five halocarbons detected by the three tropical microalgae were found to emit at higher rates at exponential phases, with exception of two brominated compounds, CHBr_3 and CHBr_2Cl by *Amphora* sp. UMACC 370. Manley & de la Cuesta (1997) reported consistency of higher emission rates of CH_3I at exponential for the Bacillariophytes *Navicula* sp., *Nitzschia* sp., and *Porosira glacialis* and the Chrysophyte *Phaeocystis* sp. The higher emission rates at exponential phase may be explained as follows: i) the tropical microalgal species used in the present study may be more tolerant to the stress of an aging culture, and the condition did not lead to increased production of the halocarbons. This might have to do with the low “leakage” of hydrogen peroxide from the algal cells into the medium (Palenik *et al.*, 1987; Wong *et al.*, 2003); ii) the exponential phase cells are actively metabolizing, allowing higher rate of methylation of haloperoxidase for halocarbon production, as compared to the cells that experience limiting conditions in stationary phase. The halo-enzymes at healthy state may be less susceptible to inhibition at its active site that allow higher chance of methylation to occur. This suggests that a more detailed research has to be done on relating the change in physiological cell state with varying nutrient composition such as sulfur, nitrogen, phosphate, that may affect the haloperoxidase-mechanism; iii) higher concentration of cells in stationary phase produced less superoxide per cell than those with lower density (Marshall, 2002). As oxidative radicals produced in the cells mediate the oxidation of halides present in the medium (Neidleman & Geigert, 1986), this suggest a possibility that lower algal cell density as measured by chlorophyll-

a and cell density during the exponential phase in this study, enhances the production of halocarbons and ultimately the emission rates. It has been reported that algal cells at exponential growth can be more toxic than those in stationary or late exponential phase (Tang & Gobler, 2009). The toxicity is caused by production of peroxidase and catalase that react with multiple compounds including organic hydroperoxides and lipid peroxides in cells. The enzymes can increase the rates of dismutation and decomposition reaction of other highly reactive oxidative species (ROS) into H_2O_2 . Thus, H_2O_2 surge in the cells from these reactions may be the cause to trigger halocarbon production (Tang & Gobler, 2009).

In case of the exception observed for CHBr_3 , CHBr_2Cl where emission rates are significantly ($p < 0.05$) higher at stationary phase, these brominated compounds may be preferentially produced due to the physiological cell stress created from the limiting conditions during growth transition. Previous studies have shown an overall higher emission at stationary phase for iodomethane, CH_3I (Scarratt & Moore, 1999; Smythe-Wright *et al.*, 2006; Brownell *et al.*, 2010; Hughes *et al.*, 2011) and brominated compounds, CHBr_3 , CH_2Br_2 and CHBr_2Cl (Tokarczyk & Moore, 1994; Moore *et al.*, 1996) and each of these emissions is strain-specific. Nonetheless, the discrepancies of higher emission at exponential compared with stationary phase, as compared to the present study may be largely due to: 1) non-normalized biomass emission; emission for the brominated compounds and biomass such as algal cell density were calculated separately but not normalized which makes it difficult to compare with to the emission rates in this study; emission rates were calculated in some of the previous studies but it was not possible to make comparison in terms of different growth phases, and another study compared lag and exponential phases but not stationary phase. 2) the difference in method used, such as gas-phase using head-space were used in many previous studies

while water-phase using purge-and -trap system was used, 3) it could just be that the emission rates of halogenated compounds are strain-specific.

5.2 Comparison of emission rates

5.2.1 Tropical marine phytoplankton and seaweeds

In order to assess the importance of the source of CHBr_3 , CH_3I , CH_2Br_2 and CHBr_2Cl from the tropical region, a comparison is made between the emission rates found in this study and those reported from tropical macroalgae by Keng *et al.*, 2013. Table 5.1 summarizes the emission rates of both the macroalgae and microalgae.

Table 5.1: Comparison of emission rate between tropical macroalgae and marine microalgae for CHBr_3 , CH_3I , CH_2Br_2 and CHBr_2Cl under dry-weight normalization

Emission rate ($\text{pmol g DW}^{-1} \text{ hr}^{-1}$)						
Compound	Tropical seaweeds (Keng <i>et al.</i> , 2013)			Tropical marine microalgae (present study)		
	<i>Sargassum binderi</i>	<i>Turbinaria conoides</i>	<i>Padina australis</i>	<i>Synechococcus sp. UMACC 371</i>	<i>Parachlorella sp. UMACC 245</i>	<i>Amphora sp. UMACC 370</i>
CHBr_3	4.7	6.5 $\times 10^3$	68.7	0.79 (Day 4)	0.28 (Day 4)	1.83 (Day 10)
CH_3I	11.6	20.7	34.7	0.85 (Day 2)	0.66 (Day 2)	2.72 (Day 10)
CH_2Br_2	105	620	15.1	0.02 (Day 10)	0.05 (Day 2)	0.24 (Day 6)
CHBr_2Cl	88.3	175	21.1	0.02 (Day 2)	0.01 (Day 10)	0.20 (Day 8)

For the comparison to be made possible, both laboratory-based studies were done and analyzed using similar water-phased method, which was through the GCMS equipped with purge-and-trap system conducted at 12light:12dark cycle at a range of irradiance level of 40-47 $\mu\text{mol photons m}^{-2}\text{s}^{-1}$.

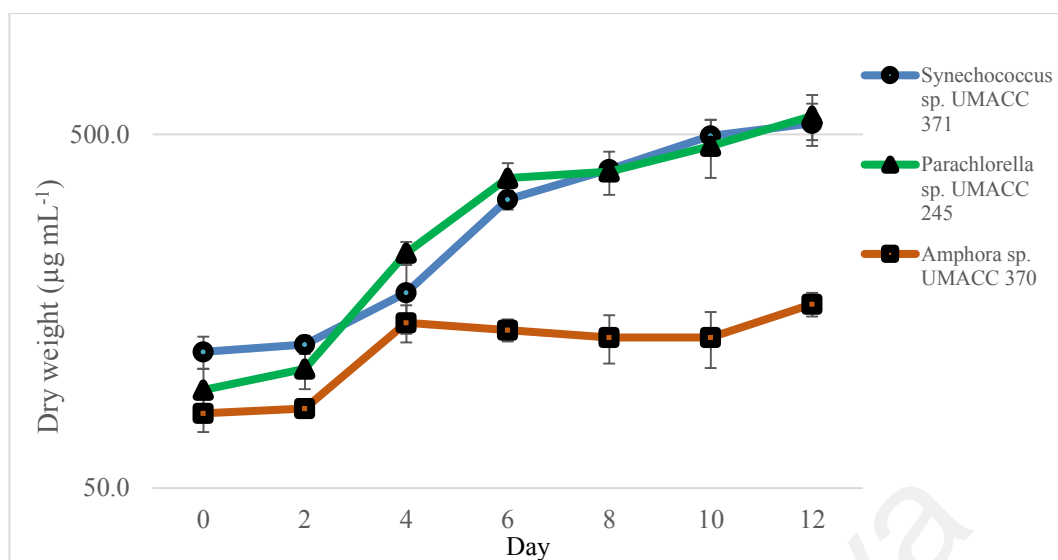


Figure 5.1: Dry weight (DW) of three tropical microalgae over a growth period of 12 days.

Our results, using dry-weight (DW) as shown in Figure 5.1 and converted to the same units give emission rates of the selected four compounds. Whilst our halocarbon emission rate per unit mass range from 3 to 30000 times lower than that for seaweeds reported by Keng *et al.* (2013), the importance of marine microalgae is potentially greater due to the fact that they inhabit more than 70% of the earth's surface. However, extensive data covering larger time and spatial scales, have to be available to allow extrapolation to natural populations to properly quantify the regional (tropical) significance of the marine microalgae as source of volatile halocarbons.

5.2.2 Previous related-studies from polar and temperate regions

Brownell *et al.* (2010) reported CH₃I emission by the temperate *Synechococcus* sp. CCMP 2370 (clone WH 8102) over the course of 27 days. The emission peaked at approximately 22-25 pmol L⁻¹ on Day 15 during its late stationary phase, with chlorophyll-a of 0.5-1.0 µg L⁻¹. In the present study, the emission of CH₃I by our tropical *Synechococcus* sp. UMACC 371 peaked at 0.53 pmol L⁻¹ on Day 10 during its mid-stationary phase, with chlorophyll-a content at approximately 2.0 mg L⁻¹. While there was a consistency of CH₃I emissions peak during the stationary phase for both cyanobacteria

strains, the emission by *Synechococcus* sp. CCMP 2370 was at an order of five times higher than that from UMACC 371. The difference may be due to: i) incubation conditions where experiments done were under lower controlled temperature of 20-21°C, higher irradiance at 60-70 $\mu\text{mol photons m}^{-2} \text{ s}^{-1}$ and at nutrient-repleted condition as compared to this study. It is assumed that biological processes affected by constant environmental factors such as differences in temperature, irradiance and nutrients (Brownell *et al.*, 2010) were responsible for the lower emission of CH_3I by *Synechococcus* sp. UMACC 371. ii) resultant physiological condition of the two cyanobacterial strains. The difference in starting cell density of inocula as well as chlorophyll-a content obtained during the same phase when maximum CH_3I emission was achieved for both studies may contribute to the variation in emission. Hughes *et al.* (2011) made a similar report on CH_3I emission by the temperate *Synechococcus* sp. CCMP 2370 grown at 22°C under light intensity of 40 $\mu\text{E m}^{-2} \text{ day}^{-1}$ for over a total of 24 days, with exponential phase starting from Day 4 to 16. The CH_3I concentration measured throughout the experiment range from 2-4 pmol L^{-1} which are close to the medium-only control, suggesting relatively low emission of the CH_3I compound despite a long exponential phase. In other words, the emission of this iodomethane from the *Synechococcus* of different climatic zones is clearly strain-specific.

In the present study, *Amphora* sp. UMACC 370, a Bacillariophyte, had significantly ($p < 0.05$) higher emission and emission rates as compared to the other two taxa from the Cyanophyta and Chlorophyta. Manley & de la Cuesta (1997) also reported higher CH_3I emission in both exponential and stationary phases from Bacillariophyta, as compared to species from Chlorophyta, Chrysophyta, Cyanophyta and Dinophyta, which further supported results from the present study of higher CH_3I emission from the Bacillariophyta than Chlorophyta and Cyanophyta. *Synechococcus*, a Cyanophyta from present and previous studies (Hughes *et al.*, 2011; Brownell *et al.*, 2010, Sæmundsdottir & Matrai,

1998; Manley & de la Cuesta, 1997) has consistently been shown as a weak emitter of CH₃I; showing either low (close to control level) or no emission and brominated compound such as CH₃Br with no emission.

5.3 Emission rates amongst the five detected compounds

From the total combined halogen mass emitted as halocarbons calculated in percentage as summarized in Table 7, the emission contribution from iodine dominates over bromine and chlorine for the taxa that emit the highest (*Amphora*) and second highest (*Synechococcus*).

Table 5.2: Total mass of emitted halides. Total halogen mass emitted as halocarbons and percentage contribution to the total from bromine, chlorine and iodine. Taxa are arranged in decreasing total mass halogens emitted order.

Taxa	Total halogens emitted (pg)	% Br	% Cl	% I
<i>Amphora</i> sp. UMACC 370	5223.6	34.39	5.93	59.7
<i>Synechococcus</i> sp. UMACC 371	2033.9	35.43	13.40	51.17
<i>Parachlorella</i> sp. UMACC 245	1573.8	32.29	47.01	21.02

Halogenating enzymes, peroxidases, catalyze the formation of carbon-hydrogen bonds using halide ions, hydrogen peroxide and an organic substrate activated for electrophilic attack. Iodoperoxidases catalyze the formation of carbon iodine bonds, whereas bromoperoxidase catalyzes iodination and bromination process, and chloroperoxidases catalyze the iodination, bromination and chlorination of organic substrates (Moore *et al.*, 1996). The higher ratio of percentage of iodine to bromine and especially chlorine suggests that *Amphora* sp. UMACC 370 and *Synechococcus* sp. UMACC 371 on the cellular level may possess more iodoperoxidase than chloroperoxidase to catalyze iodide.

On the contrary, *Parachlorella* sp. UMACC 245 emitted higher chloride than the other two halides suggests that higher concentration of chloroperoxidase may be present.

Whilst iodine-containing halocarbons are not directly involved in the depletion of stratospheric ozone, they do, however through photolysis, release iodine to react rapidly with ozone to form iodine oxides (IO/OIO), which will influence the tropospheric oxidizing capacity (McFiggans *et al.*, 2000). Calvert & Lindberg (2004) reported the potential influence of iodine-containing compounds on tropospheric chemistry, where small amounts of iodinated compounds that are present in polar air mass containing representative of Br₂-BrCl- trace gas mixtures do significantly enhance ozone depletion. With significant concentration of CH₃I observed in oceanic atmospheres (Calvert & Lindberg, 2004; Yamamoto *et al.*, 2001; Blake *et al.*, 1997), it is possible that the contribution of iodine from biogenic source like *Amphora* and *Synechococcus* may be significant over the tropical region. This encourages the local measurement of IO and precursor iodine-containing compounds as well as their interaction with currently acknowledged important trace gases like O₃ and BrO in the tropics for future studies and understanding.

5.4 Effect of irradiance and photosynthetic performance on halocarbon emission by selected microalgae

The data acquired through this study showed that the emission rates of five halocarbons, CHBr₃, CH₃I, CHCl₃, CH₂Br₂ and CHBr₂Cl from the three tropical marine microalgae were influenced by irradiance through short-term exposure to higher irradiance. Both ultraviolet radiation a and b were not detected where the incubation flasks were placed. The maximum quantum yield, F_v/F_m , of the algal cultures at different irradiances were shown to be significantly different ($p < 0.05$). Different irradiances were shown to influence the changes in F_v/F_m and halocarbon emission rates in general. The

correlation between F_v/F_m and the emission rates of all five compounds were weak for all three taxa. The halocarbon emission rates normalized to chlorophyll-a, cell density and both were well correlated ($p < 0.01$).

Halocarbon production has long been thought to be a defense mechanism in response to bacterial infection or as a chemical defense against oxidative stress. A few suggestions may be made to explain the results from the present light stress experiment. The significant ($p < 0.05$) increase in chlorophyll-a and cell density normalized emission rate of monohalogenated compounds including CHBr_3 , CHCl_3 , CH_3I and CH_2Br_2 under different irradiances, may be a result of the process of methylation of the corresponding halide ions catalyzed by halide ion methyl transferase that involves S-adenosylmethionine (SAM) (Manley, 2002). The production of a poly-halogenated compound, in case of this study, CHBr_2Cl , may involve enzymatic halogenation via haloperoxidases that were able to oxidase halogen anions. (Theiler *et al.*, 1978).

Parachlorella sp. UMACC 245 was shown to be the most light sensitive based on the significant ($p < 0.05$) changes in emission rates of all five halocarbons under different irradiances as compared to the other two algal taxa. This may indicate that *Parachlorella* sp. UMACC 245 is more sensitive to the trigger of halocarbon production when exposed to higher irradiance and during dark cycle. This clearly indicates that the effect of irradiance on halocarbon production is species-dependent. The release of halocarbons has been a form of defense mechanism to abiotic stresses and herbivory-predators (Bravo-Linares & Mudge, 2009; Paul & Pohnert, 2011). These halocarbons may be produced from hydrogen peroxide (H_2O_2) and the sources to produce H_2O_2 include mitochondrion transport chain (Cadenas, 1989), through the Mehler reaction or pseudocyclic photophosphorylation during photosynthesis (Pedersén *et al.*, 1996) and other cellular sources. *Parachlorella* sp. UMACC 245 in the tropics may have adapted to the ability of

producing higher concentration of H_2O_2 as a defense mechanism to cope with higher irradiance and possibly better at recovery from photoinhibition than *Synechococcus* sp. UMACC 371 and *Amphora* sp. UMACC 370.

The emission of short-lived CH_3I was shown to vary the most as compared to other halocarbons namely, CHBr_3 , CHCl_3 , CHBr_2Cl and CH_2Br_2 when exposed to higher irradiance, especially by *Amphora* sp. UMACC 370. Due to the fact that other trace gases were produced, the cells might have involved haloperoxidase enzymes to mediate the halogenation of organic compounds in the medium through the breakdown of hydrogen peroxide (Butler and Walker, 1993). Other possible pathways of the CH_3I production include iodination of inorganic iodine species such as atomic iodine (I^*) by methyl groups or radicals arising from photochemical reactions (Moore & Zafiriou, 1994), and the breakdown of higher molecular weight iodine-containing organics (Fenical, 1982). Although there was a low positive correlation between F_v/F_m and halocarbon emissions under different irradiances across all three taxa (except emission normalized to cell density by *Synechococcus* sp. UMACC 371), the results may indicate a link between cell stress, increased cell membrane permeability and higher emission rate of CH_3I . A loss of membrane integrity increases the release of CH_3I precursors to the surrounding medium while the cellular responses to limiting conditions promote the formation of this iodinated compound. Both oxidative stress and the associated breakdown of cellular membranes could lead to enhanced CH_3I production (Hughes et al., 2011).

The emission of other short-lived compounds including CHBr_3 , CHCl_3 , CH_2Br_2 and CHBr_2Cl by the three taxa after exposure to higher (excessive) irradiance may be, in general, linked to the oxidative damage in the photosynthetic apparatus that results in a decrease in photosynthetic efficiency. One of the reasons for this damage may be the damage in photosystem II (PSII) caused by the oxidation of lipids, proteins and pigments

by reactive oxygen species such as singlet oxygen ($^1\text{O}_2$), H_2O_2 and the hydroxyl radical (OH) (Hughes *et al.*, 2006).

Results from this irradiance experiment also showed higher production of halocarbons, especially CH_3I , during 12 hours of complete darkness. Whilst a mechanism behind this may not be available yet, nonetheless suggestions that could be made are 1) the cells may still be able to mediate the halide precursors in the dark and thus once exposed to the first return of photons, the halocarbons are synthesized as an indication of stress. 2) Mitochondrion transport chains, one of the sources of H_2O_2 production (Cadenas, 1989), are metabolically active during the dark reaction and the transport of electrons drive the production of H_2O_2 as a by-product (Bienert *et al.*, 2006). With the availability of H_2O_2 , the biosynthesis of halogenated compounds may be made possible, 3) In the dark, chloroplast and mitochondrion in photosynthetic cells are interdependence and the possible changes of their biophysical membrane, the lipid composition of the bilayers, due to the nutrient limitation may result in higher permeability for the diffusion of H_2O_2 to occur. Higher fluxes of H_2O_2 ultimately results a chance in the production of organohalogen (Hoefnagel *et al.*, 1998; Bienert *et al.*, 2006).

In general, the weak correlation between the halocarbon emission and F_v/F_m under the influence of three different irradiances implies that the halocarbon emissions in the three algae are not strongly influenced by photosynthetic performance. This may be due to the short-term exposure even at the highest irradiance. The release of CH_3I by *Parachlorella* sp. UMACC 245, CHBr_3 , CH_3I , CHCl_3 and CHBr_2Cl by *Amphora* sp. UMACC 370 as well as CH_3I , CHCl_3 , CH_2Br_2 (chlorophyll-a normalized) and CHCl_3 (cell density normalized) by *Synechococcus* sp. UMACC 371, was positively correlated with the F_v/F_m values. In these cases, the increase of halogenated compounds with increased F_v/F_m values might be due to the build-up of H_2O_2 from photosynthesis in the microalgae without H_2O_2

reaching a level that could cause cell stress or membrane destruction that inhibits photosynthesis and respiration in the cells. Four out of the five compounds, CHBr_3 , CHCl_3 , CH_2Br_2 and CBr_2Cl emitted by *Parachlorella* sp. UMACC 245, as well as brominated compounds, CHBr_3 and CH_2Br_2 emitted by *Synechococcus* sp. UMACC 371 and CH_2Br_2 emitted by *Amphora* sp. UMACC 370 were negatively correlated with the F_v/F_m values. Nonetheless, the fluorescence-based measures of F_v/F_m that reflects the ability of Photosystem II (PSII) reaction centers to make use of the available excitation energy, based on the correlation results, does not directly explain the physiological cell stress and the formation of halocarbons might not be photosynthetically related. Controversial studies have been reported that nutrient limitation in the batch culture medium, may or may not affect the maximum quantum yield and its measurement (Parkhill *et al.*, 2001; Cullen *et al.*, 1992). The possible stress of the cells resulting from the short-term exposure to the higher irradiance could also be explained from the production of H_2O_2 that originated from mitochondrial respiration, where the intracellular redox state may play a role in the maintenance and production of H_2O_2 , and enzymatic catalysis such as peroxisome-associated catalase (Gross, 1993) that chemically interacts with dissolved organic matter by the microalgal cells (Lin & Manley, 2012; Wever *et al.*, 1991).

In order to give more insight on the effect of irradiance on halocarbon emissions, studies based on a longer period of exposure to the same irradiance level, and the incorporation of additional photosynthetic parameters such as the maximum Electron Transport Rate (ETR_{max}), Non-Photochemical Quenching (NPQ) and Alpha, as well as the biochemical profiling that includes fatty acid content of the cells, would be useful to fully assess the correlation between halocarbon emission and cell stress for exact explanation and source of the stress.

The emission of each halide contributed from the five detected compounds within the 12-hour light exposure in terms of total halide mass calculated in percentage is summarized in Table 5.3. From the results, *Amphora* sp. UMACC 370 was the stronger emitter of halocarbons in terms of total halogen emission (pg) as compared to the other two taxa. *Amphora* sp. UMACC 370 was shown to contribute the highest amount of iodine as compared to bromine and chlorine and even amongst the other two taxa. This was consistent with the earlier halocarbon experiment on growth-stages.

When comparing the light stress experiment to the previous growth-cycle experiment, *Parachlorella* sp. UMACC 245 showed higher ratio of iodine to bromine and chlorine as compared to the higher ratio of chlorine to bromine and iodine, respectively. *Synechococcus* sp. UMACC 371 showed a change in the ratio of three halide composition. These clearly imply a positive influence of light stress on the emission of halocarbons, despite the short stress period that lasted only for 12 hours. Comparing the iodine release between growth stage and irradiance experiments, the percentage of iodine contributed by *Amphora* sp. UMACC 370 and *Parachlorella* sp. UMACC 245 has shown to increase from 60% to 87% and 21% to 71% respectively. Several explanations could be that these two taxa possess cell structure and size that may be more susceptible to lysis when exposed to higher irradiance, thus releasing more CH₃I (Hughes *et al.*, 2011). The possible higher concentration of iodoperoxidase present in these two taxa may also enhance the production of iodine, though the total iodine percentage emitted by *Amphora* sp. UMACC 370 is several times higher than *Parachlorella* sp. UMACC 245.

Table 5.3: Total mass of emitted halides. Total halogen mass emitted as halocarbons and percentage contribution to the total from bromine, chlorine and iodine. Taxa are arranged in decreasing total mass halogens emitted order.

Taxa	Total halogens emitted (pg)	% Br	% Cl	% I
<i>Amphora</i> sp. UMACC 370	500.5	3.35	9.73	86.92
<i>Synechococcus</i> sp. UMACC 371	471.7	14.29	46.88	38.83
<i>Parachlorella</i> sp. UMACC 245	98.3	14.59	14.59	70.82

A previous study reported higher CH₂Br₂ concentration produced by polar *Nitzschia* sp. CCMP 580 and polar *Porosira glacialis* CCMP 651 cultures when exposed to higher irradiance (Moore et al., 1996). In low light (12 $\mu\text{mol photons m}^{-2} \text{s}^{-1}$), CH₂Br₂ emitted by *Nitzschia* sp. and *Porosira glacialis* CCMP 651 ranged from 0- 200 pmol L⁻¹ and 0- 380 pmol L⁻¹ respectively. In higher light (40 $\mu\text{mol photons m}^{-2} \text{s}^{-1}$), the range of CH₂Br₂ emitted increased up to 1300 pmol L⁻¹ and 1600 pmol L⁻¹ respectively over a period of 30 days (Moore et al., 1996). This was consistent with the present light stress experiments as observed from Figure 4.23 to 4.28 where there was higher CH₂Br₂ concentration, or an increase in the emission when exposed to higher irradiance for *Synechococcus* sp. UMACC 370 and *Parachlorella* sp. UMACC 245, but not *Amphora* sp. UMACC 370, which showed no obvious changes in CH₂Br₂ concentration. Moore et al. (1996) also reported no clear trend of “higher level of illumination produces higher halocarbon concentration”, while the present study had shown the significant ($p < 0.05$) differences in the emission rates when exposed to higher irradiance. The discrepancies between the studies could be due to 1) the use of different microalgal strains, 2) temperature used for acclimatization, 3) the amount of time exposed to higher irradiance, 4) Cultures in the previous study were exposed to the range from 12 to 40 $\mu\text{mol photons m}^{-2} \text{s}^{-1}$ whereas in the present study the cultures were exposed from 40 to 120 $\mu\text{mol photons m}^{-2} \text{s}^{-1}$.

Scarratt and Moore (1999) showed a decrease in CH₃I emission by a red microalgae, *Porphyridium purpureum* despite exposure to higher irradiance (from 20 to 800 $\mu\text{mol photons m}^{-2} \text{ s}^{-1}$) for a period of 24 hours. In our present study, an increase in CH₃I emission across all three taxa was observed, contrary to Scaratt and Moor's report; but this may be due to the use of different algae, thus indicating a species-specific response.

The experimental results and comparisons made were based on the laboratory incubation of microalgae instead of an *in-situ* experiment. Hence, there are still many uncertainties that may exist in the natural habitats that might further influence the emission rates of the tropical marine microalgae.

5.5 Proposed areas for future research

It should be noted that the present studies report the emissions of short-lived halocarbons by a limited number of marine tropical microalgae under a limited range of conditions. Eight compounds (others include CH₂BrI, CHBrCl₂, CH₂I₂) were initially screened while only five compounds (CH₃I, CHBr₃, CHCl₃, CH₂Br₂, CHBr₂Cl) were detected above the detection limit by GCMS to calculate for the emission (rates). More data should be collected by studies on a wide array of marine tropical microalgae and further screened for a more complete regional data of short-lived halocarbons contributed by marine microalgae from the tropics.

Our results provide the first report of halocarbon emission by monospecific marine microalgal cultures from the tropics, both on the effect of growth-stages as well as different irradiances on halocarbon emission. This contributes to the library of existing reports on halocarbon emission by phytoplankton from polar and temperate regions. Controlled studies where the algae are subjected to other environmental stress either in the laboratory or on-site, should be done for more accurate global scale normalization. Satellite-based modeling to obtain regional phytoplankton biomass such as chlorophyll-a

to normalize with extrapolated data from controlled studies will be helpful to establish a direct link of exact source to the emission of the halocarbons.

Area for future research:

- 1) To relate the effect of different environmental factors such as the changes in temperature, salinity and pH or $p\text{CO}_2$ have on the emissions of the marine microalgae.
- 2) To establish a link between enzymatic mechanisms responsible for the production of halocarbons.
- 3) To venture into molecular work that can identify the genes responsible for halocarbon production.
- 4) To further relate the process of photosynthesis through various photosynthetic parameters other than F_v/F_m to the production and emission of halocarbons.
- 5) To establish a direct link of sources of halocarbon emission in the local open ocean waters from satellite modeling observation through chlorophyll content or even ribotype abundance patterns to the halocarbon emission measured on-site and from controlled experiments in the laboratory.
- 6) To investigate the link between oxidative stress and halocarbon production from the tropical marine microalgae.

CHAPTER 6: CONCLUSIONS

The compounds CH₃I, CHBr₃, CHCl₃, CH₂Br₂ and CHBr₂Cl were shown to be emitted by tropical marine microalgae, *Synechococcus* sp. UMACC 371, *Parachlorella* sp. UMACC 245 and *Amphora* sp. UMACC 370. *Amphora* was found to have significantly ($p<0.05$) higher emission rates of the five short-lived halocarbons, especially CH₃I.

The emission rates for the three tropical microalgae differ between the exponential and stationary growth phases, with higher emission rates at exponential phase. Results show that the emissions of volatile short-lived halogenated compounds by the three tropical microalgae strains are not only strain-specific but also growth phase-dependent, which implies the significant role of cell growth physiological state when determining the emission rates.

The short-term exposure to a range of irradiances under controlled laboratory condition was shown to influence the emission of the five halocarbons, CH₃I, CHBr₃, CHCl₃, CH₂Br₂ and CHBr₂Cl by the three tropical marine microalgae, *Synechococcus* sp. UMACC 371, *Parachlorella* sp. UMACC 245 and *Amphora* sp. UMACC 370. Halocarbons emitted were shown to increase and decrease when exposed to both higher irradiance and even complete darkness as compared to the control irradiance level, though the significance ($p<0.05$) in changes of emission for each compound that is specific to each irradiance level differ for each taxa. This clearly indicates that the effect of different irradiance on halocarbon production are species- dependent.

Parachlorella sp. UMACC 245 was shown to be the most sensitive to a change in irradiance as compared to the other two taxa based on the significant ($p<0.05$) changes of emission rates amongst the five halocarbons. The emission of CH₃I, especially the most abundant by *Amphora* sp. UMACC 370, was shown to be dominant in terms of their total

halide mass (pg) and significance ($p < 0.05$) when compared amongst the five halogenated compounds.

The different irradiances were shown to influence significantly ($p < 0.05$) the maximum quantum yield, F_v/F_m across all three taxa; a significant ($p < 0.05$) decrease in F_v/F_m was observed for *Parachlorella* sp. UMACC 245 and *Amphora* sp. UMACC 371 when exposed to higher irradiance at $120 \mu\text{mol photons m}^{-2} \text{s}^{-1}$ from $40 \mu\text{mol photons m}^{-2} \text{s}^{-1}$, the controlled light level. However, when exposed to complete darkness, the changes in F_v/F_m across all three taxa, despite showing increase and decrease in emission rate, did not vary significantly ($p < 0.05$).

The changes in halocarbon emission rates were weakly correlated and not significant to the changes in F_v/F_m when compared across all three different irradiances for all three microalgae, though both positive and negative correlation specific to each compound were observed. This suggests the possibility of other physiological stress sources such as the production of H_2O_2 from not mainly photosynthesis but mitochondrion respiration, nutrient limitation and even a change of lipid composition in membrane bilayers that stimulate and drive the production of halocarbons.

The tropical marine microalgae are widely-distributed in open-water surfaces, and are amongst the most significant sources of halogen load in the stratosphere, hence there is a need to measure and monitor such emissions not only in controlled laboratory scale but also extend to look further the actual emissions under the natural environment in the tropics in the future. Studies on biological responses to climate change should transcend transient acclimation physiology to investigate long-term adaptation and evolution, besides the essential need of a comprehensive library of regional and global emission data linking compounds to algal species for the assessment and prediction of halocarbon emissions over the world-wide oceans.

The research questions can be answered as follows:

- (i) The main short-lived halogenated compounds emitted by the three tropical marine microalgae, *Synechococcus* sp. UMACC 371, *Parachlorella* sp. UMACC 245 and *Amphora* sp. UMACC 370 were CHBr_3 , CH_3I , CHCl_3 , CHBr_2Cl and CH_2Br_2 .
- (ii) The emission of short-lived halocarbons by the three tropical marine microalgae were shown to be species- and growth phase- dependent, highlighting the importance of taking cell growth physiological state when determining emission rates into consideration.
- (iii) The range of irradiances was shown to significantly ($p>0.05$) influence the changes in F_v/F_m and halocarbon emission rates. However, the correlation between F_v/F_m and halocarbon emission rates were weakly correlated ($p>0.05$), indicating that the emission of the halocarbons might not be due to algal cell stress from photosynthetic performance but may be due to other physiological mechanisms in cells.

REFERENCES

- Abrahamsson, K., Loren, A., Wuff, A., & Wangberg, S. A. (2004). Air-sea exchange of halocarbons: the influence of diurnal and regional variations and distribution of pigments. *Deep-Sea Research II*, 51, 2789-2805.
- Amachi, S., Kagamata, Y., Kanagawa, T., & Muramatsu, Y. (2001). Bacteria mediate methylation of iodine in marine and terrestrial environments. *Applied Environmental Microbiology*, 67, 2718-2722.
- Arrigo K. R., Perovich, D. K., Pickart, R. S., Brown, Z. W., van Dijken, G. L., Lowry, K. E., Mills, M. M., Palmer, M. A., Balch, W. M., Bahr, F., Bates, N. R., Benitez-Nelson, C., Bowler, B., Brownlee, E., Ehn, J. K., Frey, K. E., Garley, R., Laney, S. R., Lubelczyk, L., Mathis, J., Matsuoka, A., Mitchell, B.G., Moore, G. W. K., Ortega-Retuerta, E., Pal, S., Polashenski, C. M., Reynolds, R. A., Schieber, B., Sosik, H. M., Stephens, M., & Swift, J. H. (2012). Massive phytoplankton blooms under Arctic sea ice. *Science*, 336, 1408.
- Asare, N. K., Turley, C. M., Nightingale, P. D., & Nimmo, M. (2012). Microbially-mediated methyl iodide production in water samples from an estuarine system. *Journal of Environment*, 01(03), 75–83.
- Aschmann, J., Sinnhuber, B. M., Atlas, E. L., & Schauffler, S. M. (2009). Modeling the transport of very short-lived substances into the tropical upper troposphere and lower stratosphere. *Atmospheric Chemistry and Physics*, 9(23), 9237-9247.
- Bayersdorf, A. J., Blake, D. R., Swanson, A., Meinardi, S., Rowland, F. S., & Davis, D. (2010). Abundances and variability of tropospheric volatile organic compounds at South Pole and other Antarctic locations. *Atmospheric Environment*, 44, 4565-4574.
- Beakes, G., Canter, H. M., & Jaworski, G. H. M. (1988). Zoospore ultrastructure of *Xygorbizidium affluens* Canter and *Z. planktonicum* Cantor, two chytrids parasitizing the diatom *Asterionella formosa* Hassall. *Canadian Journal of Botany*. 66, 1054- 1067.
- Bell, N., & Hsu, L. (2002). Methyl iodide: Atmospheric budget and use as a tracer of marine convection in global models. *Journal of Geophysical Research*, 107, 4340.
- Berg, W. W., Sperry, P. D., Rahn, K. A., & Gladney, E. S. (1983). Atmospheric bromine in the Arctic. *Journal of Geophysical Research*, 88: 6719—6736.
- Bergman, J. W., Jensen, E.J., Pfister, & L., Yang, Q. (2012) Seasonal differences of vertical-transport efficiency in the tropical tropopause layer: on the interplay between tropical deep convection, large-scale vertical ascent, and horizontal circulations. *Journal of Geophysical Research*, 117, D05302.
- Bienert, G. P., Schjoerring, J. K., & Jahn, T. P. (2006). Review: Membrane transport of hydrogen peroxide. *Biochimica et Biophysica Acta*, 1758, 994-1003.
- Blake, N. J., Blake, D. R., Chen, T. -Y., Collins, Jr. J. E., Sachse, G. W., Anderson, B. E., & Rowland, F. S. (1997). Distribution and seasonality of selected

- hydrocarbons and halocarbons over the western Pacific basin during PEM-West A and PEM-West B. *Journal of Geophysical Research—Atmospheres* 102, 28315–28331.
- Boonyapiwat, S. (1997). Proceedings of the first Technical Seminar on Marine Fishery Sources Survey in the South China Sea, Area I: Gulf of Thailand East Coast of Peninsular Malaysia. Oceanic Fisheries Division, Department of Fisheries.
- Bravo-Linares, C. M., & Mudge, S. M. (2009). Temporal trends and identification of the sources of volatile organic compounds in coastal seawater. *Journal of Environmental Monitoring*, 11, 628-641.
- Brinckmann, S., Engel, A., Bönisch, H., Quack, B., & Atlas, E. (2012). Short-lived brominated hydrocarbons – observations in the source regions and the tropical tropopause layer. *Atmospheric Chemistry and Physics*, 12, 1213–1228.
- Brownell, D. K., Moore, R. W., & Cullen, J. J. (2010). Production of methyl halides by *Prochlorococcus marinus* and *Synechococcus*. *Global Biogeochemical Cycle*, 24, GB2002.
- Burford, M. A., Rothlisberg, P. C., & Wang, Y. G. (1995). Spatial and temporal distribution of tropical phytoplankton species and biomass in the Gulf of Carpentaria, Australia. *Marine Ecology Progress Series*, 118: 255-266.
- Butler, A., & Walker, J.V. (1993). Marine haloperoxidases. *Chemical Reviews*, 93, 1937-1944.
- Cadenas, E. (1989). Biochemistry of oxygen toxicity. *Annual Review of Biochemistry*, 58, 79-110.
- Calvet, J. G., & Lindberg, S. E. (2004). Potential influence of iodine-containing compounds on the chemistry of the troposphere in the polar spring. I. Ozone depletion. *Atmospheric Environment*, 38, 5087-5104.
- Carlsson, A., Beilen van, J., Möller, R., Clayton, D., & Bowles, D. (2007). Micro- and macroalgae - utility for industrial applications: Realising the Economic Potential of Sustainable Resources - Bioproducts from Non-food Crops. CNAP, University of York: pp 86.
- Carpenter, L. J., & Liss, P. S. (2000). On temperate sources of bromoform and other reactive organic bromine gases. *Journal of Geophysical Research*, 105(D16), 20539-20548.
- CCMP (Provasoli-Guillard Center for Culture of Marine Phytoplankton, Bigelow Laboratory for Ocean Sciences, Mc Kown Point, West Boothbay Harbor, Maine 04575, USA. <http://ncma.bigelow.org/>. Accessed 10 May 2016.
- Chipperfield, M. P. (2015). Global Atmosphere - The Antarctic Ozone Hole, in Still Only One Earth: Progress in the 40 Years Since the First UN Conference on the Environment. *Royal Society of Chemistry*, 1-33.

- Clowes, M. (2014). The basic of organic chemistry. The Rosen Publishing Group, New York.
- Colomb, A., Yassaa N., Williams, J., Peeken, I., & Lochte, K. (2008). Screening volatile organic compounds (VOCs) emissions from five marine phytoplankton species by head space gas chromatography/mass spectrometry (HS-GC/MS). *Journal of Environmental Monitoring* 10(3), 325-30.
- Cubillos, J. C., Wright, S. W., Nash, G., de Salas, M. F., Griffiths, B., Tilbrook, B., Poisson, A., & Hallegraeff, G. M. (2007). Calcification morphotypes of the coccolithophorid *Emiliana huxleyi* in the Southern Ocean: changes in 2001 to 2006 compared to historical data. *Marine Ecology Progress Series*, 348, 47-54.
- Cullen, J. J., Yang, X., & MacIntyre, H. L. (1992). Nutrient limitation of marine photosynthesis. In Falkowski, P. G., Woodhead, A. D. (Eds.) Primary productivity and biogeochemical cycles in the sea. Plenum Press, New York, pp. 31-45.
- Day, J. W., Yáñez-Arancibia, A., & Rybczyk, J. M. (2011). Climate change: Effects, Causes, Consequences: Physical, Hydromorphological, Ecophysiological, and Biogeographical Changes. *Treatise on Estuarine and Coastal Science*, 8, 303-315.
- Deshler, T., Johnson, B. J., Hofmann, D. J., & Nardi, B. (1996). Correlations between ozone loss and volcanic aerosols at altitudes below 14km over McMurdo Station, Antarctica. *Geophysical Research Letter*, 23(21), 2931-2934.
- Ekdahl, A., Pedersen, M., & Abrahamsson, K. (1998). A study of the diurnal variation of biogenic volatile halocarbons. *Marine Chemistry*, 63, 1-8.
- Fahey, D.W., & Hegglin, M. I. (2011). Twenty Questions and Answers about the Ozone Layer: 2010 Update, Scientific Assessment of Ozone Depletion: 2010. World Meteorological Organization, Geneva, Switzerland.
- Faraday, M. (1821). On two new compounds of chlorine and carbon, and on a new compound of iodine, carbon, and hydrogen. *Philosophical Transactions*, 111, 47.
- Fisherman, D. B., Adlerstein, S. A., Vanderploeg, H. A., Fahnenstiel, G. L., & Scavia, D. (2010). Phytoplankton community composition of Saginaw Bay, Lake Huron, during the zebra mussel (*Dreissena polymorpha*) invasion: A multivariate analysis. *Journal of Great Lakes Research*, 36(1), 9-19.
- Fenical, W. (1982). Natural products chemistry in the marine environment. *Science*, 215, 923-928.
- Forster, P., & Joshi, M. (2005). The role of halocarbons in the climate change of the troposphere and stratosphere. *Climatic Change*, 71(1), 249-266.
- Frederick, J. E. (2015). Ozone depletion and related topics: Ozone as a *uv* filter. *Reference Module in Earth Systems and Environmental Sciences- Encyclopedia of Atmospheric Sciences (Second Edition)*, 359-363.
- Fueglistaler, S., Dessler, A. E., Dunkerton, T. J., Folkins, I., Fu, Q., & Mote, P. W. (2009). Tropical Tropopause Layer. *Reviews of Geophysics*, 47, RG1004.

- Granfors, A., Andersson, M., Chierici, M., Fransson, A., Gardfeldt, K., Torstensson, A., Wulff, A., & Abrahamsson, K. (2013). Biogenic halocarbons in young Arctic sea ice and frost flowers. *Marine Chemistry*, 155, 124-134.
- Gribble, G. W. (1998). Naturally occurring organohalogen compounds. *Accounts of Chemical Research*, 31(3), 141-152.
- Gross, W. (1993). Peroxisomes in algae: their distribution, biochemical function, and phylogenetic importance. *Progress in Phycological Research*, 9, 47-48.
- Guillard, R. R. L., & Ryther, J. H. (1962). Studies of marine planktonic diatoms: i. *cyclotella nana* hustedt, and *detonula confervacea* (cleve) gran. *Canadian Journal of Microbiology*, 8(2), 229-239.
- Godish, T., Davis, W. T., & Fu, J. S. (2015). Air quality 5/E. Publisher: Crc press.
- Hallegraeff, G. M. (2003). Harmful algal blooms: a global overview. in Hallegraeff, G.M., Anderson, D.M., & Cembella, A.D. (eds) 2003. *Manual on Harmful Marine Microalgae*, UNESCO, Paris.
- Harper, D. B. (2000). The global chloromethane cycle: biosynthesis, biodegradation and metabolic rate. *Natural Product Reports*, 17, 337-348.
- Hasle, G. R., & Syvertsen, E. E. (1996). Marine diatoms. In: Tomas CR (ed) Identifying marine diatoms and dinoflagellates. Academic, San Diego, pp 5-385.
- Helbling. E. W., & Villafane, V. E. (2001). Phytoplankton and primary production. *Fisheries and Aquaculture –Vol. v.*
- Hill, M. K. (2010). Understanding Environmental Pollution, third edition. Cambridge, United Kingdom. Cambridge University Press. (last accessed: 18 April 2017).
- Hoefnagel, M. H. N., Atkin, O. K., & Wiskich, J. T. (1998). Independence between chloroplasts and mitochondria in the light and dark. *Biochimica et Biophysica Acta*, 1366, 235-255.
- Houghton J.T., *et al.*, (2001). (Eds.), *Climate Change 2001: The Scientific Basis*, Cambridge University Press, Cambridge. (available at www.ipcc.ch/)
- Hossaini, R., Chipperfield, M. P., Montzka, S. A., Rap, A., Dhomse, S., & Feng, W. (2015) Efficiency of short-lived halogens at influencing climate through depletion of stratospheric ozone. *National Geosciences*, 8, 186-190.
- Hughes, C., Malin, G., Nightingale, P. D., & Liss, P. S. (2006). The effect of light stress on the release of volatile iodocarbons by three species of mainre microalgae. *Limnology and Oceanography*, 51(6), 2849 – 2854.
- Hughes, C., Franklin, D. J., & Malin, G. (2011). Iodomethane production by two important marine cyanobacteria: *Prochlorococcus marinus* (CCMP 2389) and *Synechococcus* sp. (CCMP 2370). *Marine Chemistry*, 125, 19 –25.

- Hughes, C., Johnson, M., Utting, R., Turner, S., Malin, G., Clarke, A., & Liss, P. S. (2013). Microbial control of bromofrom concentrations in coastal waters of the western Antarctic Peninsula. *Marine Chemistry*, 151, 35-46.
- IPCC. (2007). Climate Change 2007: The Physical Science Basis. Contribution of Working Group I to the Fourth Assessment Report of the Intergovernmental Panel on Climate Change. Cambridge, United Kingdom & New York, USA: Cambridge University Press.
- Itoh, N., Tsujita, M., Takayuki, A., Hisatomi, G., & Higashi, T. (1997): Formation and emission of monohalomethanes from marine algae, *Phytochemistry*, 45, 67-73.
- Jacob, D.J., & Winner, D.A. (2009). Effect of climate change on air quality. *Atmospheric Environment*, 43, 51-63.
- Jordan, A. (2003). Volcanic formation of halogenated organic compounds. *The Handbook of Environmental Chemistry*, 3(part P), 121-139.
- Karlsson, A., Auer, N., Schulz-Bull, D., & Abrahamsson, K. (2008). Cyanobacterial blooms in the Baltic — A source of halocarbons. *Marine Chemistry*, 110(3-4), 129-139.
- Keng, F. S. -L., Phang, S. -M., Abd Rahman, N., Leedham, E. C., Hughes, C., Robinson, A. D., Harris, N. R. P., Pyle, J. A., & Sturges, W. T. (2013). Volatile halocarbon emissions by three tropical brown seaweeds under different irradiances. *Journal of Applied Phycology*, 25(5), 1377-1386.
- Kiehl, J. T., & Trenberth, K. E. (1997). Earth's Annual Global Mean Energy Budget (PDF). *Bulletin of the American Meteorological Society*, 78(2), 197-208.
- Kinney, P. L. (2008). Climate change, air quality, and human health. *American Journal of Preventive Medicine*, 35, 459-467. Theme Issue: Climate Change and the Health of the Public.
- Kline, P. C., Verdel, E. F., Wani, S., & Woods, A. E. (2000). Purification and partial characterization of haloperoxidase from fresh water algae *Cladophora glomerata*. *Comparative Biochemistry and Physiology. Part B Biochemistry and Molecular Biology*, 125(2), 179-87.
- Krysell, M. (1991). Bromoform in the Nansen Basin in the Arctic Ocean, *Marine Chemistry*, 33, 187-197.
- Leedham, E. C., Hughes, C., Keng, F. S. L, Phang, S. M., Malin, G., & Sturges, W. T. (2013). Emission of atmospherically significant halocarbons by naturally occurring and farmed tropical macroalgae. *Biogeosciences*, 10, 3615-3633.
- Leedham Elvidge, E. C., Phang, S. M., Sturges, W. T., & Malin, G. (2015). The effect of dessication on the emission of volatile halocarbons from two common temperate macroalgae. *Biogeosciences*. 12, 387-398.

- Levine, J. G., Braesicke, P., Harris, N. R. P., Savage, N. H., & Pyle, J. A. (2007). Pathways and timescales for troposphere-to-stratosphere transport via the tropical tropopause layer and their relevance for very short lived substances. *Journal of Geophysical Research*, 112, D04308.
- Laube, J.C., Engel, A., Bönisch, H., Möbius, T., Worton, D.R., Sturges, W.T., Grunow, K., & Schmidt, U. (2008). Contribution of very short-lived organic substances to stratospheric chlorine and bromine in the tropics—a case study. *Atmospheric Chemistry and Physics*, 8(23), 7325-7334.
- Li, Y., Horsman, M., Wu, N., Lan, C. Q., & Dubois-Calero, N. (2008). Biofuels from microalgae. *Biotechnology Progress*, 24(1), 815-820.
- Lin, C.Y., & Manley, S.L. (2012). Bromoform production from seawater treated with bromoperoxidase. *Limnology and Oceanography*, 57, 1857-1866.
- Malviya, S., Scalco, E., Audic, S., Vincent, F., Veluchamy, A., Poulain, J., Wincker, P., Ludicone, D., de Vargas, C., Bittner, L., Zingone, A., & Bowler, C. (2016). Insights into global diatom distribution and diversity in the world's ocean. *Proceedings of National Academic Science, USA* 113(11), E1516-25.
- Mactavish, F., & Buckle, S. (2013). Climate change, greenhouse gases and radiative forcing. Imperial College London. Grantham briefing note 6 (version 2).
- Manley, S. L. (2002). Phytogenesis of halomethanes: A product of selection or a metabolic accident? *Biogeochemistry*, 60, 163—180.
- Manley, S. L. & Dastoor, M. N. (1987). Methyl halide (CH₃X) production from the giant kelp, *Macrocystis*, and estimates of global CH₃X production by kelp. *Limnology and Oceanography*, 32(3), 709-715.
- Manley, S. L., & de la Cuesta, J. L. (1997). Methyl iodide production from marine phytoplankton cultures. *Limnology and Oceanography*, 42(1), 142 – 147.
- Manley, S. L., Goodwin, K., & North, W. J. (1992). Laboratory production of bromoform, methylene bromide, and methyl-iodide by macroalgae and distribution in nearshore southern California waters. *Limnology and Oceanography*, 37, 1652 – 1659.
- Marshall, J. A. (2002). Photosynthesis does influence superoxide production in the ichthyotoxic alga *Chattonella marina* (Raphidophyceae). *Journal of Plankton Research*, 24(11), 1231–36.
- Mead, M. I., Khan, M. A. H., Whitem I. R., Nickless, G., & Shallcross, D. E. (2008) Methyl halide emission estimates from domestic biomass burning in Africa. *Atmospheric Environment*, 42, 5241-5250.
- McFiggans, G, Plane, J. M. C., Allan, B. J., Carpenter, L.J., Coe, H., & O'Dowd, C.A. (2000). Modeling study of iodine chemistry in the marine boundary layer. *Journal of Geophysical Research*, 105, 14371- 14385.

- McLeod, D. J., Hallegraeff, G. M., Hosie, G. W., & Richardson, A. J. (2012). Climate-driven range expansion of the red-tide dinoflagellate *Noctiluca scintillans* into the Southern Ocean. *Journal of Plankton Research*, 34, 332-337.
- McMurray, J. (Ed.). (2008). Organic Chemistry 7th Edition. Thompson Brooks/Cole, Belmont, CA.
- Mohanakuma, K. (2008). Stratosphere troposphere interactions: an introduction. Springer. pp. 34.
- Molina, M. J., & Rowland, F. S. (1974). Stratospheric sink for chlorofluoromethanes: chlorine catalyzed destruction of ozone. *Nature*. 249, 810 – 814.
- Mohd Nadzir, M. S., Phang, S. M., Abas, M. R., Abdul Rahman, N., Abu Samah, A., Sturges, W. T., Oram, D. E., Mills, G. P., Leedham, E. C., Pyle, J. A., Harris, N. R. P., Robinson, A. D., Ashfold, M. J., Mead, M. I., Latif, M. T., Mohd Hanafiah, M., Khan, M. F., & Amiruddin, A. M. (2014). Bromocarbons in the tropical coastal and open ocean atmosphere during the Prime Expedition Scientific Cruise 2009 (PESC 09). *Atmospheric Chemistry and Physics*, 14(15), 8137-8148.
- Moline, M. A., Claustre, H., Frazer, T. K., Schofield, O., & Vernet, M. (2004). Alteration of the food web along the Antarctic Peninsula in response to a regional warming trend. *Global Change Biology*, 10, 1973–1980.
- Moline, M. A., & Prézelin, B. B. (1996). Palmer LTER 1991-1994: Long-term monitoring and analysis of physical factors regulating variability in coastal Antarctic phytoplankton biomass, *in situ* productivity, and taxonomic composition over subseasonal, seasonal, interannual time scales. *Marine Ecology Progress Series*, 145, 143-160.
- Moore, R. M. (2003). Marine sources of volatile organohalogenes. *The Handbook of Environmental Chemistry*, 3(part P), 85-101.
- Moore, R. M., Geen, C. E., & Tait, V. K. (1995). Determination of Henry Law Constants for a Suite of Naturally-Occurring Halogenated Methanes in Seawater, *Chemosphere*, 30: 1183-1191.
- Moore, J., & Stanitski, C. (2014). Chemistry: The molecular science, chapter 8: properties of gases. Cengage learning. pp. 358.
- Moore, R. M., & Tokarczyk R. (1993). Volatile biogenic halocarbons in the northwest Atlantic. *Global Biogeochemical Cycles* 7, 195 – 210.
- Moore, R. M., Tokarczyk, R., Tait, V. K., Poulin, & M., Geen, C. (1994). Marine phytoplankton as a natural source of volatile organohalogenes. In: International conference on naturally-produced organohalogenes. Springer Science? Business Media Dordrecht, Netherland. *Environmental Chemistry*, 1, 283–294.
- Moore, R. M., Webb, M., Tokarczyk, R., & Wever, R. (1996). Bromoperoxidase and iodoperoxidase enzymes and production of halogenated methanes in marine diatom cultures. *Journal of Geophysical Research-Oceans*, 101, 20899-20908.

- Moore, R. M., & Zafiriou, O. C. (1994). Photochemical production of methyl iodide in seawater. *Journal of Geophysical Research*, 99(D8), 16415-16420.
- Mora, C., Frazier, A. G., Longman, R. J., Dacks, R. S., Walton, M. M., Tong, E. J., Sanchez, J. J., Kaiser, L. R., Stender, Y. O., Anderson, J. M., Ambrosino, C. M., Fernandes-Silva, I., Giuseffi, L. M., & Giambelluca, T. W. (2013) The projected timing of climate departure from recent variability. *Nature* 502, 183–187.
- Morris, J. J., Kirkegaard, R., Szul, M. J., Johnson, Z. I., & Zinser, E. R. (2008). Facilitation of robust growth of *Prochlorococcus* colonies and dilute liquid culture by "helper" heterotrophic bacteria. *Applied Environmental Microbiology*, 74, 4530 - 4534.
- Navarro, M. A., Atlas, E. L., Saiz-Lopez, A., Rodriguez-Iloveras, X., Kinnison, D. E., Lamarque, J.-F., Tilmes, S., Filus, M., Harris, N. R. P., Meneguz, E., Ashfold, M. J., Manning, A. J., Cuevas, C. A., Schauffler, S. M., & Donets, V. (2015) Airborne measurements of organic bromine compounds in the Pacific tropical tropopause layer. *Proceedings of the National Academic of Sciences, USA* 112(45), 13789–13793.
- Nash, E., & Newman, P. (2011). NASA confirms arctic ozone depletion trigger. *Image of the day*. NASA.
- Neidleman SL, & Geigert J. (1986). Biohalogenation - principles, basic roles and applications; Ellis Horwood Ltd Publishers; Chichester, UK, pp 113-130.
- Nightingale, P. D., Malin, G. & Liss, P.S. (1995). Production of chloroform and other lowmolecular-weight halocarbons by some species of macroalgae. *Limnology and Oceanography*, 40(4), 680-689.
- NOAA (National Oceanic and Atmospheric Administration) (2010). Section II: The ozone depletion process. 20 Questions: 2010 Update. <http://www.esrl.noaa.gov/csd/assessments/ozone/2010/twentyquestions/Q10.pdf>
- OBIS, Ocean Biogeographic Information System (2015) Intergovernmental Oceanographic Commission of UNESCO. www.iobis.org. (Last accessed 15 August 2016).
- O'Dowd, C. D., Jimenez, J. L., Bahreini, R., Flagan, R. C., Seinfeld, J. H., Hameri, H., Pirjola, L., Kulmala, K., Jennings, S. G., & Hoffmann, T. (2002). Marine aerosol formation from biogenic iodine emissions, *Nature*, 417, 632 – 636.
- Palenik, B., Zafiriou, O. C., & Morel, F. M. M. (1987). Hydrogen peroxide production by a marine phytoplankton. *Limnology and Oceanography*, 32, 1365-1369.
- Parkhill J. -P., Maillet, G., & Cullen, J. J. (2001). Fluorescence-based maximal quantum yield for PSII as a diagnostic of nutrient stress. *Journal of Phycology*, 37, 517-529.
- Paul, C., & Pohnert, G. (2011). Production and role of volatile halogenated compounds from marine algae. *Natural Product Reports*, 28, 186-195.

- Pedersén, M., Collén, J., Abrahamsson, K., & Ekdahl, A. (1996). Production of halocarbons from seaweeds: an oxidative stress reaction? *Scienza Marina*, 60: 257-263.
- Penkitt, S.A., Butler, J.H., Reeves, C.E., Singh, H., Toohey, D. & Weiss, R. (1995). Chapter 10 – Methyl Bromide. In: Ennis, C.A. (Ed.), Scientific Assessment of Ozone Depletion: 1994. Geneva: World Meteorological Organization.
- Pisciotta, J. M., Zou, Y., & Baskakov, I. V. (2010). Yang, C.-H., (ed) Light-dependent electrogenic activity of cyanobacteria, *PloS ONE*, 5(5), e10821.
- Poppoff, I. G., Whitten, R. C., Turco, R. P., & Capone, L. A. (1978). An assessment of the effect of supersonic aircraft operations on the stratospheric ozone content. NASA Reference Publication. 1026.
- Pyle, J. A., Warwick, N. J., Harris, N. R. P., Abas, M. R., Archibald, A. T., Ashfold, M. J., Ashworth, K., Barkley, M. P., Carver, G. D., Chance, K., Dorsey, J., Fowler, D., Gonzi, S., Gostlow, B., Hewitt, C. N., Kurosu, T. P, Lee, J. D, Langford, B., Mills, G., Moller, S., MacKenzie, A. R., Manning, A. J, Misztal, P., Nadzir, M. S. M., Nemitz, E., Newton, H., O'Brien, L. M., Ong, S., Oram, D., Palmer, P. I., Peng, L. K., Phang, S. M., Pike, R., Pugh, T. A. M., Rahman, N. A., Robinson, A. D., Samah, A. A., Sentian, J., Skiba, U., Ung, H. E., Yong, S. E., & Young, P. (2011b). The impact of local surface changes in Borneo on atmospheric composition at wider spatial scales: coastal processes, land-use change and air quality. *Philosophical Transactions of the Royal Society B*, 366, 3210–3224.
- Pyle, J. A., Ashfold, M. J., Harris, N. R. P., Robinson, N. D., Warwick, N. J., Carver, G. D., Gostlow, B., O'Brien, L. M., Manning, M. J., Phang, S. M., Yong, S. E., Leong, K. P., Ung, E. H., & Ong, S. (2011a). Bromoform in the tropical boundary layer of the Maritime Continent during OP3. *Atmospheric Chemistry and Physics*, 11, 529–542.
- Ramanathan, V., & Feng, Y. (2009). Air pollution, greenhouse gases and climate change: global and regional perspectives. *Atmospheric Environment*, 43, 37-50.
- Robinson, A. D., Harris, N. R. P., Ashfold, M. J., Gostlow, B., Warwick, N. J., O'Brien, L. M., Beardmore, E. J., Nadzir, M. S. M., Phang, S.-M., Samah, A. A., Ong, S., Ung, H. E., Peng, L. K., Yong, S. E., Mohamad, M., & Pyle, J. A. (2014). Long term halocarbon observations from a coastal and an inland site in Sabah Malaysian Borneo. *Atmospheric Chemistry and Physics*, 14(16), 8369–8388.
- Roy, R. (2010). Short-term variability in halocarbons in relation to phytoplankton pigments in coastal waters of the central eastern Arabian Sea. *Estuarine, Coastal and Shelf Science*, 88, 311- 321.
- Sturges, W. T., Sullivan, C. W., Schnell, R. C., Heidt, L. E., & Pollock, W. H. (1993). Bromoalkane production by Antarctic ice algae. *Tellus*, 45(B), 120- 126.
- Sæmundsdottir, S., & Matrai, P. A. (1998). Biological production of methyl bromide by cultures of marine phytoplankton. *Limnology and Oceanography*, 43(1), 81—87.

- Saini, H. S., Attieh, J. M., & Hanson, A.D. (1995). Biosynthesis of halomethanes and methanethiol by higher plants via a novel methyltransferase reaction. *Plant, Cell and Environment*, 18, 1027–1033.
- Scarratt, M. G., & Moore, R. M. (1996). Production of methyl chloride and methyl bromide in laboratory cultures of marine phytoplankton. *Marine Chemistry*, 54, 263-272
- Scarratt, M. G., & Moore, R. M. (1999). Production of chlorinated hydrocarbons and methyl iodide by red microalga *Porphyridium purpureum*. *Limnology and Oceanography*, 44(3), 703 – 707.
- Schauffler, S. M., Atlas, E. L., Blake, D. R., Flocke, F., Lueb, R. A., Lee-Taylor, J. M., Stroud, V., & Travnick, W. (1999). Distributions of brominated organic compounds in the troposphere and lower stratosphere, *Journal of Geophysical Research*, 104, 21513–21535.
- Scheff, J., & Frierson, D. M. W. (2014). Scaling potential evapotranspiration with greenhouse warming. *Journal of Climate*, 27, 1539-1558.
- Sherman, K., & Hempel, G., (eds.) 2009. The UNEP Large Marine Ecosystem Report. Perspective on Changing Conditions in LMEs of the World's Regional Seas. UNEP Regional Seas Report and Studies No. 182. UNEP, Nairobi, Kenya. 872 pp.
- Sivasakthivel, T., & Siva Kumar Reddy, K. K. (2011). Ozone layer depletion and its effects: a review. *International Journal of Environmental Science and Development*, 2(1), 30-37.
- Smythe-Wright, D., Boswell, S. M., Breithaupt, P., Davidson, R. D., Dimmer, C. H., & Diaz, L. B. E. (2006). Methyl iodide production in the ocean: Implications for climate change, *Global Biogeochemical Cycles*, 20, GB3003.
- Sneader, W. (2005). Chapter 8: Systematic medicine. *Drug Discovery: a history*. Chichester, England: John Wiley and Sons. pp. 74-87.
- Solomon, S. (1999). Stratospheric Ozone Depletion: A review of concepts and history. Aeronomy laboratory. National Oceanic and Atmospheric Administration (NOAA). *American Geophysical Union*, 37/3.
- Sparling, B. (2001). Antarctic Ozone Hole. NASA Advanced Supercomputing Division. www.nas.nasa.gov
- Strickland, J. D. H., & Parsons, D. R. (1968). A practical handbook of seawater analysis. Pigment analysis, *Journal of the Fisheries Research Board of Canada*, 167.
- Strzepek, R. F., & Harrison, P. J. (2004). Photosynthetic architecture differs in coastal and oceanic diatoms. *Nature*, 431, 689-692.
- Swart, F. (1908). Cours de Chimie Organique. Librairie Scientifique, A. Hmermann (Paris).

- Tang, Y. Z., & Gobler, C. J. (2009). Characterization of the toxicity of *Cochlodinium polykrikoides* isolates from Northeast US estuaries to finfish and shellfish. *Harmful Algae*, 8(3), 454–62.
- Tait, V. K., & Moore, R. M. (1995). Methyl chloride (CH₃Cl) production in phytoplankton culture. *Limnology and Oceanography*, 40(1), 189 – 195.
- Tebbani, S., Titica, M., Ifrim, G., & Caraman, S. (2014). Control of the light-to-microalgae ratio in a photobioreactor. in *Proceedings 18th International Conference System Theory, Control Computing (ICSTCC)*, Sinaia, Romania, 393-398.
- Theiler, R., Cook, J. C., & Hager, L. P. (1978). Halohydrocarbon synthesis by bromoperoxidase. *Science*, 202, 1094 – 1096.
- The National Aeronautics and Space Administration (NASA). (2009). Ozone facts: What is the ozone hole? *Ozone Hole Watch*. NASA.
- Thompson, R. J. (1932). Freon, a refrigerant. *Industrial and Engineering Chemistry*, 24(6), 620.
- Thorenz, U. R., Carpenter, L. J., Huang, R. J., Kundel, M., Bosie, J., & Hoffmann, T. (2014). Emission of iodine containing volatiles by selected microalgae species. *Atmospheric Chemistry and Physics*, 14, 14575 – 14598.
- Tibbitts, T. W. (1994). Guidelines for lighting of plants in controlled environments. NASA-CP-95-3309.
- Tokarczyk, R., & Moore, R.M. (1994). Production of volatile organohalogenes by phytoplankton cultures. *Geophysical Research Letter*, 21(4), 285 – 288.
- Toon, O. B., & Turco, R. P. (1991). Polar stratospheric clouds and ozone depletion. *Scientific American*, 264(6), 68-74.
- UNEP (United Nations Environment Programme). (2010). Data reported to the ozone secretariat. Retrieved on 14 September 2016 from http://ozone.unep.org/Data_Reporting/
- Urhahn, T., & Ballschmiter, K. (1998). Chemistry of the biosynthesis of halogenated methanes: C1-organohalogenes as pre-industrial chemical stressors in the environment. *Chemosphere*, 37, 1017–1032.
- Velders, G. J. M., Andersen, S. O., Daniel, J. S., Fahey, D. W., & McFarland, M. (2007). The importance of the Montreal Protocol in protecting climate. *Proceedings of the National Academy of Sciences*, 104 (12), 4814–4819.
- Vello, V., Phang, S. -M., Chu, W. -L., Abdul Majid, N., Lim, P. E., & Loh, S. K. (2014) Lipid productivity and fatty acid composition- guided selection of *Chlorella* strains isolated from Malaysia for biodiesel production. *Journal of Applied Phycology*, 26(3), 1399-1413.

- Watson, L., Lacressonnière, G., Gauss, M., Engardt, M., Andersson, C., Josse B, Marécal V., Nyiri A., Sobolowski, S., Siour, G., Szopa, S., & Vautard, R. (2016). Impact of emissions and +2 °C climate change upon future ozone and nitrogen dioxide over Europe. *Atmospheric Environment*, 142, 271-285.
- Wever, R., Tromp, M.G.M., Krenn, B.E., Marjani, A., & Van Tol, M. (1991). Brominating activity of the seaweed *Ascophyllum nodosum*: impact on the biosphere. *Environmental Science and Technology*, 25, 446-449.
- WMO (2014). Scientific assessment of ozone depletion: 2014, world meteorological organization, global ozone research and monitoring project report no. 55, Geneva, Switzerland. World Meteorological Organization.
- WMO. (2011). Scientific Assessment of Ozone Depletion: 2010, Global Ozone Research and Monitoring Project – Report No. 52, (pp. 516). Geneva, Switzerland: World Meteorological Organization.
- WMO (2007). Scientific Assessment of Ozone Depletion: 2006 Global Ozone Research and Monitoring Project - Report No. 50 (pp. 572). Geneva, Switzerland: World Meteorological Organization.
- Wong, G. T. F., Dunstan, W. M., & Kim, D.-B. (2003). The decomposition of hydrogen peroxide by marine phytoplankton. *Oceanologica Acta*, 26(2), 191-198.
- Wuosmaa, A. M., & Hager, L. P. (1990). Methyl Chloride Transferase: A carbocation route for biosynthesis of halometabolites. *Science*, 249, 160 – 162.
- Yamamoto, H., Yokouchi, Y., Otsuki, A., & Itoh, H. (2001). Depth profiles of volatile halogenated hydrocarbons in seawater in the Bay of Bengal. *Chemosphere*, 45, 371-377.

LIST OF PUBLICATIONS AND PAPERS PRESENTED

Yong-Kian Lim, William Sturges, Noorsaadah Abdul Rahman, Siew-Moi Phang (2016). Emission of short-lived halocarbons by selected tropical marine microalgae. Conference: Asia Oceanic Geosciences Society, Beijing, China. Date presented: 3rd August, 2016. Presentation ID: BG08-D3-AM1-311B(L3N)-006

Y-K. Lim, S-M. Phang, N. Abdul Rahman, W. T. Sturges, G. Malin. (2017). Halocarbon emissions from marine phytoplankton and climate change. *International Journal of Environmental Science and Technology*, 1-16. DOI: 10.1007/s13762-016-1219-5